Nathielly Pires Martins

Limitação de fósforo e aumento de CO_2 na atmosfera: uma perspectiva dos mecanismos de aquisição de nutrientes na floresta Amazônica

Dr. Carlos Alberto Quesada – Dra. Lucia Fuchslueger

Tese apresentada ao Instituto Nacional de Pesquisas da Amazônia como parte dos requisitos para obtenção do título de Doutora em Ciências de Florestas Tropicais

Manaus, Amazonas – Brasil

Junho, 2023

Instituto Nacional de Pesquisas da Amazônia

Programa de Pós-graduação em Ciências de Florestas Tropicais

Limitação de fósforo e aumento de CO_2 na atmosfera: uma perspectiva dos mecanismos de aquisição de nutrientes na floresta Amazônica

Nathielly Pires Martins

Dr. Carlos Alberto Quesada e Dra. Lucia Fuchslueger

Tese apresentada ao Instituto Nacional de Pesquisas da Amazônia como parte dos requisitos para obtenção do título de Doutora em Ciências de Florestas Tropicais

Manaus, Amazonas – Brasil

Junho, 2023

SINOPSE:

Foram estudados os efeitos da limitação de fósforo (P) e aumento nas concentrações de dióxido de carbono (CO_2) na atmosfera sobre as múltiplas estratégias para disponibilidade e aquisição de nutrientes na Amazônia Central. O efeito da presença das raízes finas e limitação de P na ciclagem direta de nutrientes foi avaliado através de um experimento de decomposição de detritos de madeira. Além disso, para monitorar a dinâmica das raízes finas, atividade microbiana e concentração de nutrientes na serapilheira e solo em resposta ao aumento de CO_2 um experimento distinto simulando o aumento na concentração de CO_2 na atmosfera em 200ppm foi implementado no sub-bosque da floresta Amazônica.

Palavras-chave: Mudanças climáticas, efeito de fertilização por CO_2, Amazônia, limitação de P; ciclagem de nutrientes; estratégias para aquisição de nutrientes.

In memoriam ao meu amado pai, Geraldo Pires da Silva.

Agradecimentos

Os meus maiores agradecimentos à minha família.

Ao meu querido e amado pai Geraldo P. da Silva (*in memoriam*), que sempre prezou pela educação das filhas. Em minhas memorias visualizo meu pai pedalando por quilômetros uma bicicleta vermelha comigo e minha irmã na garupa, a paisagem ao longo do caminho variava entre um cerradinho ralo e algumas pastagens, as estradas de um cascalho solto e as vezes longas distâncias com areias traiçoeiras. O destino era uma simples casinha de tábua coberta com folhas de babaçu, que ladeava um córrego de água cristalina e gelada. Nessa casinha, que na verdade foi a minha primeira escola o meu pai me alfabetizou. Do trabalho na roça ele tirava o nosso sustento, mas o conciliava com o dom de ensinar as crianças da redondeza. Sem dúvida esse sempre será o meu maior agradecimento e orgulho, porque foi onde tudo começou, obrigada pai.

À minha mãe, guerreira e protetora Maria Elena M. da Silva Pires que me trouxe a vida aos seus dezoito anos, e literalmente salvou a minha vida em alguns episódios ainda na infância. Me ensinou o amor, o afeto, a confiança e a importância de estar presente, minha eterna gratidão pela vida mãezinha.

À minha irmã e alma gêmea Sabrina P. Martins, que sempre foi o meu exemplo de força e coragem. Que sempre segurou a minha mão, me abraçou ou simplesmente olhou em meus olhos e disse que eu iria conseguir, que eu poderia ir que nunca estaria sozinha, e mesmo distante há tantos anos eu sinto que não estou. Obrigada pela parceria de vida maninha, e pelos dois presentinhos mais lindos do universo, meus sobrinhos Vitor Gabriel Martins e João Emanoel Martins.

À minha querida amiga, e primeira orientadora Dra. Mônica Elisa Bleich (*in memoriam*) que acreditou na minha carreira acadêmica antes mesmo que eu entendesse o que era ser uma cientista. Mônica me orientou na graduação, trabalhamos juntas por mais de três anos, ela conciliava as aulas e os projetos na universidade com o doutorado em Ecologia no INPA. Ela me ensinou a importância da ecologia, e a importância do conhecimento para a conservação das florestas, e sempre me dizia que eu deveria vir para o INPA, que o INPA era a minha "cara" e que aqui eu me encontraria. Ela acreditou tanto que me convenceu e me preparou para chegar até aqui, e não errou em nada. Eu me encontrei como cientista, e encontrei o meu lugar no mundo, e por isso serei eternamente grata, minha querida amiga.

À minha companheira, Gabriela Ushida que segurou a minha mão e me ajudou a superar o momento mais difícil da minha vida. Que sempre me deu total apoio e suporte, inclusive nas muitas horas triando raízes, peneirando solo e madrugadas adentro de trabalho no laboratório. Obrigada por todo o carinho e cuidado demonstrado de inúmeras formas ao longo desses últimos anos. Obrigada por acreditar e me incentivar nos momentos de desânimos e dificuldades, e pelos abraços mágicos que sempre resolvem todos os problemas.

Aos gatinhos mais lindos e fofos desse planeta. Adolfo, Iná, Paçoca, Café e Sagui por serem doses diárias de amor e carinho, todas as ronronadas e mordidas nas barriguinhas dessas fofuras contribuíram para uma mente mais tranquila ao longo desses anos.

À Jussara Dayrell e Barbara Brum minhas amigas e companheiras de moradia. Obrigada por todos os muitos dias de convivências e vivências nos últimos três anos, por estarem presente, e do jeitinho de cada uma me apoiarem nessa incrível jornada. Que sorte poder compartilhar a vida com duas mulheres incríveis como vocês.

Aos melhores orientadores, Dra. Lucia Fuchslueger e Dr. Carlos Alberto Quesada. Sete anos compartilhando muitas ideias, conhecimentos e algumas cervejas. Obrigada por acreditarem lá no início, por me incentivarem a sempre buscar o melhor em todos os sentidos. Pela paciência em ensinar os detalhes de como fazer ou ser, por me desafiarem a realizar uma ciência única. Por diariamente me ajudarem a construir o meu sonho, me tornar uma cientista. Que sorte a minha em poder contar com duas pessoas incríveis ao longo dessa jornada, eu tenho e vou levar comigo um pouquinho de cada um de vocês. Obrigada.

A todos os amigos e colegas do laboratório de Ciclos Biogeoquímicos. Bruno Takeshi e Roberta de Souza por tornarem tudo possível, vocês são inspirações. Juliane Menezes, Alacimar Guedes, Iokanam Pereira, França e Eliseu por todo o suporte logístico para manter o experimento das câmaras de topo aberto funcional e funcionando durante uma pandemia. Aos meus fiéis escudeiros, Yago Santos, Carine Cola, Gabriela Ushida, Vanessa Ferrer, Ana Caroline Miron, Maria Pires, Ana Caroline Martins, Lara Siebert, Crisvaldo Cassio, Gyovanni Ribeiro, Karst Schaap, Raffaello Diponzio, Jessica Rosa, Fernanda Luz, Amanda Damasceno que de alguma forma contribuíram para a realização deste projeto. Seja nos intermináveis campos coletando raízes, peneirando solo ou nas inúmeras madrugadas no laboratório, sem vocês não seria possível. A Cilene Palheta por lá no início me ensinar muito do que sei sobre as raízes, obrigada por dividir a sua experiencia e conhecimentos, por toda a paciência e por estar presente diariamente nos

apoiando em literalmente tudo. As minhas amigas, Laynara Lugli, Sabrina Garcia e Flavia Santana por todo o suporte, discussões cientificas e reflexões sobre a vida ao longo dessa jornada.

Aos amigos e colegas que por algum momento viveram ou passaram por Manaus, e se fizeram presente ao longo dessa jornada. Luciana Bachega, Laynara Lugli, Amanda Longhi, Tatiane Reichert, Oscar Valverde-Barrantes, Florian Hofhansl, Tomás Domingues, Erick Oblitas, David Lapola, Iain Hartley e Richard Norby obrigada pelas diferentes contribuições, pelos incentivos e inspirações.

A equipe do Laboratório Temático de Solos e plantas (INPA), Gabriela Carvalho, Erison Gomes, Raimundo Filho, Roberta Nascimento, Laura Cristina, Priscila Moraes e Jonas Filho, por contribuírem para o meu aprendizado e auxiliarem em todas as análises apresentadas nessa tese. Sem essa equipe, não seria possível.

Ao Instituto Nacional de Pesquisas da Amazônia (INPA), e ao programa de Pós-graduação em Ciências de Florestas Tropicais, em especial aos discentes por toda a troca de conhecimento. À CAPES e o Programa de Bolsas FUNBIO por financiarem essa pesquisa. A todos os envolvidos na execução do programa AmazonFACE, eu tenho muito orgulho em ter iniciado a minha carreira nesse projeto tão incrível. Mesmo após tantos anos, o meu sentimento é o de início de uma longa jornada, vida longa de contribuições com esse projeto que terá um impacto gigantesco nas questões climáticas globais.

RESUMO

A floresta Amazônica é a maior extensão de floresta tropical contínua do planeta, exercendo papel importante na dinâmica de carbono (C) global, sobretudo pela sua capacidade de atuar como sumidouro de C. Os solos altamente intemperizados presentes em aproximadamente 60% destas florestas apresentam baixa disponibilidade de fósforo (P), o que potencialmente pode limitar a produtividade primária líquida (PPL) em diversas escalas, incluindo a nível de ecossistema. Modelos climáticos globais, que dentre o efeito das mudanças climáticas simulam o efeito de aumento nas concentrações de gás carbônico (CO_2) na atmosfera, sugerem uma grande capacidade da floresta em assimilar C em sua biomassa e consequentemente auxiliar na mitigação dos efeitos causados pelas alterações no clima. Entretanto, essa capacidade pode estar sendo superestimada, já que a maioria dos modelos não incluem uma resposta dos nutrientes, em particular do P para a Amazônia. Portanto, uma maior compreensão e representatividade dos processos que envolvem o ciclo dos nutrientes e suas múltiplas estratégias de aquisição será de extrema relevância para um maior entendimento de como a Amazônia poderá responder ao aumento nas concentrações atmosféricas de CO_2. Reduzindo as incertezas nas projeções relacionadas à resposta das florestas tropicais às mudanças climáticas.

A ciclagem e decomposição da matéria orgânica fresca acima do solo (folhas, detritos de madeira) é uma das principais fontes de nutrientes – em especial P - para esses locais, e a grande diversidade de espécies arbóreas comumente encontrada em florestas tropicais desenvolveram múltiplas estratégias para aumentar a eficiência na disponibilização e aquisição destes nutrientes. Contudo, existem lacunas de conhecimento relacionadas a essas estratégias, principalmente na floresta Amazônica e considerando o aumento nas concentrações de CO_2 na atmosfera. Com o objetivo de ampliar a compreensão destes diferentes processos, foi proposto para esta tese dois diferentes experimentos. No **capítulo 1**, avaliamos o efeito da presença das raízes finas e aumento na disponibilidade de P na decomposição de detritos de madeira de diferentes espécies. Foi observado um efeito positivo da presença de raízes e uma redução na razão C:P na decomposição e liberação de nutrientes, principalmente para os detritos de menor densidade. No entanto, o efeito da presença das raízes na liberação dos nutrientes foi observado somente nas últimas coletas do experimento. Esses resultados sugerem que a proliferação das raízes finas e decomposição microbiana podem contribuir para aliviar a limitação de nutrientes na Amazônia, no entanto em condições naturais de limitação de P a mobilização dos nutrientes poderá ocorrer ao longo de décadas influenciando diretamente os fluxos de C. No **capítulo 2**, para compreender o efeito do aumento nas concentrações de CO_2 da atmosfera no ciclo do P e mecanismos de aquisição de nutrientes na Amazônia, foi simulado experimentalmente um aumento nas concentrações de CO_2 em aproximadamente 200ppm em relação a concentração ambiente no sub-bosque da floresta. Nós avaliamos os múltiplos mecanismos de aquisição de nutrientes relacionados a dinâmica das raízes finas na serapilheira e no solo, decomposição e liberação de nutrientes da serapilheira das folhas, atividade microbiana e concentração de nutrientes no solo. Observamos diferentes estratégias de aquisição de nutrientes na serapilheira fresca e no solo em resposta ao aumento de CO_2. Na serapilheira as plantas aumentaram o investimento para aquisição direta de P através da exsudação de fosfatases e alterações nos traços morfológicos das raízes sem mudanças na produtividade. No solo, por outro lado, observamos uma redução na produtividade de raízes finas, redução no comprimento a área específica das raízes, acompanhada de uma maior colonização por micorrizas arbusculares. Além disso, a redução na concentração do P total na serapilheira sem mudanças na taxa de decomposição registrada em condições de aumento de CO_2 indica

um aumento na mineralização bioquímica. O mesmo processo pode estar relacionado com a redução do P orgânico no solo em condições de aumento de CO_2, que pode indicar um aumento na absorção de P pelas plantas, considerando que essa redução na fração orgânico não resultou em alteração nas frações inorgânicas ou mobilização de P na biomassa microbiana

Em síntese, os nossos resultados indicam que os detritos de madeira e a serapilheira foliar representam uma fonte crucial de nutrientes para as plantas, e a presença das raízes finas atua como um eficiente mecanismo para aumentar a aquisição direta de nutrientes na camada da serapilheira, influenciando diretamente a disponibilidade e interceptação desses nutrientes. Além disso, com o aumento nas concentrações de CO_2 na atmosfera, observamos que as plantas apresentam uma plasticidade direcionando o uso do C extra em diferentes estratégias de aquisição na camada da serapilheira e solo, de modo a otimizar a eficiência na aquisição e disponibilidade, principalmente do P. Em condições de maior concentração de CO_2 na atmosfera, essa capacidade das plantas em alterar a disponibilidade do P e aumentar a eficiência na aquisição através de múltiplas estratégias é um importante mecanismo que pode influenciar a resiliência da floresta Amazônica às mudanças climáticas, impactando o ciclo de C global.

ABSTRACT

The Amazon rainforest is the largest continuous tropical forest in the world and plays an important role in the global carbon (C) dynamics, particularly as a carbon sink. The highly weathered soils found in approximately 60% of these forests have low phosphorus (P) availability, which has the potential to limit net primary productivity (NPP) at various scales, including the ecosystem level. Global climate models, which simulate the effects of climate change, including increased concentrations of carbon dioxide (CO_2) in the atmosphere, suggest that the forest has a great capacity to assimilate carbon into its biomass and thereby mitigate the effects of climate change. However, this capacity may be overestimated as most models do not include a nutrient response, particularly phosphorus in the Amazon. Therefore, a greater understanding and representation of the processes involving nutrient cycling and multiple nutrient acquisition strategies will be extremely relevant for a better understanding of how the Amazon will respond to the increase in atmospheric CO_2 concentrations, reducing uncertainties in projections related to the response of tropical forests to climate change.

The cycling and decomposition of fresh aboveground organic matter (leaves, woody debris) are among the main sources of nutrients, especially phosphorus, in these areas. The high diversity of tree species commonly found in tropical forests has developed multiple strategies to enhance the efficiency of nutrient availability and acquisition. However, there are knowledge gaps related to these strategies, particularly in the Amazon forest considering the increase in atmospheric CO_2 concentrations. In order to enhance the understanding of these different processes, two different experiments were proposed for this thesis. **In Chapter 1**, we evaluated the effect of the presence of fine roots and increased phosphorus availability on the decomposition of woody debris from different species. We observed a positive effect of root presence and a reduction in the C:P ratio in the decomposition and nutrient release, particularly for the lower density debris. However, the effect of root presence on nutrient release was only observed in the later stages of the experiment. These results suggest that the proliferation of fine roots and microbial decomposition may contribute to alleviating nutrient limitation in the Amazon, but under natural conditions of phosphorus limitation, nutrient mobilization may occur over decades, directly influencing carbon fluxes.

In Chapter 2, to understand the effect of increased atmospheric CO_2 concentrations on the phosphorus cycle and nutrient acquisition mechanisms in the Amazon, an experimental increase of 200ppm in CO_2 concentrations relative to ambient conditions was simulated in the forest understory. We evaluated multiple nutrient acquisition mechanisms related to the fine root dynamics in the litter layer and soil, decomposition and nutrient release from leaf litter, microbial activity, and soil nutrient concentrations. We observed different nutrient acquisition strategies in the fresh litter and soil in response to increased CO_2. In the litter layer, plants increased investment in direct phosphorus acquisition through phosphatase exudation and changes in root morphological traits without changes the productivity. In the soil, however, we observed a reduction in fine root productivity, decreased root length and specific area, accompanied by an increase in the arbuscular mycorrhizal fungi colonization. Furthermore, the reduction in total P concentration in the litter without changes in decomposition rate under increased CO_2 conditions indicates an increase in biochemical mineralization. The same process may be related to the reduction of organic phosphorus in the soil under increased CO_2 conditions, which may indicate an increase in phosphorus uptake by plants, considering that this

reduction in the organic fraction did not result in changes on the inorganic fractions or microbial P mobilization.

In summary, our results indicate that woody debris and leaf litter represent a crucial nutrient source for plants, and the presence of fine roots acts as an efficient mechanism to enhance direct nutrient acquisition in the litter layer, directly influencing the availability and interception of these nutrients. Additionally, with the increase in atmospheric CO_2 concentrations, we observed that plants exhibit plasticity in directing the extra carbon use towards different acquisition strategies in the litter layer and soil, optimizing efficiency in acquisition and availability, especially of phosphorus. Under conditions of higher atmospheric CO_2 concentration, this ability of plants to alter P availability and increase efficiency through multiple strategies is an important mechanism that can influence the resilience of the Amazon rainforest to climate change, impacting the global C cycle.

SUMÁRIO

LISTA DE TABELAS

Capítulo 1:

LISTA DE FIGURAS

Capítulo 1:

– baseline; se methods section) and shown as a standardized effect size by the difference of elevated (eCO_2) and ambient (aCO2) (n=4); the bars represent the 95% confidence interval. The red circles indicate the process in the litter layer and the beige circles in the soil. SRL, specific root length; SRA, specific root area; RTD, root tissue density; APase, acid phosphomonoesterase activity (phosphatase); ELRLP, ecosystem level root length phosphatase; ELRAP, ecosystem level root area phosphatase. CB, cellobiosidase; BG, β-glucosidase; NAG, (insert NAG real). The P values obtained by linear generalized mixed models are indicated in the variables where the eCO_2 was significantly different from aCO_2……..……55

Introdução geral

As florestas tropicais são responsáveis por armazenar aproximadamente metade do carbono (C) total global que está alocado na vegetação, o equivalente a aproximadamente 1,2 Pg C ano^{-1} entre 1990 e 2007 (Pan et al. 2011). Além disso, é o ecossistema com maior biodiversidade do planeta com grandes valores sociais e econômicos (Beech et al. 2017; Lapola et al. 2018). A maior extensão contínua de floresta tropical encontra-se na bacia Amazônica e aloca cerca de 25% do C que está fixado na biomassa vegetal acima do solo (Feldpausch et al. 2012), o que confere a esse sistema grande potencial para mitigação dos efeitos negativos relacionados às mudanças no clima. Monitoramentos em parcelas permanentes distribuídas pela Amazônia e África indicaram que nos últimos vinte anos as florestas tropicais, principalmente a Amazônia, estão perdendo a capacidade de armazenar C em sua biomassa (Brienen et al. 2015; Hubau et al. 2020). Esta redução é primariamente atribuída ao aumento na mortalidade das árvores, que pode estar relacionado à intensificação de eventos extremos de seca e precipitação (Lewis et al. 2011; Feldpausch et al. 2016; Aleixo et al. 2019; Gloor et al. 2015). Com uma maior frequência na ocorrência desses eventos extremos, prevê-se um aumento no estoque de detritos de madeira morta (Seidl et al. 2017; McDowell et al. 2018), o que pode influenciar diretamente o balanço de C e ciclagem de nutrientes da floresta, já que a decomposição desse material pode levar décadas.

Aproximadamente 60% da floresta Amazônica está localizada em solos geologicamente antigos, que apresentam baixa disponibilidade de fósforo (P), em decorrência do processo de lixiviação que vem ocorrendo por milhares de anos de intemperismo (Quesada et al. 2010; 2011). A maioria do P total está na forma orgânica ou adsorvido em partículas minerais de ferro (Fe) e alumínio (Al), indisponível para as plantas (Walker and Syers 1976). Assim, uma importante fonte de nutrientes para estes ecossistemas é a ciclagem de nutrientes através da decomposição de diferentes materiais que compõem a camada da serapilheira (Luizao and Schubart 1987; Luizao 1989). Alguns fatores relacionados às condições climáticas (i.e., temperatura, precipitação), qualidade do substrato (i.e., composição química) e comunidade microbiana podem influenciar diretamente a decomposição e ciclagem destes nutrientes (Chapin, Matson, and Vitousek 2011; Powers et al. 2009; Mooshammer et al. 2014).

De forma geral, a comunidade microbiana produz enzimas extracelulares para degradar as macromoléculas de material orgânico, disponibilizando nutrientes e outros

compostos (Schimel and Bennett 2004) para os microrganismos e plantas. Assim, a quantidade de nutrientes liberados para o ecossistema depende da demanda da comunidade microbiana por C e nutrientes em razão da quantidade de nutrientes na serapilheira (Waring 2013; Mooshammer et al. 2014). Em algumas regiões da Amazônia, ocorre uma intensa proliferação de raízes na camada da serapilheira, formando um tapete de raízes que atua na interceptação direta dos nutrientes recém mineralizados via decomposição (Stark and Jordan 1978; Went and Stark 1968). Além de atuar na aquisição direta de nutrientes, as raízes finas podem aumentar a mobilização de P sem influenciar na degradação de moléculas de C, através da mineralização bioquímica (McGill and Cole 1981; Luizão, Luizão, and Proctor 2007; Martins et al. 2021).

A grande diversidade de espécies nas regiões tropicais possibilita múltiplas estratégias e mecanismos para aquisição de nutrientes (Weemstra et al. 2016; Lugli et al. 2019). Essas estratégias podem ser ajustadas de acordo com a forma e a disponibilidade do substrato, com o potencial para aumentar a eficiência na disponibilização e aquisição de nutrientes (Lloyd et al. 2001; Lambers et al. 2008, Reichert et al. 2022). Por exemplo, as plantas podem sintetizar e exsudar através das raízes enzimas fosfatases, que são responsáveis por hidrolisar as moléculas de $PO4^-$, deixando-o disponível para as plantas sem precisar quebrar as moléculas de C (Dijkstra et al. 2013; Nannipieri et al. 2011). De forma mais indireta as plantas podem exsudar compostos de C lábil (Wen et al. 2021; Shen et al. 2011), que atuam como fonte de energia para os microrganismos realizarem a decomposição da matéria orgânica (i.e., efeito *priming*) (Kuzyakov, Friedel, and Stahr 2000). Para aumentar a aquisição dos nutrientes já disponíveis as plantas podem alterar as estruturas morfológicas das raízes finas como comprimento radicular específico (*Specific Root Length* - SRL), área radicular específica (*Specific Root Area* - SRA) e diâmetro radicular (Lambers et al. 2006), de modo a aumentar o volume de serapilheira ou solo explorados. Por outro lado, as plantas podem "terceirizar" essa maior exploração através do investimento na simbiose com os fungos micorrízicos (Smith, Smith, and Jakobsen 2004), que atuam como uma extensão das raízes aumentando a capacidade de exploração por nutrientes.

Evidências empíricas indicam que a disponibilidade de P pode limitar a produtividade primária líquida na Amazônia a nível de ecossistema (Cunha et al. 2022). Entretanto os modelos climáticos projetam que as florestas tropicais têm grande potencial para atuarem como sumidouros de C nas próximas décadas (Koch, Hubau, and Lewis 2021; Friedlingstein et al. 2022), decorrentes de uma maior assimilação do CO_2 presente

na atmosfera e sua alocação em biomassa (i.e., efeito de fertilização por CO_2; Bacastow and Keeling 1973; Walker et al. 2021), o que contradiz as observações *in situ* que indicam uma tendência de redução na capacidade das florestas tropicais em estocar C na biomassa (Hubau et al. 2020). A representação incompleta de alguns fatores cruciais para o melhor entendimento dessa dinâmica, como os ciclos dos nutrientes, pode explicar essas divergências. Modelos que incluíram o ciclo do P demonstraram que sua disponibilidade pode reduzir a resposta das florestas tropicais ao efeito de fertilização por CO_2 (Fleischer et al. 2019), gerando impactos diretos no balanço global de C. Esses resultados reforçam a importância de uma maior representatividade dos processos que envolvem o ciclo dos nutrientes e as múltiplas estratégias para aquisição de nutrientes, obtendo com isso projeções mais acuradas nos modelos globais.

Experimentos que utilizam a tecnologia de enriquecimento de CO_2 ao ar livre (*Free Air CO_2 Enrichment* – FACE) vêm sendo implementados nos últimos 30 anos com o objetivo de avaliar o efeito do aumento das concentrações de CO_2 no funcionamento de florestas (Norby and Zak 2011). Grande parte desses experimentos foram implementados em florestas temperadas que são naturalmente limitadas por nitrogênio (N). Os resultados indicam um aumento da assimilação de C em condições de aumento das concentrações de CO_2 (Ainsworth and Long 2005), mas apontam que a alocação desse C extra em biomassa vegetal depende da capacidade das plantas em aumentar sua eficiência na aquisição de nutrientes (Finzi et al. 2007; Walker et al. 2021). No primeiro experimento FACE em uma floresta madura limitada por P, realizado em uma floresta de eucaliptos na Austrália (EucFACE), foi observado um aumento significativo na assimilação de C em condições de aumento de CO_2 sem maior alocação acima do solo (Ellsworth et al. 2017; Jiang et al. 2020). Por outro lado, foi observado um aumento na mineralização de N e P nos primeiros seis meses (Hasegawa, Macdonald, and Power 2016; Ochoa-Hueso et al. 2017) e estudos posteriores indicaram um efeito das raízes na disponibilidade de nutrientes, possivelmente estimulando a comunidade microbiana através da exsudação de compostos de C lábil na rizosfera (Pihlblad et al. 2023). No entanto, ainda são poucos os estudos que investigaram o efeito do aumento de CO_2 nos mecanismos de aquisição de nutrientes em solos limitados por P, sobretudo em florestas com alta diversidade, como a Amazônia, que podem apresentar múltiplas estratégias para aumentar a eficiência na aquisição de nutrientes.

Considerando o contexto brevemente apresentado, esta tese está dividida em dois capítulos que abordam, experimentalmente, duas importantes lacunas relacionadas aos

mecanismos e múltiplas estratégias para aquisição de nutrientes em florestas tropicais em resposta às mudanças climáticas. No **capítulo 1**, investigamos como a proliferação das raízes finas e limitação por P podem influenciar a decomposição e liberação de nutrientes em detritos de madeira, uma importante fonte de nutrientes e estoque de C em ecossistemas tropicais, cujo acúmulo tem se intensificado em decorrência do aumento na mortalidade das árvores causado por eventos extremos mais frequentes. No **capítulo 2**, investigamos como as múltiplas estratégias de aquisição de nutrientes respondem ao aumento das concentrações de CO_2 na atmosfera em uma floresta limitada pela baixa disponibilidade natural de P. Para isso, nós simulamos o aumento nas concentrações de CO_2 em câmaras de topo aberto (*Open Top Chambers* - OTCs) instaladas no sub-bosque de uma floresta primária de terra-firme na Amazônia Central e medimos a produtividade, características morfológicas das raízes, atividade da fosfatase e percentual de colonização por micorrizas na camada da serapilheira e solo, assim como a concentração de nutrientes e atividade dos microrganismos no solo.

Referências

Ainsworth, Elizabeth A., and Stephen P. Long. 2005. “What Have We Learned from 15 Years of Free-Air CO2 Enrichment (FACE)? A Meta-Analytic Review of the Responses of Photosynthesis, Canopy Properties and Plant Production to Rising CO2.” *New Phytologist* 165 (2): 351–72. https://doi.org/10.1111/j.1469-8137.2004.01224.x.

Aleixo, Izabela, Darren Norris, Lia Hemerik, Antenor Barbosa, Eduardo Prata, Flávia Costa, and Lourens Poorter. 2019. “Amazonian Rainforest Tree Mortality Driven by Climate and Functional Traits,” no. May. https://doi.org/10.1038/s41558-019-0458-0.

Bacastow, R, and C K Keeling. 1973. “Atmospheric Carbon Dioxide and Radiocarbon in the Natural Carbon Cycle: II. Changes from A. D. 1700 to 2070 as Deduced from a Geochemical Model.” In *Brookhaven Symposia in Biology*, 30:86–135.

Beech, E., M. Rivers, S. Oldfield, and P. P. Smith. 2017. “GlobalTreeSearch: The First Complete Global Database of Tree Species and Country Distributions.” *Journal of Sustainable Forestry* 36 (5): 454–89. https://doi.org/10.1080/10549811.2017.1310049.

Brienen, R. J.W., O. L. Phillips, T. R. Feldpausch, E. Gloor, T. R. Baker, J. Lloyd, G. Lopez-Gonzalez, et al. 2015. “Long-Term Decline of the Amazon Carbon Sink.” *Nature* 519 (7543): 344–48. https://doi.org/10.1038/nature14283.

Chapin, F. Stuart, Pamela A Matson, and Peter M. Vitousek. 2011. *Priciples of Terrestrial Ecosysten Ecology*. Second.

Cunha, Hellen F.V., Flavia Delgado Santana, Izabela Fonseca Aleixo, Anna Martins Moraes, Sabrina Garcia, Raffaello Di Ponzio, Erick Oblitas Mendoza, et al. 2022. “Direct Evidence for Phosphorus Limitation on Amazon Forest Productivity,” no. September 2021. https://doi.org/10.1038/s41586-022-05085-2.

Dijkstra, Feike A, Yolima Carrillo, Elise Pendall, and Jack A Morgan. 2013. “Rhizosphere Priming: A Nutrient Perspective.” *Frontiers in Microbiology* 4 (July): 216. https://doi.org/10.3389/fmicb.2013.00216.

Ellsworth, David S., Ian C. Anderson, Kristine Y. Crous, Julia Cooke, John E. Drake, Andrew N. Gherlenda, Teresa E. Gimeno, et al. 2017. “Elevated CO2 Does Not Increase Eucalypt Forest Productivity on a Low-Phosphorus Soil.” *Nature Climate Change* 7 (4): 279–82. https://doi.org/10.1038/nclimate3235.

Feldpausch, T. R., J. Lloyd, S. L. Lewis, R. J.W. Brienen, M. Gloor, A. Monteagudo Mendoza, G. Lopez-Gonzalez, et al. 2012. “Tree Height Integrated into Pantropical Forest Biomass Estimates.” *Biogeosciences* 9 (8): 3381–3403. https://doi.org/10.5194/bg-9-3381-2012.

Feldpausch, T R, O L Phillips, R J W Brienen, E Gloor, J Lloyd, Y Malhi, A Alarcón, et al. 2016. “Amazon Forest Response to Repeated Droughts.” *Global Biogeochemical Cycles* 30 (7): 964–82. https://doi.org/10.1002/2015GB005133.Received.

Finzi, Adrien C, Richard J Norby, Carlo Calfapietra, Anne Gallet-Budynek, Birgit Gielen, William E Holmes, Marcel R Hoosbeek, et al. 2007. “Increases in Nitrogen

Uptake Rather than Nitrogen-Use Efficiency Support Higher Rates of Temperate Forest Productivity under Elevated CO 2." www.pnas.org/cgi/content/full/.

Fleischer, Katrin, Anja Rammig, Martin G. De Kauwe, Anthony P. Walker, Tomas F. Domingues, Lucia Fuchslueger, Sabrina Garcia, et al. 2019. "Amazon Forest Response to CO2 Fertilization Dependent on Plant Phosphorus Acquisition." *Nature Geoscience* 12 (September): 736–741. https://doi.org/10.1038/s41561-019-0404-9.

Friedlingstein, Pierre, Michael O'Sullivan, Matthew W. Jones, Robbie M. Andrew, Luke Gregor, Judith Hauck, Corinne Le Quéré, et al. 2022. "Global Carbon Budget 2022." *Earth System Science Data* 14 (11): 4811–4900. https://doi.org/10.5194/essd-14-4811-2022.

Gloor, M, J Barichivich, G Ziv, R Brienen, J Schöngart, and P Peylin. 2015. "Recent Amazon Climate as Background for Possible Ongoing Special Section :" *Global Biogeochemical Cycles* 29 (9): 1384–99. https://doi.org/10.1002/2014GB005080.Received.

Hasegawa, Shun, Catriona A. Macdonald, and Sally A. Power. 2016. "Elevated Carbon Dioxide Increases Soil Nitrogen and Phosphorus Availability in a Phosphorus-Limited Eucalyptus Woodland." *Global Change Biology* 22 (4): 1628–43. https://doi.org/10.1111/gcb.13147.

Hubau, Wannes, Simon L. Lewis, Oliver L. Phillips, Kofi Affum-Baffoe, Hans Beeckman, Aida Cuní-Sanchez, Armandu K. Daniels, et al. 2020. "Asynchronous Carbon Sink Saturation in African and Amazonian Tropical Forests." *Nature* 579 (7797): 80–87. https://doi.org/10.1038/s41586-020-2035-0.

Jiang, Mingkai, Belinda E. Medlyn, John E. Drake, Remko A. Duursma, Ian C. Anderson, Craig V.M. Barton, Matthias M. Boer, et al. 2020. "The Fate of Carbon in a Mature Forest under Carbon Dioxide Enrichment." *Nature* 580 (7802): 227–31. https://doi.org/10.1038/s41586-020-2128-9.

Koch, Alexander, Wannes Hubau, and Simon L. Lewis. 2021. "Earth System Models Are Not Capturing Present-Day Tropical Forest Carbon Dynamics." *Earth's Future* 9 (5): 1–19. https://doi.org/10.1029/2020EF001874.

Kuzyakov, Yakov., J K. Friedel, and K. Stahr. 2000. "Review of Mechanisms and Quantification of Priming Effects." *Soil Biology and Biochemistry* 32 (11–12): 1485–98. https://doi.org/10.1016/S0038-0717(00)00084-5.

Lambers, Hans, John A. Raven, Gaius R. Shaver, and Sally E. Smith. 2008. "Plant Nutrient-Acquisition Strategies Change with Soil Age." *Trends in Ecology and Evolution* 23 (2): 95–103. https://doi.org/10.1016/j.tree.2007.10.008.

Lambers, Hans, Michael W. Shane, Michael D. Cramer, Stuart J. Pearse, and Erik J. Veneklaas. 2006. "Root Structure and Functioning for Efficient Acquisition of Phosphorus: Matching Morphological and Physiological Traits." *Annals of Botany* 98 (4): 693–713. https://doi.org/10.1093/aob/mcl114.

Lapola, David M., Patricia Pinho, Carlos A. Quesada, Bernardo B. N. Strassburg, Anja Rammig, Bart Kruijt, Foster Brown, et al. 2018. "Limiting the High Impacts of Amazon Forest Dieback with No-Regrets Science and Policy Action." *Proceedings of the National Academy of Sciences* 115 (46): 11671–79.

https://doi.org/10.1073/pnas.1721770115.

Lewis, Simon L, Paulo M Brando, Oliver L Phillips, Geertje M F Van Der Heijden, and Daniel Nepstad. 2011. "The 2010 Amazon Drought" 331 (February): 2011.

Lloyd, J., M.I. Bird, E.M. Veenendaal, and B. Kruijt. 2001. "Should Phosphorus Availability Be Constraining Moist Tropical Forest Responses to Increasing CO2 Concentrations?" *Global Biogeochemical Cycles in the Climate System*, no. December: 95–114. https://doi.org/10.1016/b978-012631260-7/50010-8.

Lugli, Laynara F., Kelly M. Andersen, Luiz E.O.C. Aragão, Amanda L. Cordeiro, Hellen F.V. Cunha, Lucia Fuchslueger, Patrick Meir, et al. 2019. "Multiple Phosphorus Acquisition Strategies Adopted by Fine Roots in Low-Fertility Soils in Central Amazonia." *Plant and Soil*. https://doi.org/10.1007/s11104-019-03963-9.

Luizao, F. J. 1989. "Litter Production and Mineral Element Input to the Forest Floor in a Central Amazonian Forest." *GeoJournal* 19 (4): 407–17. https://doi.org/10.1007/BF00176910.

Luizao, F. J., and H. O.R Schubart. 1987. "Litter Production and Decomposition in a Terra-Firme Forest of Central Amazonia." *Experientia* 43 (3): 259–65. https://doi.org/10.1007/BF01945549.

Luizão, Regina C.C, Flávio J Luizão, and John Proctor. 2007. "Fine Root Growth and Nutrient Release in Decomposing Leaf Litter in Three Contrasting Vegetation Types in Central Amazonia." *Plant Ecology* 192 (2): 225–36. https://doi.org/10.1007/s11258-007-9307-8.

Martins, Nathielly P., Lucia Fuchslueger, Katrin Fleischer, Kelly M. Andersen, Rafael L. Assis, Fabricio B. Baccaro, Plínio B. Camargo, et al. 2021. "Fine Roots Stimulate Nutrient Release during Early Stages of Leaf Litter Decomposition in a Central Amazon Rainforest." *Plant and Soil* 469: 287–303. https://doi.org/10.1007/s11104-021-05148-9.

McDowell, Nate G., Sean T. Michaletz, Katrina E. Bennett, Kurt C. Solander, Chonggang Xu, Reed M. Maxwell, and Richard S. Middleton. 2018. "Predicting Chronic Climate-Driven Disturbances and Their Mitigation." *Trends in Ecology and Evolution* 33 (1): 15–27. https://doi.org/10.1016/j.tree.2017.10.002.

McGill, W B, and C V Cole. 1981. "Comparative Aspects of Cycling of Organic C, N, S and P through Soil Organic Matter." *Geoderma* 26: 267–86. https://doi.org/doi.org/10.1016/0016-7061(81)90024-0.

Mooshammer, Maria, Wolfgang Wanek, Sophie Zechmeister-Boltenstern, and Andreas Richter. 2014. "Stoichiometric Imbalances between Terrestrial Decomposer Communities and Their Resources: Mechanisms and Implications of Microbial Adaptations to Their Resources." *Frontiers in Microbiology* 5: 1–10. https://doi.org/10.3389/fmicb.2014.00022.

Nannipieri, P, L Giagnoni, L Landi, and G Renella. 2011. "Role of Phosphatase Enzymes in Soil." In *Phosphorus in Action. Biological Processes in Soil Phosphorus Cycling*, 26:215–43. https://doi.org/10.1007/978-3-642-15271-9.

Norby, Richard J., and Donald R. Zak. 2011. "Ecological and Evolutionary Lessons from Free Air Carbon Enhancement (FACE) Experiments." *Annual Review of*

Ecology, Evolution, and Systematics 42. https://doi.org/10.1146/annurev-ecolsys-102209-144647.

Ochoa-Hueso, Raúl, John Hughes, Manuel Delgado-Baquerizo, John E. Drake, Mark G. Tjoelker, Juan Piñeiro, and Sally A. Power. 2017. "Rhizosphere-Driven Increase in Nitrogen and Phosphorus Availability under Elevated Atmospheric CO2 in a Mature Eucalyptus Woodland." *Plant and Soil* 416 (1–2): 283–95. https://doi.org/10.1007/s11104-017-3212-2.

Pan, Yude, Richard a Birdsey, Jingyun Fang, Richard Houghton, Pekka E Kauppi, Werner a Kurz, Oliver L Phillips, et al. 2011. "A Large and Persistent Carbon Sink in the World's Forests." *Science* 333: 1239–43. https://doi.org/10.1126/science.1201609.

Pihlblad, Johanna, Louise C. Andresen, Catriona A. Macdonald, David S. Ellsworth, and Yolima Carrillo. 2023. "The Influence of Elevated CO2and Soil Depth on Rhizosphere Activityand Nutrient Availability in a Mature Eucalyptus Woodland." *Biogeosciences* 20 (3): 505–21. https://doi.org/10.5194/bg-20-505-2023.

Powers, Jennifer S., Rebecca A. Montgomery, E. Carol Adair, Francis Q. Brearley, Saara J. Dewalt, Camila T. Castanho, Jerome Chave, et al. 2009. "Decomposition in Tropical Forests: A Pan-Tropical Study of the Effects of Litter Type, Litter Placement and Mesofaunal Exclusion across a Precipitation Gradient." *Journal of Ecology* 97 (4): 801–11. https://doi.org/10.1111/j.1365-2745.2009.01515.x.

Quesada, C. A., J. Lloyd, L. O. Anderson, N. M. Fyllas, M. Schwarz, and C. I. Czimczik. 2011. "Soils of Amazonia with Particular Reference to the RAINFOR Sites." *Biogeosciences* 8 (6): 1415–40. https://doi.org/10.5194/bg-8-1415-2011.

Quesada, C. A., J. Lloyd, M. Schwarz, S. Patiño, T. R. Baker, C. Czimczik, N. M. Fyllas, et al. 2010. "Variations in Chemical and Physical Properties of Amazon Forest Soils in Relation to Their Genesis." *Biogeosciences* 7 (5): 1515–41. https://doi.org/10.5194/bg-7-1515-2010.

Reichert, Tatiana, Anja Rammig, Lucia Fuchslueger, Laynara F. Lugli, Carlos A. Quesada, and Katrin Fleischer. 2022. "Plant Phosphorus-Use and -Acquisition Strategies in Amazonia." *New Phytologist* 234 (4): 1126–43. https://doi.org/10.1111/nph.17985.

Schimel, Joshua P., and Jennifer Bennett. 2004. "NITROGEN MINERALIZATION: CHALLENGES OF A CHANGING PARADIGM." *Concepts & Synthesis* 85 (3): 591–602. https://doi.org/https://doi.org/10.1890/03-8002.

Seidl, Rupert, Dominik Thom, Markus Kautz, Dario Martin-Benito, Mikko Peltoniemi, Giorgio Vacchiano, Jan Wild, et al. 2017. "Forest Disturbances under Climate Change." *Nature Climate Change* 7 (6): 395–402. https://doi.org/10.1038/nclimate3303.

Shen, Jianbo, Lixing Yuan, Junling Zhang, Haigang Li, Zhaohai Bai, Xinping Chen, Weifeng Zhang, and Fusuo Zhang. 2011. "Phosphorus Dynamics: From Soil to Plant." *Plant Physiology* 156 (3): 997–1005. https://doi.org/10.1104/pp.111.175232.

Smith, Sally E., F. Andrew Smith, and Iver Jakobsen. 2004. "Functional Diversity in Arbuscular Mycorrhizal (AM) Symbioses: The Contribution of the Mycorrhizal P

Uptake Pathway Is Not Correlated with Mycorrhizal Responses in Growth or Total P Uptake." *New Phytologist* 162 (2): 511–24. https://doi.org/10.1111/j.1469-8137.2004.01039.x.

Stark, Nellie M ., and Carl F. Jordan. 1978. "Nutrient Retention by the Root Mat of an Amazonian." *Ecology* 59 (3): 434–37. https://doi.org/doi.org/10.2307/1936571.

Walker, Anthony P., Martin G. De Kauwe, Ana Bastos, Soumaya Belmecheri, Katerina Georgiou, Ralph F. Keeling, Sean M. McMahon, et al. 2021. "Integrating the Evidence for a Terrestrial Carbon Sink Caused by Increasing Atmospheric CO2." *New Phytologist* 229 (5): 2413–45. https://doi.org/10.1111/nph.16866.

Walker, T W., and J. K. Syers. 1976. "The Fate of Phosphorus during Pedogenesis." *Geoderma* 15 (1): 1–19. https://doi.org/10.1016/0016-7061(76)90066-5.

Waring, Bonnie G. 2013. "Exploring Relationships between Enzyme Activities and Leaf Litter Decomposition in a Wet Tropical Forest." *Soil Biology and Biochemistry* 64: 89–95. https://doi.org/10.1016/j.soilbio.2013.04.010.

Weemstra, Monique, Liesje Mommer, Eric J W Visser, Jasper Van Ruijven, Thomas W Kuyper, Godefridus M J Mohren, and Frank J Sterck. 2016. "Tansley Review Towards a Multidimensional Root Trait Framework : A Tree Root Review." *New Phytologist* 211: 1159–69. https://doi.org/10.1111/nph.14003.

Wen, Zhihui, Philip J. White, Jianbo Shen, and Hans Lambers. 2021. *Linking Root Exudation to Belowground Economic Traits for Resource Acquisition*. *New Phytologist.* https://doi.org/10.1111/nph.17854.

Went, F.W, and N. Stark. 1968. "THE BIOLOGICAL AND MECHANICAL ROLE OF SOIL FUNGI." *Botany*, no. 1: 497–504. https://doi.org/10.1073 / pnas.60.2.497.

Capítulo 1

Fine root presence and increased phosphorus availability stimulate wood decay in a Central Amazonian rainforest

Nathielly P. Martins*, Oscar Valverde-Barrantes, Lucia Fuchslueger, Laynara. F. Lugli, Adriana Grandis, Florian Hofhansl, Bruno Takeshi, Gabriela Ushida, Carlos. A. Quesada

Status of manuscript: under review – Oikos journal

Picture: João Rosa - AmazonFACE

Fine root presence and increased phosphorus availability stimulate wood decay in a Central Amazonian rainforest

Nathielly P. Martins[1]*, Oscar Valverde-Barrantes[2], Lucia Fuchslueger[1,3], Laynara. F. Lugli[1,4], Adriana Grandis[6], Florian Hofhansl[5], Bruno Takeshi[1], Gabriela Ushida[1], Carlos. A. Quesada[1]

[1]Coordination of Environmental Dynamics (CODAM), National Institute of Amazonian Research, Manaus, Amazonas, Brazil.

[2]International Center of Tropical Biodiversity, Florida International University, Miami, Florida, United States.

[3]Centre of Microbiology and Environmental Systems Sciences, University of Vienna, Vienna, Austria.

[4]Land Surface – Atmosphere Interactions, Technical University of Munich, Freising, Bavaria, Germany.

[5]Biodiversity, Ecology, and Conservation (BEC) Research Group, Biodiversity and Natural Resources (BNR) Program, International Institute for Applied Systems Analysis (IIASA), Laxenburg, Austria.

[6]Department of Botany, Biosciences Institute, University of São Paulo, São Paulo, Brazil.

*Author for correspondence: Nathielly P. Martins: nathiellymartins9@gmail.com

Fine root presence and increased phosphorus availability stimulate wood decay in a Central Amazonian rainforest

Abstract

Dead logs and branches encompass ~ 14% of all carbon stored in terrestrial ecosystems and represent an important nutrient pool in tropical forests. Approximately 60% of rainforest in the Amazon basin is thriving on geologically old and highly weathered soils, depleted in phosphorus (P) and cations. In this system, nutrient cycling is relatively closed, and plants strongly rely on direct nutrient recycling from decomposing organic matter. Woody debris decomposition is poorly studied and often not considered in ecosystem carbon (C) and nutrient budgets.

We hypothesized that woody debris decomposition is accelerated by colonizing fine roots mining for nutrients, depending on wood density and nutrient stoichiometry. We tested this by conducting a wood decomposition experiment in a Central Amazonian rainforest over two years including logs of five different local woody species covering a range of wood density, with factorial root presence and P addition treatments.

We found that root colonization and P addition increased wood decay rates and, although fine root colonization increased when P was added, wood decay did not change. Nutrient loss from wood was accelerated by P addition, whereas a root presence effect on nutrient mobilization was only detectable at the end of the experiment. Our results highlight the role of fine roots in priming wood decay, although direct nutrient acquisition by plants seem to only occurs in more advanced stages of decomposition. On the other hand, the positive effect of P addition indicates that microbial nutrient mobilization in woody material is driven mainly by wood stoichiometry rather than priming by root activity.

Keywords: Amazon rainforest; coarse wood debris; fine root presence; P limitation; wood density; wood decomposition

Introduction

Tropical forests are the main global terrestrial carbon (C) sink, with an uptake estimated by 1.2 Pg C year-1 from 1990-2007 (Pan et al. 2011). The Amazon basin contributes around 25% to the terrestrial C sink (Phillips et al. 2009; Pan et al. 2011; Feldpausch et al. 2012), but its sink strength has started to decline, mainly due to a sustained long-term increase in tree mortality potentially induced by rising temperatures and greater drought frequency (Brienen et al. 2015; Hubau et al. 2020). This surge in climate extreme events is predicted to increase dead wood stocks and subsequently, the decomposition of woody material could strongly alter the forest C balance (Seidl et al. 2017; McDowell et al. 2018). Moreover, approximately 60% of the rainforests in the Amazon basin are growing on geologically old and highly weathered soils, depleted in phosphorus (P) and cations (Quesada et al. 2010; 2011). Thus, nutrients stored in woody debris are quantitatively important at the ecosystem-scale and the recycling and release of nutrients from litter are critical to maintain ecosystem productivity (Grau et al. 2017; Bauters et al. 2022). Nonetheless, there is still little information about the factors controlling the decomposition and nutrient release from woody debris in tropical forests.

Wood decomposition is controlled by abiotic factors with faster decay rates at warm and wet conditions (Bradford et al. 2014), wood quality and chemical composition, in particular wood density, lignin and cellulose concentration, and stoichiometry (Cornwell et al. 2008; Hu et al. 2018; Parton et al. 2007) as well as the presence of saprotrophic organisms. Moreover, plants with rapid acquisition resources strategies (e.g., with high specific leaf area, or leaf N and P content) tend to construct softer stems with lower wood density and lignin content than potentially more conservative species with denser wood (Chave et al. 2009; Cornwell et al. 2008; Freschet et al. 2010; Weedon et al. 2009). This suggests that a similar range in wood decomposition rates of woody material could also be found across tropical tree communities with higher rates of wood decomposition being associated with lower wood density (i.e., acquisitive strategies) (Baraloto et al. 2010; Freschet, Aerts, and Cornelissen 2012).

Simultaneously, wood decomposition is strongly modulated by fragmentation and degradation processes modulated by faunal, fungal, and bacterial communities (Hättenschwiler, Tiunov, and Scheu 2005; Powers et al. 2009). Microbial activity is regulated by substrate quality and the relative C to nutrient demand of decomposer communities, with the scarcest nutrients limiting decomposition (Manzoni et al. 2010;

Mooshammer et al. 2012). Woody debris have a higher C: N: P ratio (103:40:1; global average) compared to leaf and root litter, and the C present is bound in complex and large molecules as lignin or cellulose (Weedon et al. 2009; Mooshammer et al. 2014). The breakdown of these compounds requires high energetic costs, drastically slowing down the decay of high-density wood (Mooshammer et al. 2014; Nottingham et al. 2018). Consequently, the rather large abundance of complex C compounds, as well as low mineral P availability, have been shown to be the main factors limiting woody debris decomposition rates, even in hot and humid tropical climates (Chen et al. 2016).

A characteristic feature of the Amazonian rainforest is the presence of large root mats on the soil surface that are responsible for taking up mineralized nutrients from the litter layer and maintaining a tight nutrient cycling (Went and Stark 1968; Herrera et al. 1978; Cuevas and Medina 1988; Martins et al. 2021). Much less is known about the rates of nutrient acquisition by fine roots from woody debris. It is possible that fine roots may also enhance woody debris decomposition as they physically disrupt the tissues in their pursuit for nutrients, and by releasing labile C as exudates, which could stimulate microbial saprotrophic activity (Kuzyakov, Friedel, and Stahr 2000). For instance, specialist saprotrophic fungi can use these labile exudates to produce extracellular lignocellulolytic enzymes and enhance the breakdown of more recalcitrant lignin (i.e., positive priming) (Blanchette 2000; Yang et al. 2022). On the other hand, a reduction in decomposition can occur when a preferential substrate utilization occurs, in this case, fungal communities with abundant nutrient supply would prefer to use labile root-derived C rather than more complex C compounds present in the organic material, reducing the degradation of the woody substrate (Cheng 1999; Cheng and Kuzyakov 2005).

We here explore whether woody debris characteristics, such as initial density and changes in nutrient stoichiometry caused by P addition may affect fine root colonization and impact decomposition rates and nutrient release. We hypothesize that (i) fine root colonization will have a stronger effect on wood decay from species with lower-density wood, as they are more accessible and a better nutrient-cost balance, (ii) P addition will increase root colonization with an additive effect on wood decay. We tested our hypotheses by conducting a wood decomposition experiment using logs of five tree species constituting a gradient of wood density in a Central Amazonian rainforest over two years (2016-2018), with factorial root presence and P addition treatments.

Materials and Methods

Site description

The study site is in the Cuieiras Reserve, about 60 km north of Manaus (Amazonas, Brazil), and is managed by the National Institute of Amazonian Research (INPA). The forest is composed of a dense, mature, and well-preserved rainforest typical of a Central Amazonian Terra-Firme vegetation, the climate is classified as a rainy tropical climate with average monthly temperatures varying from 24 to 27 °C, mean annual rainfall is 2.400 mm, with lower precipitation levels (<100 mm per month) from July to September (Alves et al. 2016). The soil is characterized as Geric Ferralsol, clay-rich and highly weathered with a low concentration of rock-derived nutrients, such as P, Ca, Mg and K. In these soils, a large proportion of P is bound to secondary soil minerals, such as iron and aluminum oxides (Quesada et al. 2010; 2011).

Experimental design

Woody material was collected from branches of recently fallen trees (identified by a botanist) after an intense storm in the area near the experimental site. We sampled woody branches measuring between 6 to 12 cm in diameter from at least three separated individuals of five canopy species abundant in the area (*Dimorphandra coccinea*, *Croton lanjouwensis*, *Inga alba*, *Byrsonima duckeana* and *Licania heteromopha*) covering a range of wood densities from soft to heavy (Table 1; (Chave et al. 2006). The diameter and length (about 10 cm) of all wood samples were measured, using a digital caliper and tape. After that, samples were dried at 65 °C for 72 h or until constant weight to calculate wood density of each log used for the decomposition experiment. Among the collected species *Dimorphandra sp*. had the lowest wood density with an average of 0.19 ± 0.01 g-1 cm^3, and *Licania sp.*, had the highest wood density, with an average of 0.38 ± 0.06 g-1 cm^3. The other three species were classified as intermediate with wood density varying between 0.24 ± 0.01 g-1 cm3 and 0.28 ± 0.04 g-1 cm3 (Table 1).

To test the effects of both root presence (R) and nutrient availability (P) on the rates of wood decomposition and nutrient release we established a factorial experiment in a paired block design in June 2016. Before the samples were installed in the forest, the total 200 logs were split in P addition (+P) and without P addition (-P). For the + P treatment, wood samples were submerged in a solution containing 570 g of $NH_4H_2PO_4$ in 60 liters of water

(0.81 M $NH_4H_2PO_4$ solution) for 3 days, corresponding in total to 347.7 g of PO_4. The samples for the -P treatment were submerged in water for 3 days. Three samples per species and +P or -P treatments were dried and used to characterize their initial wood chemical composition (Table S1).

In the forest, the samples were divided equally into two blocks, each under the canopy of a large *Caryocar pallidum* tree separated by ~300 m (giving an n=2 per species and treatment combination). Each block was divided into five sub-blocks, one for each collection time. Each sub-block contained samples from all five species, exposed to the respective treatments: half of the samples were left untouched to allow root colonization (+R), and neither roots nor fauna colonization changed until samples were harvested. The other half of the samples were inspected every two weeks and roots trying to colonize the wood debris were carefully removed (-R). In addition, P was added to the +P treatment samples by sprinkling 3 ml of the PO_4 solution (0.017 g of P) on each sample, while 3 ml of water to treatment without P (-P). These additions were done every two weeks during the 2 years (2016 – 2018) and gave in total four different treatment combinations: +R-P ('natural'), -R-P, -R+P, +R+P. The samples were tied approximately 20 cm from each other directly on the forest floor (Fig. 1).

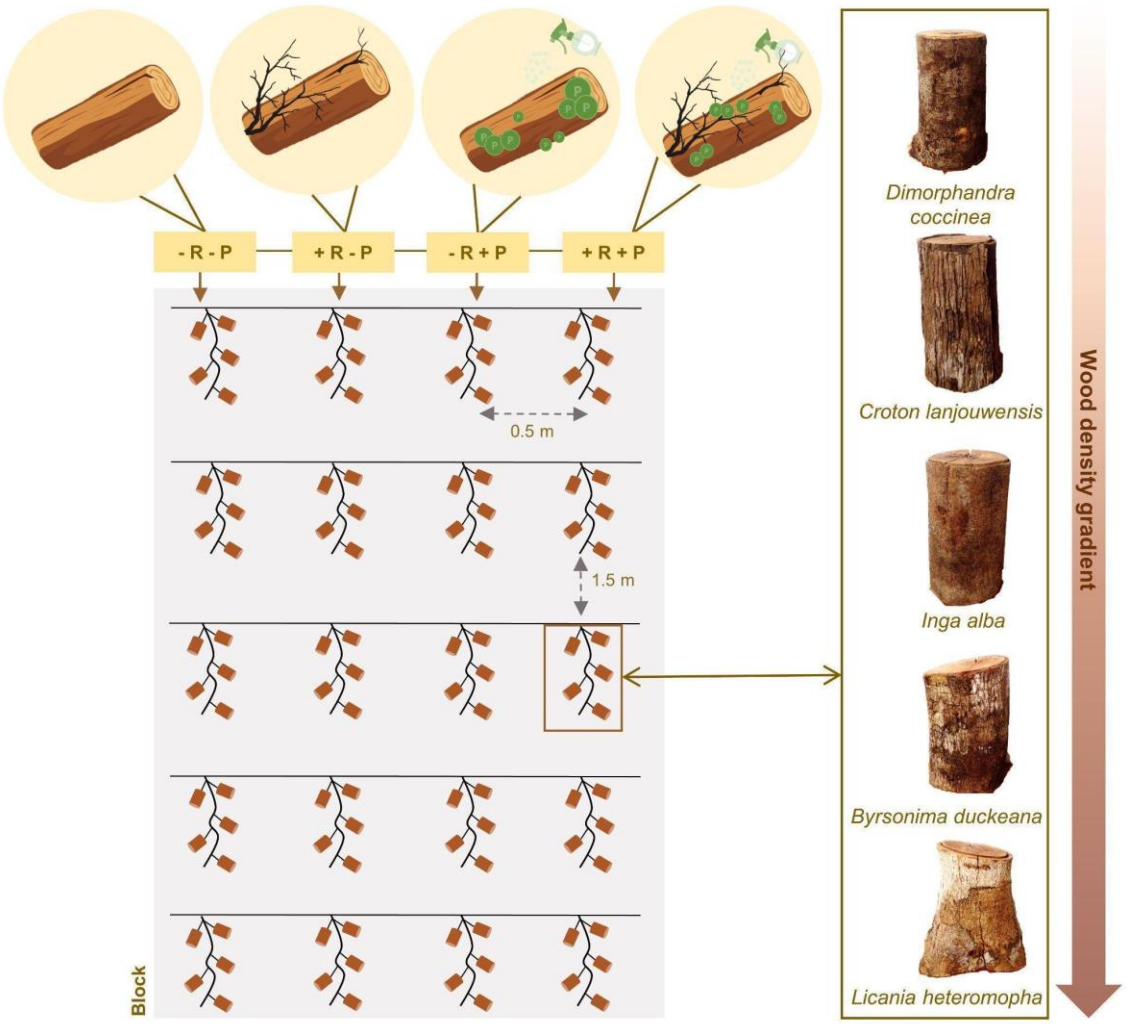

Figure 1. A conceptual overview of the experimental design of one block of the wood decomposition experiment. The decomposition experiment consisted of two blocks approximately 300 meters apart, in each of these two blocks, five sub-blocks were set up, approximately 1.5 meters from each other (at each sampling one sub-block per experiment block was collected). Each sub-block included all treatment combinations in a factorial design: root presence, no P addition (+R-P; 'natural'), without roots, no P addition (-R-P), without roots, plus P addition (-R+P), and with root presence plus P addition (+R+P), for five different species (*Dimorphandra coccinea*; *Croton lanjouwensis*; *Inga alba*; *Byrsonima duckeana*; and *Licania heteromopha)* separated from each other by approximately 20 centimeters.

Sample collection and laboratory analyses

For each collection time, a total of 40 samples (2 blocks, 5 species, 4 treatment combinations) were collected after 3, 6, 12, 18 and 24 months after the onset of the experiment. In the treatments with root presence (+R-P, +R+P), roots were carefully removed from the woody debris, washed, and dried at 65 ° C for 72 h to calculate the total colonizing root biomass.

Woody samples were cleaned with a brush to remove any soil residues and dried at 65 °C for 72 h. To calculate wood decomposition rates, we first calculated the proportion of remaining wood mass (RM) per collection time as the difference of initial wood mass by remaining wood mass (%) as follows:

$$RM=(W_{tn}/W_{t0}) *100 \quad \text{(Eq.1)}$$

where Wt0 is the initial dry weight of wood debris before the start of the experiment, and Wtn is the dry weight at a given collection time (tn). Then we calculated mass loss as the difference between 100% from the initial mass and the remaining wood mass in percentage at tn. In addition, decomposition rate constants (k values; fractional mass loss per year) were calculated using a single pool, exponential decay model (Olson 1963):

$$k=(-\ln f_0(x_t/x_0)/t) \quad \text{(Eq. 2)}$$

where t represents the time (year), Xt is the wood weight mass on time collection, and X0 is the initial wood mass.

Chemical analysis

Samples from time zero (t0, treated with +P or -P) and woody pieces sampled along the decomposition experiment duration were ground to fine powder for chemical analyses. Total nitrogen (N) was determined via Kjeldahl digestion, using sulfuric acid digestion. Concentrations of total phosphorus (P) and cations (potassium (K), calcium (Ca), and magnesium (Mg)) were analyzed after digesting samples with a nitro-perchloric acid solution as described by (Malavolta, Vitti, and Oliveira 1989)). Total P was determined colorimetrically (Murphy and Riley 1962; Olsen and Sommers 1982) and read on a UV spectrophotometer (Model 1240, Shimadzu, Kyoto, Japan). Cation concentrations were

measured by atomic absorption spectrophotometry as described by (Anderson and Ingram 1993). Wood lignin and cellulose contents were determined with the method proposed by (Soest 1963) using an acid-detergent fiber. The proportion of remaining structural compounds and nutrient contents in the wood throughout the wood decomposition experiment was calculated as described in equation 3 (McGroddy, Silver, and De Oliveira 2004):

$$RE=((X_t*W_t)/(X_0*W_0)* 100) \quad \text{(Eq. 3)}$$

where RE are the remaining elements (%), X0 is the initial mean concentration of wood elements, Xt is the concentration of elements at a given collection time (t), W0 is the initial wood dry weight and Wt is wood dry weight at a given collection time (t). Since P concentrations drastically changed when we applied the P treatment, we used the mean of the initial P concentration per species and per treatment (+ P and - P additions), but since no differences between treatment (+ P and - P additions) were detected for N, K, Ca, and Mg, we used the mean by species (Table S1).

Statistical analyses

All analyses were performed in R version 4.0.4 (R Core Team 2022). We tested differences in the initial wood density and chemical composition between the species by one-way ANOVA and a Post-hoc Tukey's test for multiple comparisons. We used Pearson's correlation analysis to identify, if fine root biomass colonization were associated to wood characteristics (initial or during the wood decomposition), such as physical (e.g., density, mean diameter) or chemical (e.g., N or P remaining, %lignin) properties (Fig S2). We applied linear mixed effect models (LMMs) using the lmer function from the lme4 package (Bates et al. 2020), to test the effect of root presence, P addition, and their interactive effects. First, we used a simple model (no interaction) to determine how fine root biomass colonizing wood samples was affected by P additions. For this, we selected only data with root presence (+R), using P treatments (+P and - P) as fixed factors. In addition, we included initial wood density as a covariate to account for species specific differences. Second, we tested the interaction between root presence (+R/-R) and P addition (+P/-P) for wood decomposition and nutrient dynamics. Since no significant interactions were detected, the root presence and P addition were tested in factorial models, that is the effect of root presence (i.e., +R; n=4) compared to all samples

where roots were excluded (i.e., –R; n=4) and the same pattern was used for P addition (i.e., +P; n=4) compared to without P addition (i.e., –P; n=4). This approach allowed us to test for potential interactive effects with species identity (e.g., fixed factors: treatment * species identity). If there was no interaction effect, we used the simple model (treatment + species identity). For all models we tested collection date and blocks as random factors. Finally, we filtered only the data from the final sample collections after 24 months to account for possible cumulative effects of root presence using species as a random factor. The final selected model was then re-run and only the significant effects are reported. Post-hoc tests for multiple comparisons were conducted using Tukey's test by emmeans package (Lenth et al. 2020) when significant interaction was observed. In all statistical analyses, we used $p < 0.05$ as a threshold for statistical significance.

Results

Wood debris characterization

The five species significantly differed in their initial wood density and chemical composition. *Dimorphandra sp.* had the lowest wood density, lignin fraction, lignin: N, lignin: P, but the highest cellulose fraction, and N and P contents, while *Licania sp.* had highest wood density, lignin fraction, lignin: N, lignin: P, but lowest cellulose fraction, and N and P concentration (Table 1; Fig. S1). The woody material of the other three species (*Croton sp*., *Inga sp*., *Byrsonima sp*.,) were more similar to each other (Table 1, Fig. S1). Before placing logs in the forest, half of the samples were treated with a P solution (see Material and Methods), which significantly increased P content by 259% in the woody debris. Consequently, N:P and lignin: P ratios decreased by 66.58%, and 69%, respectively (Table S1).

Root biomass dynamic

As expected, under 'natural conditions' (+R–P) and across the wood decomposition experiment, we observed that the highest root colonization of woody debris occurred in the lowest wood density of *Dimorphandra sp.* (Fig. S2a; R= -0.31, p=0.02; i.e., 3.13 mg roots g^{-1} wood). In contrast, wood debris from *Licania sp.* with the highest wood density, showed the lowest root colonization (1.13 ± SE 0.59 mg roots g^{-1} wood). Across all

species, fine root biomass colonizing wood debris ranged between 0.18 ± 0.13 mg roots g^{-1} wood in the first 3 months of the experiment, reaching a peak of 3.36 ± 1.28 mg roots g^{-1} wood after 24 months (Fig. 2a, without P).

P additions significantly stimulated fine root biomass colonization of wood debris after 6 months with 5.57 ± 3.08 mg roots g^{-1} wood, reaching a peak of 10.65 ± 3.05 mg roots g^{-1} wood after 24 months (Fig. 2a). Across all sample collections, the wood debris receiving P were 320 % more colonized by fine root biomass ($F_{1:87.8}$=8.71, p=0.004; –P; 1.86± 0.48 versus +P: 7.83 ± 1.83 mg roots g^{-1} wood). Moreover, we observed an interaction between P addition and initial wood density, where the impact of P additions on root biomass colonization was stronger for the species with lower to intermediate wood density (Fig. S3; $F_{1:88}$= 3.71, p=0.05).

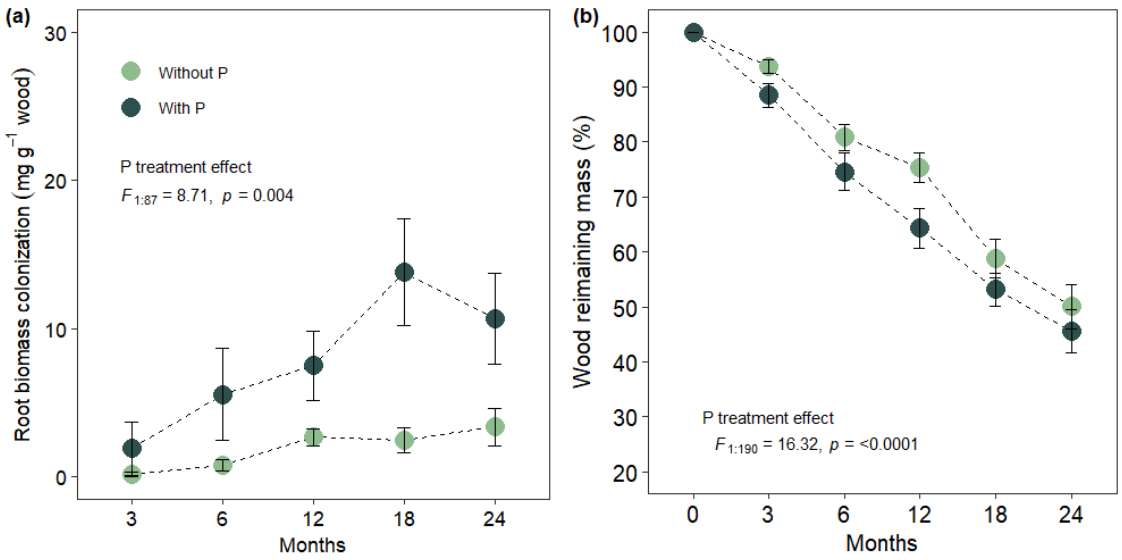

Figure 2. The influence of P additions on (a) fine roots colonization wood debris (mg roots g^{-1} dry wood) over the course of the wood decomposition (means of all species by time) and (b) wood remaining mass (%) showed by mean of the five species and two blocks by collection time (months) resulting in a without/with P addition factorial design. Error bars indicate errors for (a) n=10 and (b) n=20. Statistical results of the P addition effect were obtained by linear mixed models, reported by *p*-value, *F*-value$_{NumDF:\ DenDF}$ (numerator degrees of freedom and denominator degrees of freedom) for the fixed effect term.

Wood decomposition rates

Under 'natural conditions' (+R-P) the decomposition rate varied between 0.56 ± 0.08 yr^{-1} for the low-density *Dimorphandra sp.* and 0.25 ± 0.04 yr^{-1} for high-density *Licania sp.* Fine root presence, independently of P treatment, reduced wood remaining mass by 12.4% after 24 months (Fig. 3a; –R 50.9 ± 3.5 % and + R 44.6 ± 4.2 % of remaining mass; F1:186=6.37, p=0.001), with significant interaction with species identity (root effect*species; $F_{4:186}$=4.51, p=0.0001). We found higher mass loss with root presence for the species with the lowest density *Dimorphandra sp.* in the first six months (three months,–R: 91.6 ± 5.4% and +R: 84.2 ± 8.10%; six months: -R: 82.0 ± 9.2 % and +R: 66.3 ± 12.4%; Fig. 3b) and for the second lowest density *Croton sp.*, mainly after 18 months (18 months, –R: 61.01 ± 7.1% and +R: 40.5 ± 2.8%; 24 months: –R: 56.8 ± 5.2 % and +R: 31.0 ± 4.6%; Fig. 3b).

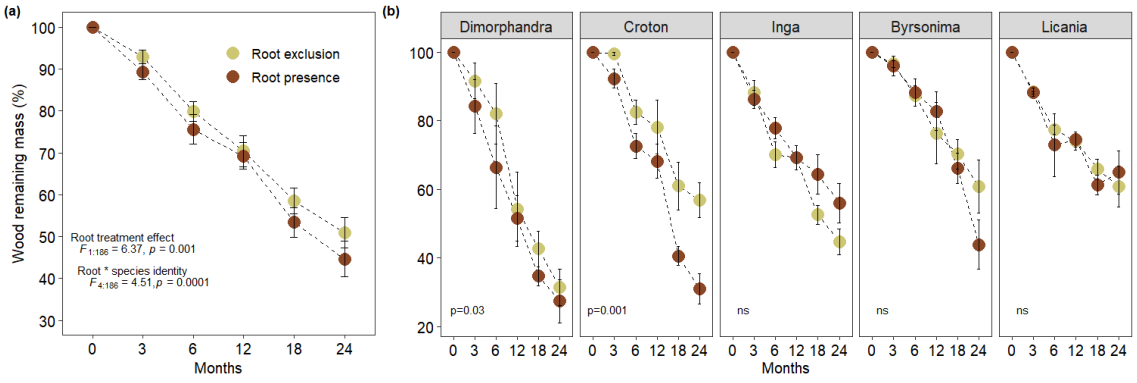

Figure 3. Root presence effect on wood remaining mass (%) over the course of the wood decomposition experiment: a) showed by mean of the five species and two blocks by collection time (months) resulting in a without/with root presence factorial design (n=20), and b) interaction with the specie identity (n=10). Error bars indicate standard errors of the mean. Statistical results of root presence effect and the interaction with specie identity was obtained by linear mixed models (LMM), reported by *p*-value, *F*-value$_{NumDF:\ DenDF}$ (numerator degrees of freedom and denominator degrees of freedom) for the fixed effect term, and the specific effect of root presence by species was tested using Post-hoc Tukey's tests of the LMM reported by *p*-value.

Similarly, P addition induced a reduction in the remaining mass by 9 % after 24 months compared to without P (–P 50.0 ± 4% and + P 45.5 ± 3.9% of remaining mass respectively; $F_{1:190}$=16.32, p<0.0001). Furthermore, P additions also significantly reduced the remaining cellulose fraction in wood debris by 6.54 % (Fig. S4b; $F_{1:108}$=13.8, p=0.003). We did not observe an interaction between fine root colonization and P additions (Table S2), as well as between P addition and plant species identity (p >0.05).

Wood nutrient dynamics over time

We observed a higher temporal variability in the remaining wood nutrient content, mainly when fine roots were present (Fig. 4 and 5). However, we did not detect a significant influence of fine root presence on the relative remaining N, P, K, Ca, and Mg contents (p >0.05; Fig. 4a, b and 5a-c) over time. Only after 24 months, both remaining K (-23.6%) and Ca (-30.9%) contents were significantly reduced with fine root presence ($F_{1:34}$=6.02, p=0.01; $F_{1:34}$=4.74, p=0.03, respectively; Fig. 5a, b).

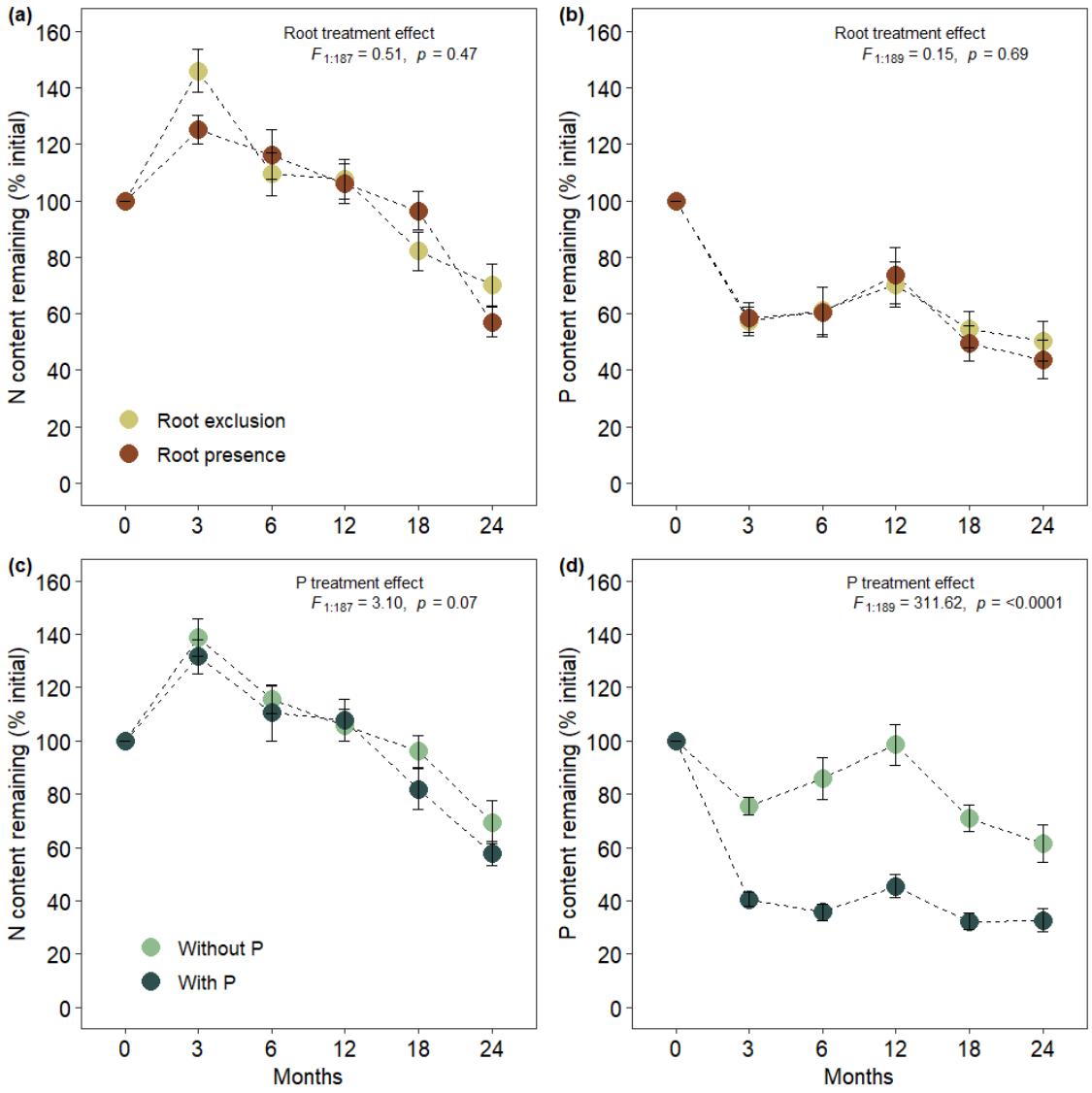

Figure 4. The influence of fine root presence and P addition on the percentage of nitrogen (a, c) and phosphorus (b, d) in the wood remaining mass over the course of the wood decomposition experiment. For each panel and collection time (months) the mean of the five species and two blocks are shown resulting in root presence/exclusion and with/without P addition factorial design (n=20). Error bars indicate standard errors of the mean. Statistical results of root presence and P addition effect were obtained by linear mixed models (LMM), reported by *p*-value, *F*-value$_{NumDF:\ DenDF}$ (numerator degrees of freedom and denominator degrees of freedom) for the respective fixed effect term.

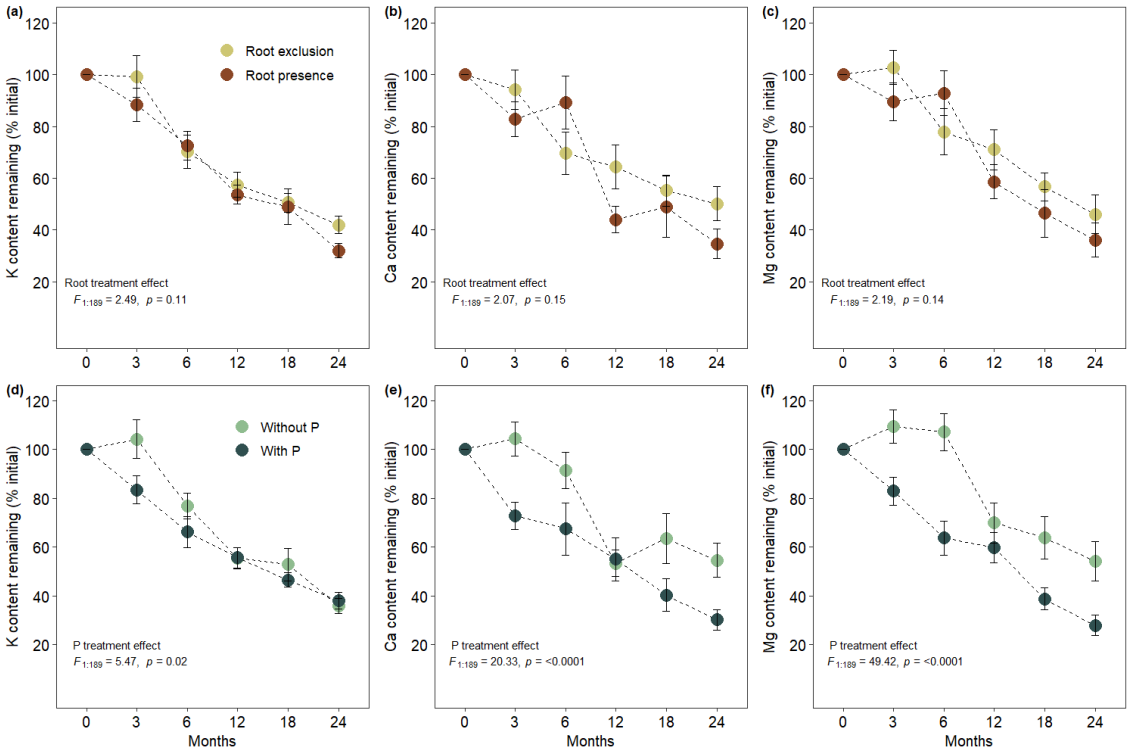

Figure 5. The influence of fine root presence and P addition on the percentage of potassium (a; d), calcium (b, e), and magnesium (c; f) contents remaining in the wood remaining mass over the course of the wood decomposition experiment. For each panel and collection time (months) the means of the five species and two blocks are shown resulting in root presence/exclusion and with/without P addition factorial design (n=20). Error bars indicate standard errors of the mean. Statistical results of root presence and P addition effect were obtained by linear mixed models (LMM), reported by *p*-value, *F*-value$_{NumDF:\ DenDF}$ (numerator degrees of freedom and denominator degrees of freedom) for the respective fixed effect term.

P additions did not influence the remaining wood N content (Fig. 4c), but we observed a significant reduction by 52.5 % of remaining wood P content over all sample collections ($F_{1:189}$=311.62, p <0.0001; Fig. 4d). Over time, P additions also significantly reduced the remaining K ($F_{1:188}$=5.47, p=0.02), Ca ($F_{1:189}$=20.33, p<0.0001), and Mg ($F_{1:189}$=49.42, p<0.0001) content by 10.7, 27.4 and 32.2 % respectively (Fig. 4d-f). The effects of fine roots and P additions were not interactive and independent of species identity.

Discussion

In this study we found a stimulative effect of fine roots on wood debris decomposition, but a possible priming effect dependent on the quality of the wood. In line with our first hypothesis, we observed that fine root colonization and its stimulative effect on wood decay were negatively related to wood density. The P additions increased wood decay, which indicates that P limits microbial decomposition in tropical forest ecosystems. Furthermore, there was a significant interaction in root colonization with wood density despite P additions, with denser wood being less prone to root colonization (Fig. S3). However, the even stronger increase in root colonization with P addition did not amplify wood decay or nutrient loss from decaying wood, possibly because of preferential substrate utilization by decomposers. We found the strongest effect of root biomass on nutrient release only for specific nutrients and for species with lower density (i.e., *Dimorphandra sp*. and *Croton sp.*) and in general during later stages of wood decay. This suggests that roots are taking up nutrients directly from wood decomposition depending on the stoichiometry of substrate and the decomposer community, which in turn appears to be stimulated by root exudates (i.e., priming effect) (Kuzyakov, Friedel, and Stahr 2000).

Structural and chemical properties of wood determine fine root colonization

Fine roots play an important role in effectively acquiring and conserving rare nutrients, especially in infertile highly weathered soils (Herrera et al. 1978; Stark and Jordan 1978; St.John 1983). For instance, plants can grow more fine roots in the uppermost litter layer and take up nutrients from leaf and woody materials before they get leached into the deeper mineral soil layers (Sayer, Tanner, and Cheesman 2006). However, little is known about the mechanisms involved in the release of nutrients stored in wood. In this study, we expected that high density wood would take longer to decompose, and softer wood material would be a more attractive substrate for fine roots. Hence, we hypothesized that the biological and physical activity of fine roots would increase decay rates and nutrient release, however, with differences associated with species-specific. Accordingly, our results confirmed that initial wood density is an important factor for root colonization (Fig. S2a), which was further supported by a strong positive correlation with wood mass loss (Fig. S2b). Furthermore, we observed that the fine root colonization was negatively

correlated with remaining lignin: P ratio, corroborating that changes in structural and chemical properties during wood decay directly affect root colonization (Fig. S2c). Our results demonstrate strong evidence that not only wood density, but also wood nutrient composition is driving the colonization by roots, which is evidenced by the three-fold increase response of fine root colonization to P additions, especially in softer woods.

Fine roots change wood decay and nutrient mobilization

Our findings suggest that fine roots play an active role in wood decomposition, as the decomposition rate was 22.8 % higher with roots (0.43 ± 0.1 yr^{-1}) compared to when roots were constantly removed (0.35 ± 0.07 yr^{-1}). Confirming our first hypothesis, we found that fine roots had a particularly strong effect on softer woods (i.e., *Dimorphandra sp.*, and *Croton sp.*, Fig. 3 a, b). We also observed a reduction in the lignin: P ratio of the remaining wood with increases in root biomass in denser woods, but at a much slower rate than in softer woods (Fig. S2c). That may suggest an overall positive effect of root presence on wood decay, but the effect may take longer than the 24 months of decomposition of this study for denser woods (Fig. S3e).

Fine roots can increase wood fragmentation, increasing the exposure area for microbial, especially fungal colonization, thereby indirectly contributing to wood decay (Hendel and Marxsen 2000). On the other hand, fine root exudates can introduce labile C and N compounds (i.e., sugars, amino acids) in the wood debris rhizosphere and this input of labile C by root exudates could change the community composition of decomposers or directly stimulate microbial activity providing the energy needed to break down complex molecules, inducing an increase in nutrient demand and leading to increased wood decomposition (Kuzyakov, Friedel, and Stahr 2000; Cheng and Kuzyakov 2005). A similar positive effect of fine roots on wood decomposition has been observed in temperate forests, where their presence promoted decay by increasing mycelial colonization (Malik 2019). In contrast, in an experiment simulating fine root exudates by adding labile C and N, (Qiao et al. 2016) observed a negative priming effect in woody debris. This reduction in wood decay in response to more labile C and N availability was attributed because of preferential substrate utilization by microbial decomposers likely switching from lignin to more readily available components, which overall may slow decomposition. In our study, fine roots could provide a greater amount of labile C to the

microbial community, which could increase microbial decomposers demand to mine for inorganic nutrients to maintain the decomposer's stoichiometric balance (Mooshammer et al. 2014). On the other hand, although root colonization increased substantially with P addition (Fig. 2a), we did not observe a significant additive effect between fine root presence and P addition on wood decay as we expected. In that case, the abundant supply of the most limiting nutrient (by P addition) and the labile C by root exudation would reduce or not change wood decomposition, similar to what was observed by (Qiao et al. 2016).

In addition to stimulating litter decomposition rates and mass loss, fine roots at the soil surface are highly efficient in the direct acquisition of nutrients (Herrera et al. 1978; Stark and Jordan 1978; Cuevas and Medina 1988). Previous studies in the Central Amazon showed that the presence of roots in the litter layer significantly increased the uptake of P and cations (K, Ca, and Mg) without increasing litter decomposition (Luizao, Luizao, and Proctor 2007; Martins et al. 2021). For woody debris, we observed a contrasting effect, fine roots increased wood decay, but not the release of P. We found an increase in the release of K by 17% and Ca by 31% when roots were present, but this effect only occurred at the final collection with more advanced stages of wood decay. These differences may be mainly related to the quality/composition of the wood versus leaf litter substrate; leaf litter has more labile C to stimulate the microbial activity and promote a faster nutrient cycling, but also yields more nutrient returns for fine roots in the litter layer, which capture intercepting nutrients before they are immobilized by microorganisms or lost into the soil. In contrast, labile exudations from fine roots could promote wood decomposition and nutrient cycling, but in a smaller and slower proportion. These results suggest that wood is not a primary source for direct nutrient acquisition but rather an alternative long-term resource for the provisioning of limiting nutrients in such a scarce environment as the Amazon forest. In the case of high-density wood, this process could signify years of decay before nutrients can be readily available for plants.

P addition effects on wood decay and nutrient dynamics

Previous studies showed that reduced soil nutrient availability (e.g., N, P, and K) decreased wood decomposition rates in a lowland tropical forest, but the moderate

increases in soil nutrients by natural litter input did not influence long-term decomposition (Gora et al. 2018). Here, we increased P concentrations in woody debris experimentally, which increased the decomposition constant k by 5.5 % (-P: 0.38 ± 0.1 yr^{-1} and +P: 0.40 ± 0.1 yr^{-1}), independent of the initial chemical/nutrient composition of the woods from different species. This response to P additions suggests that the decomposers benefited from increased P availability and increased their activity, and more importantly indicates that they may be limited by P under 'natural conditions'. Higher wood mass loss in response to P additions were also reported by (Chen et al. 2016) in a secondary mixed tropical forest in China. (Sinsabaugh et al. 1992) showed that wood decomposition is a C- limited process (i.e., higher energy demand) and then highly dependent on ligno-cellulose degrading enzymes (i.e., β-1,4-glucosidase, phenol oxidase, peroxidase). Here, we observed an increase in cellulose degradation with P addition (i.e., reduction of remaining wood cellulose content, Fig. S4). This could indicate that P additions enhanced enzymatic activity by the decomposers to break down specific compounds, which would accelerate the decomposition and then supply their stoichiometric imbalance (Mooshammer et al. 2014).

We expected that, with a higher availability of P, the microbial community would increase its immobilization to retain P especially in a nutrient-poor system (Stark and Jordan 1978; Cleveland, Reed, and Townsend 2006) as was also observed by (Chen et al. 2016). However, surprisingly remaining P in wood decreased faster with P additions compared to ambient wood logs (Fig. 4d). Such a strong P release may be related to faster total wood mass loss induced by constant P additions or caused by the fact that +P wood debris had higher concentrations of inorganic P (Pi) already from the beginning of the experiment (Fig. S5d). Moreover, P additions also increased the release of cations (K, Ca, and Mg) but not of N, which highlights the importance of P and other rock-derived limiting nutrients for microbial processes driving decomposition in tropical rainforests.

Conclusion

We found that fine root colonization and the potential alleviation of P limitation stimulated wood decomposition in Amazonian forests. Most strikingly, our findings indicate that the strength of this effect depends on initial substrate quality i.e., the type of wood and stage of decomposition. Our results highlight the importance of a better

understanding of the role of woody debris as a nutrient resource to plants in tropical forests, as well as of monitoring fine-root dynamics above and in the soil surface layers. Further experiments clarifying the mechanistic linkage between C, N, and P cycle processes and the association of fine root presence with microbial decomposer activity for a more robust gradient of species functional characteristics will be required to increase our understanding of the mechanisms regulating nutrient imbalances in tropical forest ecosystems.

Conflict of Interest Statement

All authors declare no conflict of interest.

Funding

We would like to acknowledge the AmazonFACE program of the National Institute of Amazonian Research (INPA), which was funded by the Inter-American Development Bank (IADB) through a technical cooperation agreement with the MCTI Grant BR-T1284, CAPES Grant 23038.007722/2014-77, CAPES-INPA Grant 88881.154644/2017-01, and by FAPEAM Grant 2649/2014. NM was supported by the Coordenação de Aperfeiçoamento de Pessoal de Nível Superior - Brasil (CAPES) - Finance Code 001. LF was supported by the European Union's Horizon 2020 research and innovation program under the Marie Sklodovska-Curie grant agreement No 847693 (REWIRE). F.H. gratefully acknowledges funding from the International Institute for Applied Systems Analysis (IIASA) and the National Member Organizations that support the institute. CAQ acknowledges the grants from Brazilian National Council for Scientific and Technological Development (CNPq) CNPq/LBA 68/2013, CNPq/MCTI/FNDCT no. 18/2021 and his productivity grant.

Acknowledgments

We thank Luciano Castilho for the logistical support in the field, as well Gabriela Carvalho and the Thematic Laboratory for Soils and Plants (Laboratório Temático de

Solos e Plantas—LTSP) at INPA, Manaus, for helping with the lignin and cellulose analyses.

Authors' Contributions

Nathielly P. Martins: Conceptualization (equal); Methodology (equal); Data curation (lead); Formal analysis (lead); Writing – original draft (lead); Writing – review and editing (lead). Oscar J. Valverde-Barrantes: Conceptualization (lead); Methodology (lead); Formal analysis (equal); Writing – original draft (supporting); Writing – review and editing (equal). Lucia Fuchslueger: Conceptualization (lead); Methodology (supporting); Formal analysis (equal); Writing – original draft (supporting); Writing – review and editing (equal). Laynara. F. Lugli: Methodology (supporting); Formal analysis (supporting); Data curation (supporting); Writing – review and editing (equal). Adriana Grandis: Formal analysis (supporting); Data curation (supporting); Writing – review and editing (equal). Florian Hofhansl: Conceptualization (supporting); Formal analysis (supporting); Writing – review and editing (equal). Bruno Takeshi: Project administration: (lead); Funding acquisition (lead) Writing – review and editing (supporting); Data curation (supporting); Gabriela Ushida: Data curation (supporting); Formal analysis (equal); Writing – review and editing (equal).

Carlos A. Quesada: Conceptualization (lead); Funding acquisition (lead); Data curation (supporting); Writing – review and editing (equal).

References

Alves, Eliane G., Kolby Jardine, Julio Tota, Angela Jardine, Ana Maria Yãnez-Serrano, Thomas Karl, Julia Tavares, et al. 2016. "Seasonality of Isoprenoid Emissions from a Primary Rainforest in Central Amazonia." Atmospheric Chemistry and Physics 16 (6): 3903–25. https://doi.org/10.5194/acp-16-3903-2016.

Anderson, J. M, and J. S. I Ingram. 1993. Tropical Soil Biology and Fertility: A Handbook of Methods. 2nd ed. Wallingford: CAB International.

Baraloto, Christopher, C. E.Timothy Paine, Lourens Poorter, Jacques Beauchene, Damien Bonal, Anne Marie Domenach, Bruno Hérault, Sandra Patiño, Jean Christophe Roggy, and Jerome Chave. 2010. "Decoupled Leaf and Stem Economics in Rain Forest Trees." Ecology Letters 13 (11): 1338–47. https://doi.org/10.1111/j.1461-0248.2010.01517.x.

Bates, Douglas, Martin Mächler, Benjamin M. Bolker, and Steven C. Walker. 2020. Lme4: Linear Mixed-Effects Models. R Package Version 1.1.21.

Bauters, Marijn, Oriol Grau, Sebastian Doetterl, Katherine D. Heineman, James W. Dalling, Cecilia M. Prada, Marco Griepentrog, et al. 2022. "Tropical Wood Stores Substantial Amounts of Nutrients, but We Have Limited Understanding Why." Biotropica, no. 2021: 596–606. https://doi.org/10.1111/btp.13069.

Blanchette, Robert A. 2000. "A Review of Microbial Deterioration Found in Archaeological Wood from Different Environments." International Biodeterioration & Biodegradation 46: 189–204. https://doi.org/https://doi.org/10.1016/S0964-8305(00)00077-9.

Bradford, Mark A., Robert J. Warren, Petr Baldrian, Thomas W. Crowther, Daniel S. Maynard, Emily E. Oldfield, William R. Wieder, Stephen A. Wood, and Joshua R. King. 2014. "Climate Fails to Predict Wood Decomposition at Regional Scales." Nature Climate Change 4 (7): 625–30. https://doi.org/10.1038/nclimate2251.

Brienen, R. J.W., O. L. Phillips, T. R. Feldpausch, E. Gloor, T. R. Baker, J. Lloyd, G. Lopez-Gonzalez, et al. 2015. "Long-Term Decline of the Amazon Carbon Sink." Nature 519 (7543): 344–48. https://doi.org/10.1038/nature14283.

Chave, Jerome, David Coomes, Steven Jansen, Simon L. Lewis, Nathan G. Swenson, and Amy E. Zanne. 2009. "Towards a Worldwide Wood Economics Spectrum." Ecology Letters 12 (4): 351–66. https://doi.org/10.1111/j.1461-0248.2009.01285.x.

Chave, Jerome, Helene. Muller-Landau, Timothy R. Baker, Tomás A. Easdale, Hans. ter Steege, and O. Webb, Campbell. 2006. "Regional and Phylogenetic Variation of Wood Density Across 2456 Neotropical Tree Species." Ecological Applications 16 (6): 2356–67. https://doi.org/https://doi.org/10.1890/1051-0761(2006)016[2356:RAPVOW]2.0.CO;2.

Chen, Yao, Emma J. Sayer, Zhian Li, Qifeng Mo, Yingwen Li, Yongzhen Ding, Jun Wang, Xiankai Lu, Jianwu Tang, and Faming Wang. 2016. "Nutrient Limitation of Woody Debris Decomposition in a Tropical Forest: Contrasting Effects of N and P Addition." Functional Ecology 30 (2): 295–304. https://doi.org/10.1111/1365-2435.12471.

Cheng, Weixin. 1999. “Rhizosphere Feedbacks in Elevated CO2.” Tree Physiology 19 (4–5): 313–20. https://doi.org/10.1093/treephys/19.4-5.313.

Cheng, Weuxub, and Yakov Kuzyakov. 2005. “Root Effects on Soil Organic Matter Decomposition.” In Agronomy Monograph No. 48, American Society of Agronomy, Madison, Wisconsin, USA, 119–43. https://doi.org/10.2134/AGRONMONOGR48.C7.

Cleveland, Cory C, Sasha C Reed, and Alan R Townsend. 2006. “Nutrient Regulation of Organic Matter Decomposition in a Tropical Rain Forest.” Ecology 87 (2): 492–503. https://doi.org/10.1890/05-0525.

Cornwell, William K, Johannes H C Cornelissen, Kathryn Amatangelo, Ellen Dorrepaal, Valerie T Eviner, Oscar Godoy, Sarah E Hobbie, et al. 2008. “Plant Species Traits Are the Predominant Control on Litter Decomposition Rates within Biomes Worldwide.” Ecology Letters 11 (10): 1065–71. https://doi.org/10.1111/j.1461-0248.2008.01219.x.

Cuevas, Elvira, and Ernesto Medina. 1988. “Nutrient Dynamics within Amazonian Forests - II. Fine Root Growth, Nutrient Availability and Leaf Litter Decomposition.” Oecologia 76 (2): 222–35. https://doi.org/10.1007/BF00379956.

Feldpausch, T. R., J. Lloyd, S. L. Lewis, R. J.W. Brienen, M. Gloor, A. Monteagudo Mendoza, G. Lopez-Gonzalez, et al. 2012. “Tree Height Integrated into Pantropical Forest Biomass Estimates.” Biogeosciences 9 (8): 3381–3403. https://doi.org/10.5194/bg-9-3381-2012.

Freschet, Grégoire T., Rien Aerts, and Johannes H.C. Cornelissen. 2012. “A Plant Economics Spectrum of Litter Decomposability.” Functional Ecology 26 (1): 56–65. https://doi.org/10.1111/j.1365-2435.2011.01913.x.

Freschet, Grégoire T., Johannes H.C. Cornelissen, Richard S.P. van Logtestijn, and Rien Aerts. 2010. “Evidence of the ‘plant Economics Spectrum’ in a Subarctic Flora.” Journal of Ecology 98 (2): 362–73. https://doi.org/10.1111/j.1365-2745.2009.01615.x.

Gora, Evan M., Emma J. Sayer, Benjamin L. Turner, and Edmund V.J. Tanner. 2018. “Decomposition of Coarse Woody Debris in a Long-Term Litter Manipulation Experiment: A Focus on Nutrient Availability.” Functional Ecology 32 (4): 1128–38. https://doi.org/10.1111/1365-2435.13047.

Grau, Oriol, Josep Peñuelas, Bruno Ferry, Vincent Freycon, Lilian Blanc, Mathilde Desprez, Christopher Baraloto, et al. 2017. “Nutrient-Cycling Mechanisms Other than the Direct Absorption from Soil May Control Forest Structure and Dynamics in Poor Amazonian Soils.” Scientific Reports 7 (February): 1–11. https://doi.org/10.1038/srep45017.

Hättenschwiler, Stephan, Alexei V. Tiunov, and Stefan Scheu. 2005. “Biodiversity and Litter Decomposition in Terrestrial Ecosystems.” Annual Review of Ecology, Evolution, and Systematics 36 (1): 191–218. https://doi.org/10.1146/annurev.ecolsys.36.112904.151932.

Hendel, Björn, and Jürgen Marxsen. 2000. “Extracellular Enzyme Activity Associated with Degradation of Beech Wood in a Central European Stream.” International Review

of Hydrobiology 85 (1): 95–105. https://doi.org/10.1002/(SICI)1522-2632(200003)85:1<95::AID-IROH95>3.0.CO;2-D.

Herrera, R., Tatiana Merida, Nellie Stark, and C.F. Jordan. 1978. "Direct Phosphorus Transfer from Leaf Litter to Roots." Naturwissenschaften 65 (Dl): 208–9. https://doi.org/doi.org/10.1007/BF00450594.

Hu, Zhenhong, Sean T. Michaletz, Daniel J. Johnson, Nate G. McDowell, Zhiqun Huang, Xuhui Zhou, and Chonggang Xu. 2018. "Traits Drive Global Wood Decomposition Rates More than Climate." Global Change Biology 24 (11): 5259–69. https://doi.org/10.1111/gcb.14357.

Hubau, Wannes, Simon L. Lewis, Oliver L. Phillips, Kofi Affum-Baffoe, Hans Beeckman, Aida Cuní-Sanchez, Armandu K. Daniels, et al. 2020. "Asynchronous Carbon Sink Saturation in African and Amazonian Tropical Forests." Nature 579 (7797): 80–87. https://doi.org/10.1038/s41586-020-2035-0.

Kuzyakov, Yakov., J K. Friedel, and K. Stahr. 2000. "Review of Mechanisms and Quantification of Priming Effects." Soil Biology and Biochemistry 32 (11–12): 1485–98. https://doi.org/10.1016/S0038-0717(00)00084-5.

Lenth, Russell, Henrik Singmann, Jonathon Love, Paul Buerkner, and Maxime Herve. 2020. "Package 'Emmeans.'" R Package Version 1.15-15. Vol. 34. https://doi.org/10.1080/00031305.1980.10483031>.License.

Luizao, Regina C C, Flavio J Luizao, and John Proctor. 2007. "Fine Root Growth and Nutrient Release in Decomposing Leaf Litter in Three Contrasting Vegetation Types in Central Amazonia." Plant Ecology, 225–36. https://doi.org/10.1007/s11258-007-9307-8.

Malavolta, E., G C. Vitti, and A S Oliveira. 1989. Avaliação Doestado Nutricional Das Plantas: Princípios e Aplicações. Associação Brasileira Para Pesquisa Da Potassa e Do Fosfato. Piracicaba.

Malik, Rondy J. 2019. "No 'Gadgil Effect': Temperate Tree Roots and Soil Lithology Are Effective Predictors of Wood Decomposition." Forest Pathology 49 (3): 1–9. https://doi.org/10.1111/efp.12506.

Manzoni, Stefano, John A. Trofymow, Robert B. Jackson, and Amilcare Porporato. 2010. "Stoichiometric Controls on Carbon, Nitrogen, and Phosphorus Dynamics in Decomposing Litter." Ecological Monographs 80 (1): 89–106. https://doi.org/10.1890/09-0179.1.

Martins, Nathielly P., Lucia Fuchslueger, Katrin Fleischer, Kelly M. Andersen, Rafael L. Assis, Fabricio B. Baccaro, Plínio B. Camargo, et al. 2021. "Fine Roots Stimulate Nutrient Release during Early Stages of Leaf Litter Decomposition in a Central Amazon Rainforest." Plant and Soil 469: 287–303. https://doi.org/10.1007/s11104-021-05148-9.

McDowell, Nate G., Sean T. Michaletz, Katrina E. Bennett, Kurt C. Solander, Chonggang Xu, Reed M. Maxwell, and Richard S. Middleton. 2018. "Predicting Chronic Climate-Driven Disturbances and Their Mitigation." Trends in Ecology and Evolution 33 (1): 15–27. https://doi.org/10.1016/j.tree.2017.10.002.

McGroddy, Megan E., Whendee L. Silver, and Raimundo Cosme De Oliveira. 2004. "The Effect of Phosphorus Availability on Decomposition Dynamics in a Seasonal Lowland Amazonian Forest." Ecosystems 7 (2): 172–79. https://doi.org/10.1007/s10021-003-0208-y.

Mooshammer, Maria, Wolfgang Wanek, Jorg Schnecker, Birgit Wild, Sonja Leitner, Florian Hofhansl, Andreas Blochl, et al. 2012. "Stoichiometric Controls of Nitrogen and Phosphorus Cycling in Decomposing Beech Leaf Litter." Ecology 93 (4): 770–82. https://doi.org/10.1890/11-0721.1.

Mooshammer, Maria, Wolfgang Wanek, Sophie Zechmeister-Boltenstern, and Andreas Richter. 2014. "Stoichiometric Imbalances between Terrestrial Decomposer Communities and Their Resources: Mechanisms and Implications of Microbial Adaptations to Their Resources." Frontiers in Microbiology 5: 1–10. https://doi.org/10.3389/fmicb.2014.00022.

Murphy, J, and J.P Riley. 1962. "A Modified Single Solution Method for the Determination of Phosphate in Natural Waters." Analytica Chimica Acta 27: 31–36. https://doi.org/10.1016 / s0003-2670 (00) 88444-5.

Nottingham, Andrew T., Lettice C. Hicks, Adan J.Q. Ccahuana, Norma Salinas, Erland Bååth, and Patrick Meir. 2018. "Nutrient Limitations to Bacterial and Fungal Growth during Cellulose Decomposition in Tropical Forest Soils." Biology and Fertility of Soils 54 (2): 219–28. https://doi.org/10.1007/s00374-017-1247-4.

Olsen, S.R., and L.E Sommers. 1982. "Methods of Soil Analysis: Part 2 Chemical and Microbiological Properties." In American Society of Agronomy, Inc., Soil Science Society of America, 403–30. https://doi.org/doi.org/10.2134/agronmonogr9.2.2ed.c24.

Olson, Jerry S. 1963. "Energy Storage and the Balance of Producers and Decomposers in Ecological Systems." Ecology 44 (2): 322–31. https://doi.org/doi.org/10.2307/1932179.

Pan, Yude, Richard a Birdsey, Jingyun Fang, Richard Houghton, Pekka E Kauppi, Werner a Kurz, Oliver L Phillips, et al. 2011. "A Large and Persistent Carbon Sink in the World's Forests." Science 333: 988–93. https://doi.org/10.1126/science.1201609.

Parton, William, Whendee L. Silver, Ingrid C. Burke, Leo Grassens, Mark E. Harmon, William S. Currie, Jennifer Y. King, et al. 2007. "Global-Scale Similarities in Nitrogen Release Patterns during Long-Term Decomposition." Science 315 (5810): 361–64. https://doi.org/10.1126/science.1134853.

Phillips, Oliver L., Luiz Eduardo O. C. Aragão, Simon L Lewis, Joshua B Fisher, Jon Lloyd, Gabriela López-gonzález, Yadvinder Malhi, et al. 2009. "Drought Sensitivity of the Amazon Rainforest" 323: 1344–47. https://doi.org/10.1126/science.1164033.

Powers, Jennifer S., Rebecca A. Montgomery, E. Carol Adair, Francis Q. Brearley, Saara J. Dewalt, Camila T. Castanho, Jerome Chave, et al. 2009. "Decomposition in Tropical Forests: A Pan-Tropical Study of the Effects of Litter Type, Litter Placement and Mesofaunal Exclusion across a Precipitation Gradient." Journal of Ecology 97 (4): 801–11. https://doi.org/10.1111/j.1365-2745.2009.01515.x.

Qiao, Na, Xingliang Xu, Yuehua Hu, Evgenia Blagodatskaya, Yongwen Liu, Douglas Schaefer, and Yakov Kuzyakov. 2016. “Carbon and Nitrogen Additions Induce Distinct Priming Effects along an Organic-Matter Decay Continuum.” Scientific Reports 6: 1–8. https://doi.org/10.1038/srep19865.

Quesada, C. A., J. Lloyd, L. O. Anderson, N. M. Fyllas, M. Schwarz, and C. I. Czimczik. 2011. “Soils of Amazonia with Particular Reference to the RAINFOR Sites.” Biogeosciences 8 (6): 1415–40. https://doi.org/10.5194/bg-8-1415-2011.

Quesada, C. A., J. Lloyd, M. Schwarz, S. Patiño, T. R. Baker, C. Czimczik, N. M. Fyllas, et al. 2010. “Variations in Chemical and Physical Properties of Amazon Forest Soils in Relation to Their Genesis.” Biogeosciences 7 (5): 1515–41. https://doi.org/10.5194/bg-7-1515-2010.

R Core Team. 2022. “A Language and Environment for Statistical Computing.” Vienna, Austria.: R Foundation for Statistical Computing.

Sayer, E. J., E. V J Tanner, and A. W. Cheesman. 2006. “Increased Litterfall Changes Fine Root Distribution in a Moist Tropical Forest.” Plant and Soil 281 (1–2): 5–13. https://doi.org/10.1007/s11104-005-6334-x.

Seidl, Rupert, Dominik Thom, Markus Kautz, Dario Martin-Benito, Mikko Peltoniemi, Giorgio Vacchiano, Jan Wild, et al. 2017. “Forest Disturbances under Climate Change.” Nature Climate Change 7 (6): 395–402. https://doi.org/10.1038/nclimate3303.

Sinsabaugh, R. L., R. K. Antibus, A. E. Linkins, C. A. McClaugherty, L. Rayburn, D. Repert, and T. Weiland. 1992. “Wood Decomposition over a First-Order Watershed: Mass Loss as a Function of Lignocellulase Activity.” Soil Biology and Biochemistry 24 (8): 743–49. https://doi.org/10.1016/0038-0717(92)90248-V.

Soest, P J Van. 1963. “Use of Detergents in the Analysis of Fibrous Feeds. II. A Rapid Method for the Determination of Fiber and Lignin.” Journal of the Association of Official Agricultural Chemists 73 (4): 491–97. https://doi.org/doi.org/10.1093/jaoac/73.4.491.

Stark, Nellie M ., and Carl F. Jordan. 1978. “Nutrient Retention by the Root Mat of an Amazonian.” Ecology 59 (3): 434–37. https://doi.org/doi.org/10.2307/1936571.

St.John, T. V. 1983. “Response of Tree Roots to Decomposing Organic Matter in Two Lowland Amazonian Rain Forests.” Canadian Journal of Forest Research 13 (2): 346–49. https://doi.org/https://doi.org/10.1139/x83-050.

Weedon, James T., William K. Cornwell, Johannes H.C. Cornelissen, Amy E. Zanne, Christian Wirth, and David A. Coomes. 2009. “Global Meta-Analysis of Wood Decomposition Rates: A Role for Trait Variation among Tree Species?” Ecology Letters 12 (1): 45–56. https://doi.org/10.1111/j.1461-0248.2008.01259.x.

Went, F.W, and N. Stark. 1968. “THE BIOLOGICAL AND MECHANICAL ROLE OF SOIL FUNGI.” Botany, no. 1: 497–504. https://doi.org/10.1073 / pnas.60.2.497.

Yang, Shanshan, Lourens Poorter, Eiko E. Kuramae, Ute Sass-Klaassen, Marcio F.A. Leite, Ohana Y.A. Costa, George A. Kowalchuk, et al. 2022. “Stem Traits, Compartments

and Tree Species Affect Fungal Communities on Decaying Wood." Environmental Microbiology 24 (8): 3625–39. https://doi.org/10.1111/1462-2920.15953.

Tables

Table 1 – Characterization of woody debris of the five species used in the wood decomposition experiment. Wood density was characterized for all individual samples that were placed into the forest (values are means ± SE for n=50). The other variables were determined subsamples at t0 (mean ± SE of 3 samples (n=3 by species). The wood density is expressed as g cm^3, lignin, and cellulose are expressed in %, N, P are given in g kg^{-1}, N:P ratio is expressed in molar and Lignin: NP ratio is expressed in %. Different superscript letters indicate significant differences by species (for multiple comparisons by Post hoc Tukey test).

	Dimorphandra coccinea		*Croton lanjouwensis*		*Inga alba*		*Byrsonima duckeana*		*Licania heteromopha*	
Wood density	0.19 ± 0.01	a	0.24 ± 0.01	b	0.26 ± 0.05	b c	0.28 ± 0.04	c	0.38 ± 0.06	d
Lignin	16.39 ± 0.79	a	29.72 ± 4.18	b	27.61 ± 2.49	b	30.69 ± 0.80	b	32.05 ± 1.22	b
Cellulose	64.15 ± 1.39	a	50.02 ± 0.64	c	46.25 ± 0.91	cd	58.98 ± 0.79	b	43.01 ± 1.55	d
N	4.10 ± 0.11	a	2.59 ± 0.21	b c	2.91 ± 0.21	b	2.23 ± 0.07	c	2.60 ± 0.08 b	b c
P	0.30 ± 0.01	a	0.30 ± 0.01	a	0.35 ± 0.01	b	0.28 ± 0.01	a	0.19 ± 0.01	c
N:P	31.88 ± 0.28	a	19.00 ± 2.00	b	18.08 ± 0.47	b	17.48 ± 0.70	b	29.87 ± 0.48	a
Lignin: N	38.51 ± 2.80	a	115.94 ± 0.67	b c	96.53 ± 15.89	b	137.65 ± 8.10	c	123.07 ± 4.75	b c
Lignin: P	547.58 ± 21.81	a	995.92 ± 176.49	b	783.90 ± 111.31	a b	1083.52 ± 33.16	b	1659.05 ± 45.59	c

Supplementary information

Fine root presence and increased phosphorus availability stimulate wood decay in a Central Amazonian rainforest

Table S1 – Initial woody debris characterization in the control (i.e., water immersion) and P addition. The data considers all species in time 0, for control we have a mean ± SE of 10 samples (n=10) and for P addition we have a mean ± SE of 8 samples (n=8). Different superscript letters between the column indicate significant differences by species (for multiple comparisons by Post hoc Tukey test).

	Control		P addition	
Lignin (%)	27.79 ± 2.89	a	29.64 ± 2.90	a
Cellulose (%)	52.79 ± 3.89	a	49.10 ± 3.73	a
N (g kg ^{1})	2.88 ± 0.26	a	3.38 ± 0.31	a
P (g kg ^{1})	0.27 ± 0.02	a	0.97 ± 0.10	b
N:P ¯molar	23.58 ± 2.48	a	7.88 ± 0.46	b
Lignin: N (%)	104.00 ± 16.28	a	91.78 ± 11.37	a
Lignin: P (%)	1066.69 ± 172.65	a	330.62 ± 52.59	b

Table S2 – Test interaction effect between root presence and P addition on wood debris remaining mass, structural compounds, and nutrient dynamics dynamic over the wood decomposition experiment. The statistical parameters are obtained from a linear mixed model (LMM) that considers the entire dataset controlling the "time" as a random factor.

Parameter	*LMM (response variable ~ P addition * root presence (1|time)*		
	P addition effect	Root presence effect	P addition * Root presence
Remaining mass (%)	**$F_{1:192}$= 12.39, *p*=0.0005**	**$F_{1:192}$= 4.74, *p*=0.03**	$F_{1:192}$= 1.00, *p*=0.31
Cellulose (%)	$F_{1:205}$= 1.57, *p*= 0.21	$F_{1:205}$= 0.81, *p*=0.36	$F_{1:205}$= 0.00, *p*=0.96
Lignin (%)	$F_{1:204}$= 0.11, *p*= 0.73	$F_{1:204}$= 0.50, *p*=0.47	$F_{1:204}$= 0.01, *p*=0.90
N (g kg ^{1})	$F_{1:190}$= 0.11, *p*= 0.74	$F_{1:190}$= 2.22, *p*=0.13	$F_{1:190}$= 0.00, *p*=0.92
P (g kg ^{1})	**$F_{1:191}$= 119.18, *p*= <0.0001**	$F_{1:191}$= 0.27, *p*=0.59	$F_{1:191}$= 0.00, *p*=0.96
K (g kg ^{1})	$F_{1:191}$= 0.07, *p*= 0.78	$F_{1:191}$= 0.35, *p*=0.55	$F_{1:191}$= 0.00, *p*=0.98
Ca (g kg ^{1})	**$F_{1:191}$= 6.87, *p*= 0.009**	$F_{1:191}$= 0.28, *p*=0.59	$F_{1:191}$= 0.00, *p*=0.96
Mg (g kg ^{1})	**$F_{1:191}$= 10.58, *p*= 0.001**	$F_{1:191}$= 0.37, *p*=0.53	$F_{1:191}$= 0.23, *p*=0.63
Remaining Cellulose	**$F_{1:114}$= 11.93, *p*=0.0007**	$F_{1:114}$= 0.08, *p*=0.77	$F_{1:114}$= 0.00, *p*=0.93
Remaining Lignin	$F_{1:114}$= 1.13, *p*=0.28	$F_{1:114}$= 1.17, *p*=0.27	$F_{1:114}$= 0.02, *p*=0.87
Remaining N	$F_{1:191}$= 2.79, *p*= 0.09	$F_{1:191}$= 0.43, *p*=0.51	$F_{1:191}$= 0.11, *p*=0.73
Remaining P	**$F_{1:191}$= 161.13, *p*= <0.0001**	$F_{1:191}$= 0.26, *p*=0.61	$F_{1:191}$= 0.07, *p*=0.79
Remaining K	**$F_{1:191}$= 4.85, *p*= 0.02**	$F_{1:191}$= 2.29, *p*=0.13	$F_{1:191}$= 0.00, *p*=0.97
Remaining Ca	**$F_{1:191}$= 19.27, *p*= <0.0001**	$F_{1:191}$= 2.22, *p*=0.13	$F_{1:191}$= 0.30, *p*=0.58
Remaining Mg	**$F_{1:191}$= 39.62 *p*= <0.0001**	$F_{1:191}$= 2.25, *p*=0.13	$F_{1:191}$= 0.82, *p*=0.36

* Statistical results of root presence, P addition and the interaction effect were obtained by an analysis of variance of the LMM using Satterthwaite's method, reported by *p*-value, *F*-value$_{NumDF: DenDF}$ (numerator degrees of freedom and denominator degrees of freedom) for the respective fixed effect term.

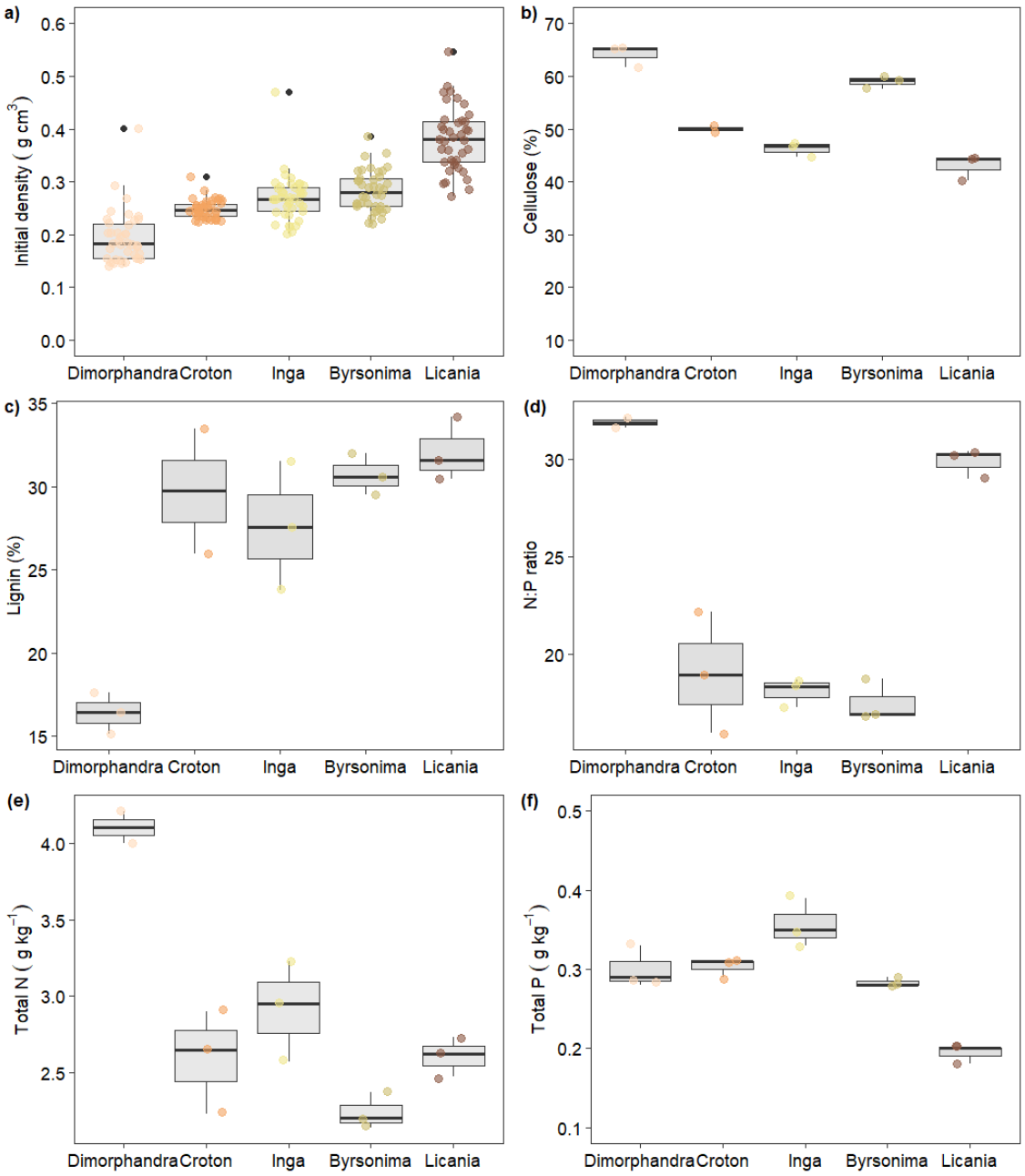

Figure S1. Characterization of woody debris of the five species at time 0 (before going to the field). Initial wood density was determined for each sample that was placed in the forest thus the values are means ± SE for n=50. For the other variables, b) cellulose, c) lignin, d) N: P ratio, e) total N concentration, and f) total P concentration, we showed the mean ± SE of 3 samples by species (n=3).

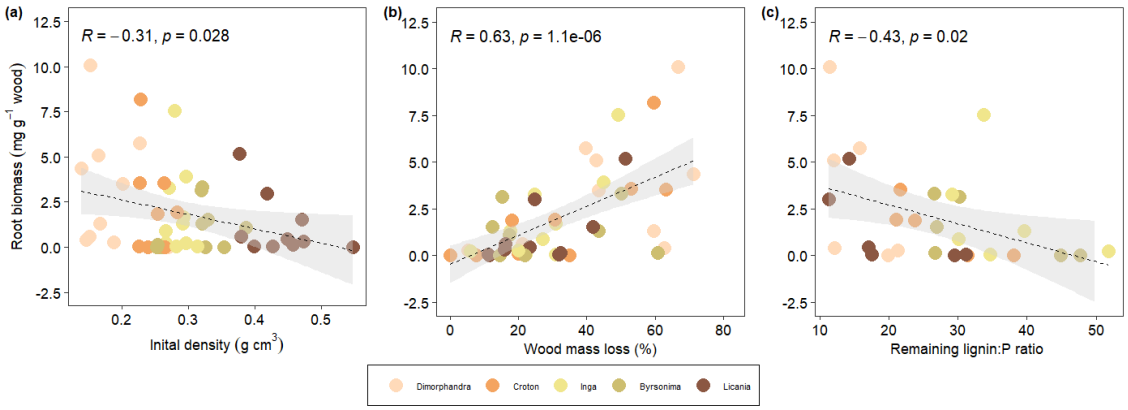

Figure S2. Correlations between fine root colonization of wood debris, with a) wood debris initial density, b) wood mass loss, and c) the ratio of percentual remaining content of lignin and P. For density we used the initial density of the wood debris, and for mass loss and remaining lignin: P ratio content we have a temporal process along of wood decay experiment. The colors represent the different species and the data presented correspond to all collection times under natural conditions data (+R- P), resulting in n=10 by species.

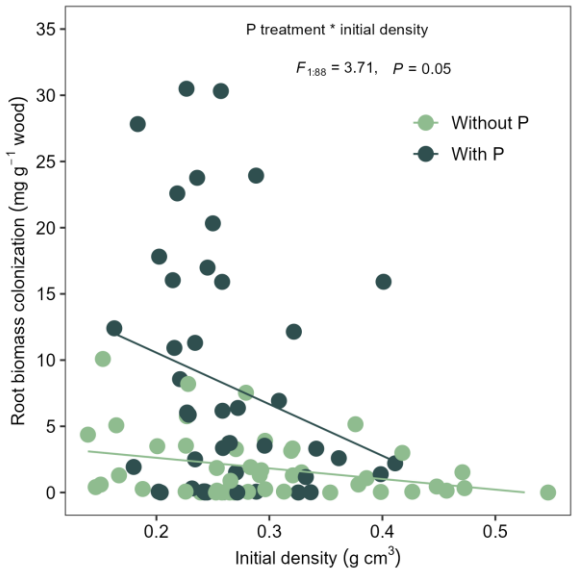

Figure S3. Influence of initial wood density on P addition effect of root colonization. Statistical results represent the interaction effect of P addition treatment and initial wood density obtained by linear mixed models (LMM), reported by *p*-value, F-value$_{NumDF:\ DenDF}$ (numerator degrees of freedom and denominator degrees of freedom).

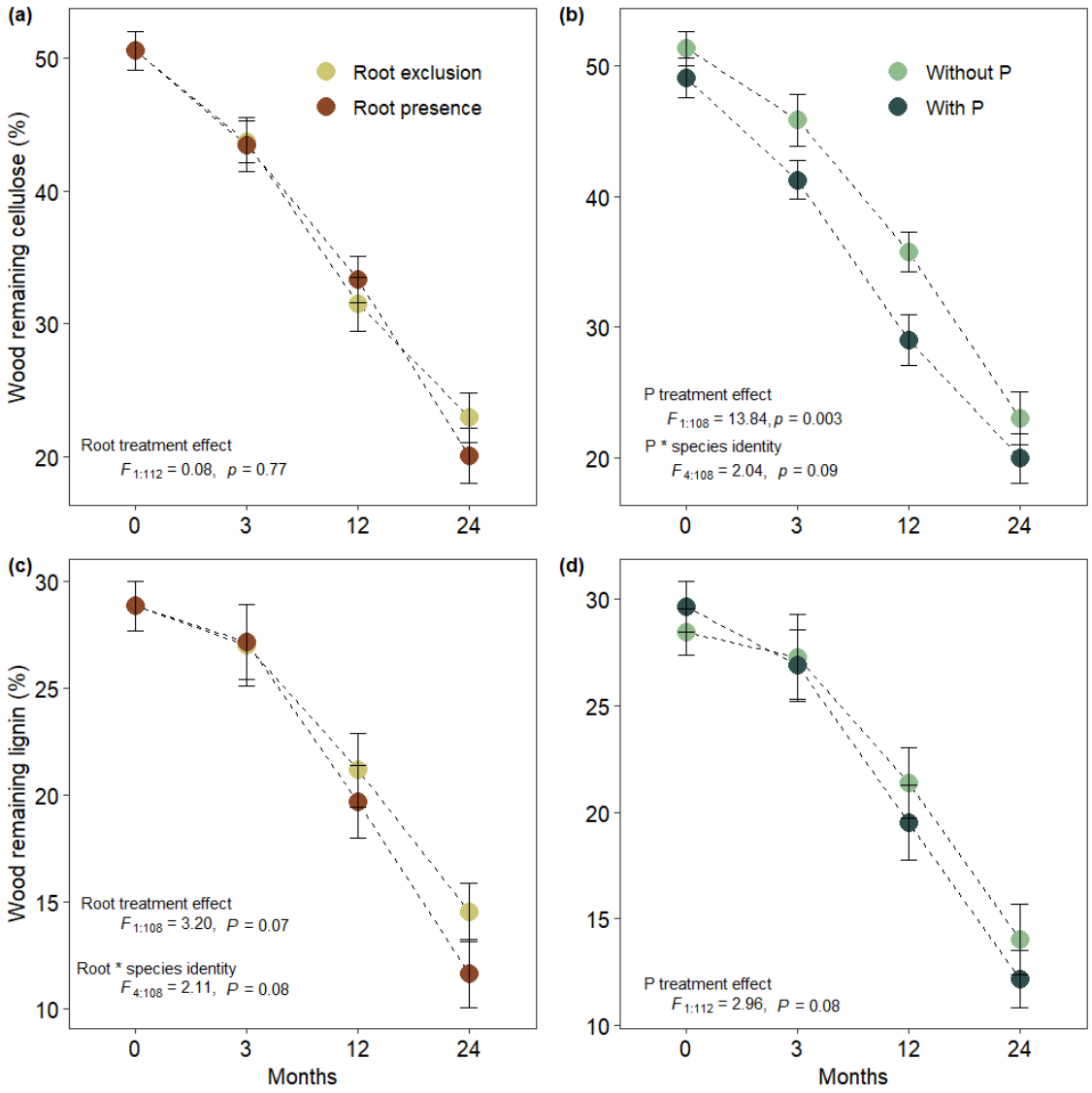

Figure S4. The effect of root presence and P addition on wood remaining structural compounds over the course of the wood decomposition experiment, (a-b) cellulose, and (c-d) lignin. For each panel and collection time (months) the mean of the five species and two blocks are shown resulting in root presence/exclusion and with/without P addition factorial design (n=20). Error bars indicate standard errors of the mean. Statistical results of root presence, P addition effect and their interaction were obtained by linear mixed models (LMM), reported by *p*-value, *F*-value$_{NumDF:\ DenDF}$ (numerator degrees of freedom and denominator degrees of freedom) for the respective fixed effect term.

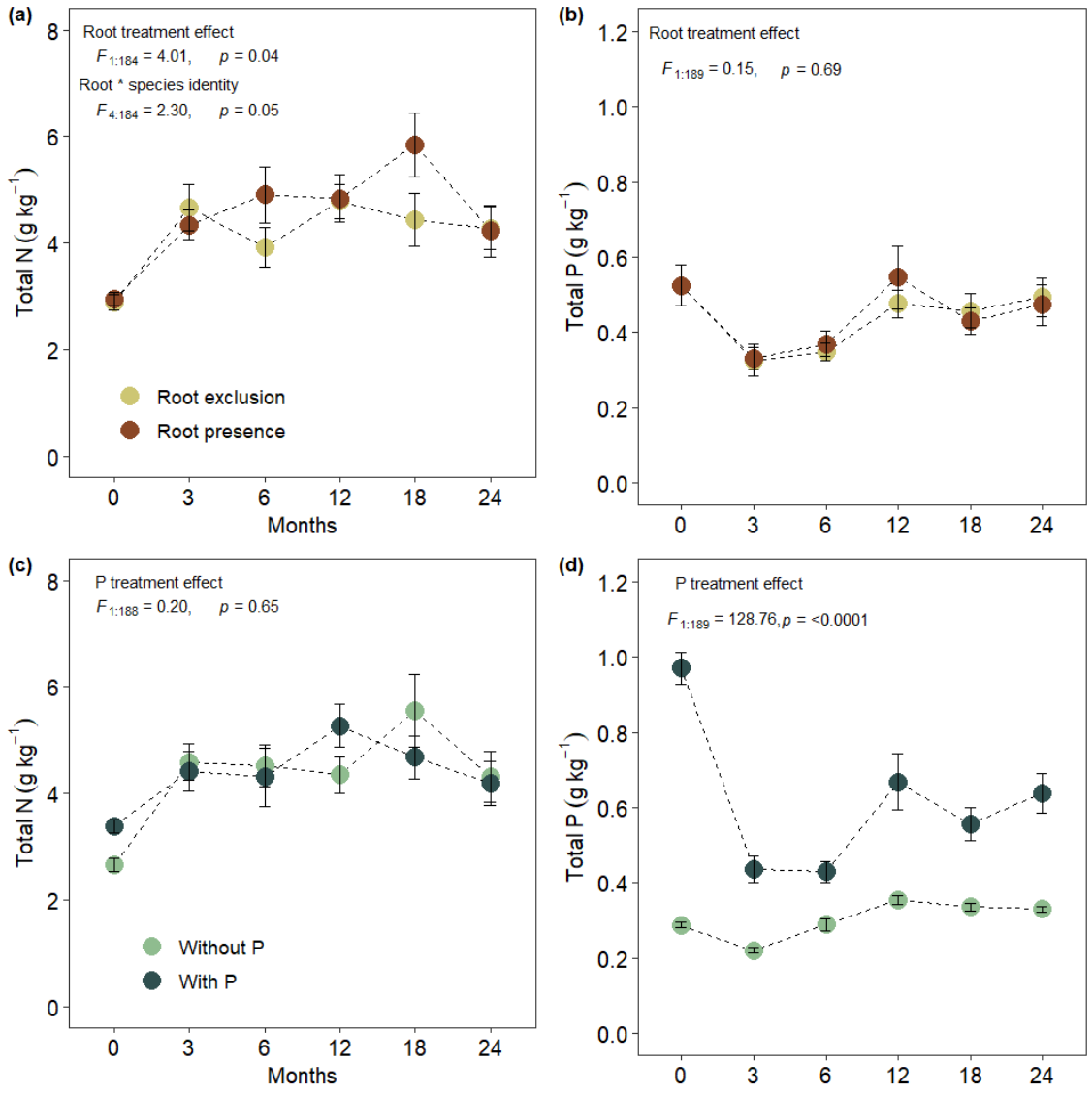

Figure S5. The effect of root presence and P addition on total wood nitrogen (N) and phosphorus (P) concentration (a-c and b-d, respectively) over the course of the wood decomposition experiment. For each panel and collection time (months) the mean of the five species and two blocks are shown resulting in root presence/exclusion and with/without P addition factorial design (n=20). Error bars indicate standard errors of the mean. Statistical results of root presence, P addition effect and their interaction were obtained by linear mixed models (LMM), reported by *p*-value, F-value$_{NumDF:\ DenDF}$ (numerator degrees of freedom and denominator degrees of freedom) for the respective fixed effect term.

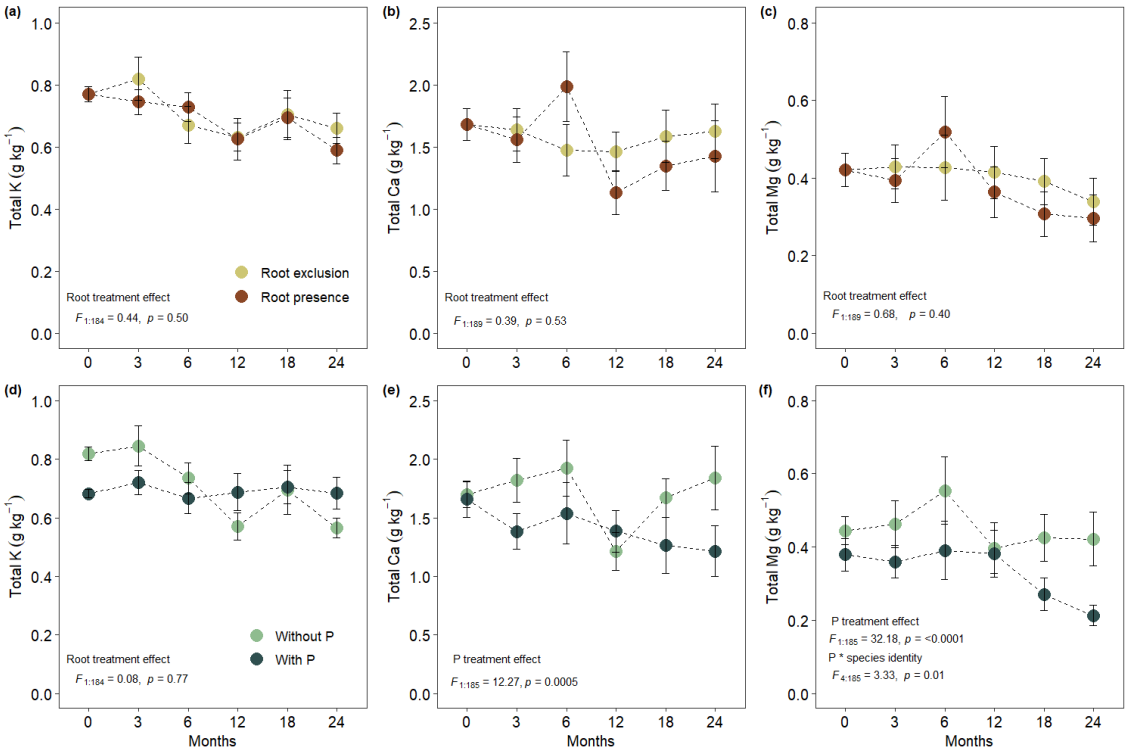

Figure S6. The effect of root presence and P addition on total wood potassium (K), calcium (Ca), and magnesium (Mg) concentration (a-d, b-e, and c-f, respectively) over the course of the wood decomposition experiment. For each panel and collection time (months) the mean of the five species and two blocks are shown resulting in root presence/exclusion and with/without P addition factorial design (n=20). Error bars indicate standard errors of the mean. Error bars indicate standard errors of the mean. Statistical results of root presence, P addition effect and their interaction were obtained by linear mixed models (LMM), reported by *p*-value, *F*-value$_{NumDF:\ DenDF}$ (numerator degrees of freedom and denominator degrees of freedom) for the respective fixed effect term.

Capítulo 2

Elevated atmospheric carbon dioxide concentration changes phosphorus acquisition strategies in the Amazonian understory

Nathielly P. Martins[1], Lucia Fuchslueger, Laynara F. Lugli, Oscar J. Valverde-Barrantes, Richard J. Norby, Iain P. Hartley, Izabela Aleixo, Fabricio B. Baccaro, Barbara Brum, Raffaello Di Ponzio, Amanda Damasceno, Vanessa R. Ferrer, Katrin Fleischer, Sabrina Garcia, Alacimar Guedes, Florian Hofhansl, David Lapola, Juliane G. Menezes; Anna C. M. Moraes, Ana Caroline Miron, Leonardo Ramos de Oliveira ,Cilene Palheta, Iokanam S. Pereira, Maria Pires, Gyovanni Ribeiro, Jessica S. Rosa, Anja Rammig, Flavia D. Santana, Yago R. Santos, Lara Siebert Silva, Bruno Takeshi, Gabriela Ushida and Carlos A. Quesada

Status of manuscript, to be submitted: Nature

Picture: João Rosa – AmazonFACE

Elevated atmospheric carbon dioxide concentration changes phosphorus acquisition strategies in the Amazonian understory

Nathielly P. Martins, Lucia Fuchslueger, Laynara F. Lugli, Oscar J. Valverde-Barrantes, Richard J. Norby, Iain P. Hartley, Izabela Aleixo, Fabricio B. Baccaro, Barbara Brum, Raffaello Di Ponzio, Amanda Damasceno, Vanessa R. Ferrer, Katrin Fleischer, Sabrina Garcia, Alacimar Guedes, Florian Hofhansl, David Lapola, Juliane G. Menezes; Anna C. M. Moraes, Ana Caroline Miron, Leonardo Ramos de Oliveira ,Cilene Palheta, Iokanam S. Pereira, Maria Pires, Gyovanni Ribeiro, Jessica S. Rosa, Anja Rammig, Flavia D. Santana, Yago R. Santos, Lara Siebert Silva, Bruno Takeshi, Gabriela Ushida and Carlos A. Quesada

***Authors for correspondence:**

Nathielly P. Martins: nathiellymartins9@gmail.com

Lucia Fuchslueger: lucia.fuchslueger@univie.ac.at

Abstract

One of the biggest uncertainties in ecosystem model projections is the response of the Amazon forest's primary productivity to human-induced atmospheric carbon dioxide enrichment[1]. Approximately 60% of the Amazon rainforest grows on highly weathered soils with low levels of rock-derived nutrients[2,3]. In such nutrient-limited ecosystems, the functional capacity and adaptability of plant communities to facilitate efficient nutrient acquisition are decisive for determining a potential CO_2 fertilization effect and ultimately for the role of the Amazon rainforest as an atmospheric carbon sink or source. To address this uncertainty, we designed an *in situ* Open Top Chamber (OTC) experiment, elevating CO_2 (eCO_2) by 250 ppm, in the understory of a highly phosphorus-limited mature Amazonian tropical forest in Manaus, Brazil. We here show for the first time the plasticity of different nutrient acquisition strategies of Amazonian rainforest understory plants under eCO_2 to possibly increase the nutrient uptake. Plants intensified the foraging in the litter layer, adopting a "do-it-yourself" strategy increasing under eCO_2 both root length and area by 328% and 217%, respectively. In contrast, roots in the soil adopted an "outsourcing" strategy increasing the arbuscular mycorrhizal colonization (AM) by 117%. Furthermore, we show that eCO_2 enhances direct biochemical phosphorus (P) mineralization in the litter layer by capturing 11% more P, without changing litter mass loss. At the same time, the soil organic P pool decreased by 77% under eCO_2. This ability of understory plants to adapt their P acquisition strategies in response to eCO_2 by tackling different sources within the litter-soil continuum to maximize nutrient acquisition is a strong indicator for a further stand level biomass growth, supporting the resilience of the Amazonian rainforest to climate change, and thus influencing the global carbon balance.

Main text

Tropical forests are amongst the most diverse ecosystems on the planet[4], with an overwhelming social and economic value[5]. They contain approximately half of the earth's C stored in terrestrial vegetation[6]. Because of their high productivity, they play a key role as terrestrial C sinks and have a high potential to mitigate the effects of climate change. Earth system models project an increased C sink of tropical vegetation for the next decades[7] due to the expected benefits of elevated CO_2 over photosynthesis, referred to as the CO_2 fertilization effect[8]. However, in situ, forest inventories across Amazonia, Africa, and Asia show a progressive decline in the C sink of mature forests which is attributed to C losses from increased tree mortality[9,10]. Moreover, on highly weathered soils P could limit plant's net primary productivity (NPP)[11], and this has been recently confirmed by experimental evidence for Central Amazonia[12]. In fact, ecosystem model simulations including P cycle feedbacks demonstrated a much lower capacity of the Amazon Forest to respond to eCO_2[1], indicating that divergences between field observations and model projections may be related to an incomplete representation of nutrient cycle feedbacks in ecosystem models[13]. Thus, understanding the role of P in controlling Amazon Forest responses to eCO_2, is essential to make accurate predictions of a future carbon sink and to understand the sensitivity of Amazonia to global change.

In the highly weathered soils of the Amazon basin, most of the P is adsorbed to iron and aluminum oxides or found in organic forms[3,11]. These P forms are difficult to access and are influenced by factors such as plant demand, accessibility, and distribution of these organic and inorganic P pools, often requiring specific multiple acquisition strategies to be obtained by plants[14,15]. For instance, large root mats growing inside the leaf litter stimulate direct biochemical P acquisition (i.e. through phosphatase enzymes) and have been pointed out as a common strategy response to low nutrient supply in many forests across Amazonia[16–19]. Furthermore, most species have a certain range of plasticity that allows them to adjust their nutrient acquisition strategies, generating a variety of adaptative trait combinations[20]. For example, to maximize the resource acquisition while minimizing the cost of root construction and maintenance, plants may adjust their morphological strategy[21], such as investing in finer roots, and exploring a larger soil volume (i.e., increasing the specific root length - SRL), while C allocation remains unchanged. In a multidimensional framework of fine root economic space, this trait combination was described as a "do-it-yourself" strategy[22,23]. In contrast, plants may invest in shorter and thicker roots, while "outsourcing" nutrient acquisition to mycorrhizal fungal or other symbionts[23]. Moreover, plants may also adjust the fine root physiological traits by regulating phosphatase exudation to hydrolyze organic P (P_o), and acquire organically bound P without the need to decompose organic material[24,25]; roots can also invest in exudation of organic acids to increase P uptake by desorption of inorganic P (P_i) or increase microbial P_o mineralization[14,26].

Over the last decades, one of the biggest uncertainties and most important questions in climate science is whether the CO_2 fertilization effect will occur in tropical forests, and if it will be sustained or limited by nutrient availability[27]. In Free Air Carbon Enrichment (FACE) experiments in temperate forests, plants increased the C allocation mainly to root productivity[28] and into labile C exudation to stimulate SOM decomposition by the soil microbial community (i.e., nutrient mining and priming effect)[29] to alleviate N limitation. In contrast to N-limited temperate forests, P-limited Amazon forests may demand a different set of acquisition strategies to maintain nutrient supply, or even increase nutrient uptake to satisfy a potential CO_2 fertilization effect. In fact, given that the P cycle is strongly dependent on biological processes, eCO_2 availability may possibly change or intensify some of the P acquisition strategies to maintain, or even increase, nutrient supply[30]. However, only a few studies have been investigating eCO_2 effects on plants growing in low-P soils, and mostly in greenhouse experiments with seedlings[31]. The first FACE experiment in a mature, P-limited Eucalyptus forest (EucFACE) demonstrated that eCO_2 significantly increased the photosynthetic capacity, but without any changes in allocation of C to above-ground growth[32,33], but with an initial increase in soil N and P mineralization rates, likely triggered by short-term increased C allocation belowground[34,35]. In addition, after five years under eCO_2, the influence of roots on the rhizosphere (root effect) was found to increase nutrient availability in deeper soils[36]. It is however nearly impossible to generalize results from monodominant, temperate or mediterranean forests to P-limited, hyperdiverse forests in the Amazon. Here, diverse tree communities likely possess diverse P acquisition strategies, varying greatly across natural soil P gradients[14]. There still exists a particular knowledge gap on how these diverse plant communities respond to eCO_2 belowground and to which extent they can adapt their root systems and rhizosphere to explore different P sources and interact with microbial communities. Such information can greatly contribute to reducing the uncertainties about the response of Amazonia to global change and improve our predictive capacity in future climate scenarios of the Amazon and globally.

We established an eCO_2 experiment in the understory of an undisturbed, mature, P-limited lowland tropical forest, using Open-Top Chambers (OTC). The experiment was located in the study site of the AmazonFACE program[37] (https://amazonface.unicamp.br/), approximately 70 km north of Manaus, Brazil. In total, eight chambers (with 2.4 m of diameter and a 3 m of height) were set up in pairs resulting in four controls with ambient CO_2 (aCO_2) and four with CO_2 increased by 250 ppm (eCO_2) relative to the respective aCO_2 chamber (see methods section). We investigated fine root biomass, productivity, morphological parameters, and phosphatase activity in the litter layer and down to 15 cm of soil. Additionally, we measured litter nutrient dynamics and decomposition, soil microbial activity (i.e., microbial CNP biomass and enzyme activity), and soil nutrient dynamics.

Under eCO_2 the understory plant communities changed their root systems intensifying foraging in the litter layer by adjusting root morphology to predominantly thinner, and longer roots. This resulted in a significant decrease in observed root diameter (Fig. 1a; aCO_2: – 0.15 ± 0.09 mm versus eCO_2: –0.31 ± 0.07 mm; Z= –1.92, p= 0.04) accompanied by a three-fold increase in specific root length (SRL) by 328 % (Fig. 1a; aCO_2: 2.40 ± 1.65 cm mg^{-1} versus eCO_2:10.28 ± 1.76 cm mg^{-1}; Z=4.2, p= <0.001), and in specific root area (SRA) by 217 % (Fig. 1a; aCO_2: 0.29 ± 0.25 cm^2 mg^{-1} versus eCO_2: 0.92 ± 0.28 cm^2 mg^{-1}; Z=2.39, p=0.01) without changing their net root productivity. Although root phosphatase activity rates did not change per root mass, phosphatase in the litter layer per root length or area increased, highlighting the litter layer as a crucial source of P for plants. We found a significant increase in phosphatase activity by 127 % when upscaling to total root length (Fig 1a; aCO_2: 63.61 ± 18.86 nmol cm root h^{-1} versus eCO_2: 144.85 ± 51.05 nmol cm root h^{-1}; Z=2.02, p=0.04) and a strong tendency of increase per total root area (Fig 1a; aCO_2: 66.68 ± 20.40 nmol cm^2 h^{-1} versus eCO_2: 118.95 ± 33.77 nmol cm h^{-1}; Z=1.68, p=0.09). This increased investment in longer and finer roots promotes substrate surface interactions and increases the litter volume the roots can intercept, suggesting that in the litter layer, it is more cost-efficient for plants to follow a "do-it-yourself" strategy[23], that is, not relying on external factors such as mycorrhizas or microbial priming to increase nutrient acquisition. Furthermore, those changes in P acquisition under eCO_2 resulted in a significant reduction in leaf litter P concentrations by 11 % (Fig 1b; aCO_2: 0.38 ± 0.02 mg kg^{-1} versus eCO_2: 0.34 ± 0.02 mg kg^1; Z= –2.09, p=0.03) without changing litter mass loss during litter decomposition (Fig 1b; aCO_2: 53.75 ± 5.84 % versus eCO_2: 51.67 ± 7.75 %; Z= –0.34, p=0.72). Therefore, the increase in root phosphatase activity in the litter layer observed under eCO_2 underpins that roots clearly invest in tackling P stored in organic material as already previously reported[19], and further point out the importance of biochemical P mineralization in scenarios of eCO_2 in the Amazonian Forest.

Strikingly, in the upper 15 cm of soil root and nutrient acquisition, strategies showed a completely opposite response to eCO_2. Soil root biomass stocks did not change under eCO_2 (Fig. 1a; aCO_2: –0.99 ± 0.72 mg cm^2 versus eCO_2: –0.52 ± 0.43 mg cm^2; Z=0.50, p=0.61), but fine root productivity in the soil decreased by 81% (Fig. 1a; aCO_2: 0.042 ± 0.02 mg cm^2 day^{-1} versus eCO_2: 0.007 ± 0.005 mg cm^2 day^{-1}; Z= – 1.79, p=0.07). In addition, roots growing in the soil became lighter (i.e., decrease on root tissue density - RTD) (Fig 1a; aCO_2: 0.44 ± 0.17 mg cm^3 versus eCO_2 0.23.4 ± 0.06 mg cm^3; Z=-1.82, p=0.06) and shorter. Here, it is unclear if the root longevity in the soil decreased and turnover increased, which would be expected since roots became lighter [38]. Furthermore, under eCO_2 soil fine roots significantly decrease the SRL and SRA (i.e., roots are shorter and have lower area) by 657 and 350 % respectively (Fig. 1a; aCO_2: 1.45 ± 3.91 cm mg^{-1} versus eCO_2: –8.00 ± 5.17 cm mg^{-1}; Z=2.10, p=0.03 and aCO_2: – 0.75 ± 0.44 cm^2 mg^{-1} versus eCO_2: – 3.39 ± 1.2 cm^2 mg^{-1}; Z= – 2.36, p=0.01 respectively), while they significantly increase

mycorrhizal colonization by 117 % (Fig. 1a; aCO_2: 25.75 ± 9.96 % versus eCO_2: 56.00 ± 10.61 %; Z=3.13, p=0.001). These combined eCO_2 induced changes of C allocation to rather light and short roots suggest that within the soil matrix, it is more efficient and C-cost efficient for plants to "outsource" nutrient uptake by fostering their accessibility by mycorrhizal symbionts[23]. This mutualistic partnership with mycorrhizae is a rather conservative strategy reducing C investments in root tissue but favoring soil exploration and P mobilization through extensive mycorrhizal hyphae, which presumably becomes cheaper for the plants under eCO_2. Although not a focus of this study, photosynthesis and relative biomass growth rates aboveground also increased during the experiment (Damasceno et al submitted), thus likely allowing greater carbohydrate supply to symbionts.

The different strategies adopted by plants under eCO_2 to improve nutrient acquisition in the litter layer and soil can directly influence soil nutrient dynamics, microbial activity, and consequently, soil organic carbon cycling since both labile C and plant litter inputs impact SOM formation and soil nutrient retention[39–41]. Our results showed that eCO_2 did not change the total and microbial pools of C, N, and P (Fig. S12 and Fig. S16; Supplementary information), but significantly reduced the total soil organic P fraction (sum of $NaHCO_3$ and NaOH organic P) (Fig 1c; aCO_2: 9.40 ± 5.07 µg g^{-1} versus eCO_2: 2.10 ± 2.50 µg g^{-1}; Z= – 1.95, p=0.05), mainly driven by a reduction of the NaOH extractable P-fractions (Fig. S14; Supplementary information). This decrease in the organic P fraction was not accompanied by a relative increase in the inorganic P pools or microbial P biomass, which may suggest that plants outcompete microbial P uptake under eCO_2. The organic P fraction is considered the most dominant fraction on old and weathered soils[3], and accessible for plants after biological and/or biochemical mineralization by microbial or plant-root phosphatase activity[16]. Although we did not observe a significant increase in soil microbial phosphatase activity, some studies indicate that arbuscular mycorrhiza has the ability to exudate acid phosphatase[42], thus it is possible that the doubling of AM colonizing fine roots under eCO_2 promoted biochemical organic P mineralization in addition to "simply" increasing soil exploration by fine roots. Furthermore, the soil extracellular enzyme C:P ratio significantly decreased (Fig 1c; aCO_2: –0.09 ± 0.04 versus eCO_2: –0.26 ± 0.04; Z=–4.03, p=<0.001) suggesting that soil microbes possibly increase investing in organic P mineralization. On the other hand, the potential activity of both enzymes responsible for hydrolyzing C (i.e., cellobiosidase and β-glucosidase) significantly decreased under eCO_2 by 156 % and 94% respectively (Fig. S17; Supplementary information), which suggests that the microbial community may not need to invest in C degradation and indicate a change in the access and availability of C substrates in the soil under eCO_2.

Our findings provide new evidence on the ability of plants living in P-limited forests to change nutrient acquisition strategies under eCO_2, highlighting the ability of plants to access potential

nutrient resources in the upper layers of soil. In contrast to N-limited temperate forests, where the extra C provided by eCO_2 was allocated mainly to root production[28] and root exudates stimulating microbial mining in soil organic matter (SOM)[29]. Our results indicate that in tropical P-limited forest ecosystems, plants have a certain plasticity to respond to eCO_2 by investing in biochemical P mineralization in the litter layer, and increasing foraging by producing longer and finer roots, while simultaneously increasing the AM colonization in the soil. On the other hand, our results suggest that in superficial, organic soils layers, eCO_2 may not stimulate microbial activity and subsequent SOM decomposition reducing or balancing soil CO_2 efflux which over longer time scales could result in a net C sequestration.

Our results reflect relatively short-term responses occurring at an interval of 8 to 24 months under elevated CO_2. Long-term monitoring experiments are needed to investigate possible acclimation effects, but also to capture different stages of plant development, and the potential effect of progressive nutrient limitations, and lead to further changes in C allocation, plant P use efficiency, and accessing of different strategies and P pools. Also, given that our results represent the response of Amazonian understory plants, which are living most of the time close to their light compensation point, it is likely that the observed responses in this study were constrained by light availability. In fact, it is remarkable that the understory community was able to change P acquisition strategies so dramatically despite light limitation. We hypothesize that although the response of adult canopy trees may follow similar strategies of changes in P acquisition strategies, the magnitude of change may be higher since they may access much more resources.

Phosphorus availability limits plant productivity across Amazonia[12,43], thus potentially constraining ecosystem level responses to eCO_2[1]. Our results provide the first in situ evidence that Amazonian plant communities are able to change their P acquisition strategies in response to eCO_2, which could, in principle, allow them to overcome P limitation, possibly resulting in further stand level biomass growth. However, it is unclear for how long the observed adaptations in P acquisition under eCO_2 may sustain growth, since the present P pools do not increase, but are only used more efficiently. Such intensification of the P cycle will likely reach a new equilibrium and may facilitate only a temporary carbon sink or increased Amazon Forest resilience. Nevertheless, given the disproportionate influence of the Amazon and other tropical forests in the terrestrial carbon balance, the response of such forests to eCO_2 will, to a large degree, dictate how long our societies must curb emissions and adhere to international agreements such as limiting warming to 1.5 C[44]. In that context, the observation that Amazon plant communities can change strategies and turn P uptake more efficiently under eCO_2 is of striking importance and means that Amazon could still buy us more time to fight climate change.

List of Figures

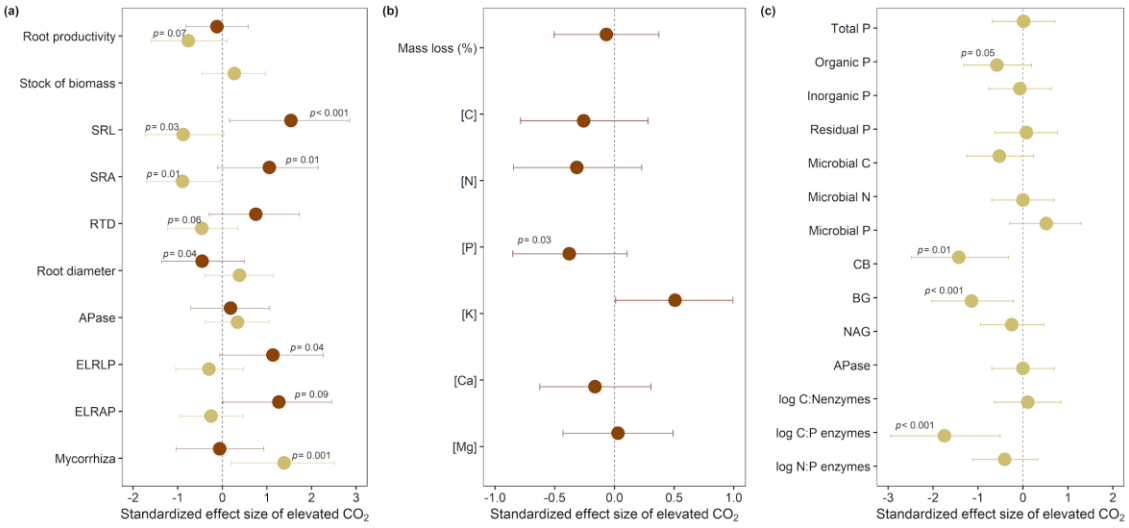

Figure 1 | Effect of elevated CO_2 on fine root nutrient mechanisms acquisition (a), litter decomposition (b), soil phosphorus concentration, and microbial activity (c). The effects of elevated CO_2 are represented by the delta effect CO2 (i.e., eCO2 experiment – baseline; se methods section) and shown as a standardized effect size by the difference of elevated (eCO_2) and ambient (aCO_2) (n=4); the bars represent the 95% confidence interval. The red circles indicate the process in the litter layer and the beige circles in the soil. SRL, specific root length; SRA, specific root area; RTD, root tissue density; APase, acid phosphomonoesterase activity (phosphatase); ELRLP, ecosystem level root length phosphatase; ELRAP, ecosystem level root area phosphatase. CB, cellobiosidase; BG, β-glucosidase; NAG, (insert NAG real). The *P* values obtained by linear generalized mixed models are indicated in the variables where the eCO_2 was significantly different from aCO_2.

Reference

1. Fleischer, K. *et al.* Amazon forest response to CO2 fertilization dependent on plant phosphorus acquisition. *Nat. Geosci.* **12**, 736–741 (2019).

2. Vitousek, P. M., Porder, S., Houlton, B. Z. & Chadwick, O. A. Terrestrial phosphorus limitation: Mechanisms, implications, and nitrogen-phosphorus interactions. *Ecol. Appl.* **20**, 5–15 (2010).

3. Quesada, C. A. *et al.* Variations in chemical and physical properties of Amazon forest soils in relation to their genesis. *Biogeosciences* **7**, 1515–1541 (2010).

4. Steege, H., Pitman, N. C. A., Sabatier, D. & Baraloto, C. Hyperdominance in the Amazonian Tree Flora. (2013). doi:10.1126/science.1243092

5. Lapola, D. M. *et al.* Limiting the high impacts of Amazon forest dieback with no-regrets science and policy action. *Proc. Natl. Acad. Sci.* **115**, 11671–11679 (2018).

6. Pan, Y. *et al.* A large and persistent carbon sink in the world's forests. *Science (80-.).* **333**, 988–993 (2011).

7. Koch, A., Hubau, W. & Lewis, S. L. Earth System Models Are Not Capturing Present-Day Tropical Forest Carbon Dynamics. *Earth's Futur.* **9**, 1–19 (2021).

8. Bacastow, R. & Keeling, C. K. Atmospheric carbon dioxide and radiocarbon in the natural carbon cycle: II. Changes from A. D. 1700 to 2070 as deduced from a geochemical model. in *Brookhaven Symposia in Biology* **30**, 86–135 (1973).

9. Brienen, R. J. W. *et al.* Long-term decline of the Amazon carbon sink. *Nature* **519**, 344–348 (2015).

10. Hubau, W. *et al.* Asynchronous carbon sink saturation in African and Amazonian tropical forests. *Nature* **579**, 80–87 (2020).

11. Walker, T. W. & Syers, J. K. The fate of phosphorus during pedogenesis. *Geoderma* **15**, 1–19 (1976).

12. Cunha, H. F. V. *et al.* Direct evidence for phosphorus limitation on Amazon forest productivity. (2022). doi:10.1038/s41586-022-05085-2

13. Fleischer, K. & Terrer, C. Estimates of soil nutrient limitation on the CO 2 fertilization effect for tropical vegetation . *Glob. Chang. Biol.* 6366–6369 (2022). doi:10.1111/gcb.16377

14. Reichert, T. *et al.* Plant phosphorus-use and -acquisition strategies in Amazonia. *New Phytol.* **234**, 1126–1143 (2022).

15. Lambers, H., Raven, J. A., Shaver, G. R. & Smith, S. E. Plant nutrient-acquisition strategies change with soil age. *Trends Ecol. Evol.* **23**, 95–103 (2008).

16. McGill, W. B. & Cole, C. V. Comparative aspects of cycling of organic C, N, S and P through soil organic matter. *Geoderma* **26**, 267–286 (1981).

17. Cuevas, E. & Medina, E. Nutrient dynamics within amazonian forests - II. Fine root growth, nutrient availability and leaf litter decomposition. *Oecologia* **76**, 222–235 (1988).

18. Luizao, R. C. C., Luizao, F. J. & Proctor, J. Fine root growth and nutrient release in decomposing leaf litter in three contrasting vegetation types in central Amazonia. *Plant Ecol.* 225–236 (2007). doi:10.1007/s11258-007-9307-8

19. Martins, N. P. *et al.* Fine roots stimulate nutrient release during early stages of leaf litter

decomposition in a Central Amazon rainforest. *Plant Soil* **469**, 287–303 (2021).

20. Dallstream, C., Weemstra, M. & Soper, F. M. A framework for fine-root trait syndromes: syndrome coexistence may support phosphorus partitioning in tropical forests. 1–16 (2022). doi:10.1111/oik.08908

21. Freschet, G. T. *et al.* Root traits as drivers of plant and ecosystem functioning: current understanding, pitfalls and future research needs. *New Phytol.* (2020). doi:10.1111/nph.17072

22. Weemstra, M. *et al.* Tansley review Towards a multidimensional root trait framework : a tree root review. *New Phytol.* **211**, 1159–1169 (2016).

23. Bergmann, J. *et al.* The fungal collaboration gradient dominates the root economics space in plants. *Sci. Adv.* **6**, 1–10 (2020).

24. Nannipieri, P., Giagnoni, L., Landi, L. & Renella, G. Role of Phosphatase Enzymes in Soil. in *Phosphorus in Action. Biological Processes in Soil Phosphorus Cycling* **26**, 215–243 (2011).

25. Dijkstra, F. A., Carrillo, Y., Pendall, E. & Morgan, J. A. Rhizosphere priming: a nutrient perspective. *Front. Microbiol.* **4**, 216 (2013).

26. Wang, Y. & Lambers, H. Root-released organic anions in response to low phosphorus availability : recent progress , challenges and future perspectives. **2050**, 135–156 (2020).

27. Hofhansl, F. *et al.* Amazon Forest Ecosystem Responses to Elevated Atmospheric CO2 and Alterations in Nutrient Availability: Filling the Gaps with Model-Experiment Integration. *Front. Earth Sci.* **4**, 1–9 (2016).

28. Iversen, C. M., Ledford, J. & Norby, R. J. CO2 enrichment increases carbon and nitrogen input from fine roots in a deciduous forest. *New Phytol.* **179**, 837–847 (2008).

29. Phillips, R. P., Finzi, A. C. & Bernhardt, E. S. Enhanced root exudation induces microbial feedbacks to N cycling in a pine forest under long-term CO2 fumigation. *Ecol. Lett.* **14**, 187–194 (2011).

30. Lloyd, J., Bird, M. I., Veenendaal, E. M. & Kruijt, B. Should Phosphorus Availability Be Constraining Moist Tropical Forest Responses to Increasing CO2 Concentrations? *Glob. Biogeochem. Cycles Clim. Syst.* 95–114 (2001). doi:10.1016/b978-012631260-7/50010-8

31. Cernusak, L. A. *et al.* Tropical forest responses to increasing atmospheric CO2: Current knowledge and opportunities for future research. *Funct. Plant Biol.* **40**, 531–551 (2013).

32. Ellsworth, D. S. *et al.* Elevated CO2 does not increase eucalypt forest productivity on a low-phosphorus soil. *Nat. Clim. Chang.* **7**, 279–282 (2017).

33. Jiang, M. The fate of carbon in a mature forest under carbon dioxide enrichment. *Nature* **580**, (2020).

34. Hasegawa, S., Macdonald, C. A. & Power, S. A. Elevated carbon dioxide increases soil nitrogen and phosphorus availability in a phosphorus-limited Eucalyptus woodland. *Glob. Chang. Biol.* **22**, 1628–1643 (2016).

35. Ochoa-Hueso, R. *et al.* Rhizosphere-driven increase in nitrogen and phosphorus availability under elevated atmospheric CO2 in a mature Eucalyptus woodland. *Plant Soil* **416**, 283–295 (2017).

36. Pihlblad, J., Andresen, L. C., Macdonald, C. A., Ellsworth, D. S. & Carrillo, Y. The influence of elevated CO2and soil depth on rhizosphere activityand nutrient availability in a mature Eucalyptus woodland. *Biogeosciences* **20**, 505–521 (2023).

37. Lapola, D. & Norby, R. *Amazon-FACE: Assessing the effects of increased atmospheric CO2 on the ecology and resilience of the Amazon forest – Science plan and implementation strategy*. *Brasilia: Ministério de Ciência, Technologia e Inovação* (2014).

38. McCormack, M. L. *et al.* Redefining fine roots improves understanding of below-ground contributions to terrestrial biosphere processes. *New Phytol.* **207**, 505–518 (2015).

39. Cotrufo, M. F., Ranalli, M. G., Haddix, M. L., Six, J. & Lugato, E. Soil carbon storage informed by particulate and mineral-associated organic matter. *Nat. Geosci.* **12**, 989–994 (2019).

40. Jansson, J. K. & Hofmockel, K. S. Soil microbiomes and climate change. *Nat. Rev. Microbiol.* **18**, 35–46 (2020).

41. Sayer, E. J. *et al.* Altered litter inputs modify carbon and nitrogen storage in soil organic matter in a lowland tropical forest. *Biogeochemistry* **156**, 115–130 (2021).

42. Joner, E. J., Van Aarle, I. M. & Vosatka, M. Phosphatase activity of extra-radical arbuscular mycorrhizal hyphae: A review. *Plant Soil* **226**, 199–210 (2000).

43. Quesada, C. A. *et al.* Basin-wide variations in Amazon forest structure and function are mediated by both soils and climate. *Biogeosciences* **9**, 2203–2246 (2012).

44. Intergovernmental Panel on Climate Change. *Global warming of 1.5°C-IPCC*. (2018).

Methods

Study site. The Open-top chambers (OTC) experiment was implemented in the experimental area of the AmazonFACE program[37] (-2° 35' 40.29, -60° 12' 28.69), located in the Central Amazon at the "*Cuieiras*" experimental reserve about 70 km north of Manaus (Amazonas, Brazil). The study area was located on a plateau with old-growth, lowland Terra-Firme Forest vegetation[45]. The soil is characterized as clay-rich (67.7% clay, 19.9% sand, and 12.3% silt) and highly weathered Geric Ferralsols, with a pH of 3.94, and a low concentration of total P and rock-derived nutrients[3,46]. Average annual rainfall is about 2500 mm with the wettest period from December to May and the dry season characterized by August to September (<100 mm of precipitation), the average temperature range between 24 °C and 27°C to April and September respectively [47].

Experimental design. A total of eight polypropylene open-top chambers (OTCs), each with a diameter of 2.4 m and a height of 3 m, were installed in the understory of the forest. To prevent root proliferation and other effects from plants outside the OTCs, each chamber was surrounded by a circular soil trench measuring 30 cm in width and 50 cm in depth. The chambers were arranged in pairs, with four control chambers maintained at ambient CO_2 [aCO_2] and four elevated CO_2 [eCO_2] treatments, in which CO_2 concentration was increased by 200 ppm relative to the respective ambient OTC. Inside each chamber, concentrations of CO_2 and water vapor (H_2O) were measured using a CO_2/H_2O non-dispersive infrared (NDIR) gas analyzer (LI-840A, Li-Cor Biosciences, Lincoln, NE, USA) connected to a central logger system (Campbell Scientific CR1000 data loggers). The CO_2 was injected into the eCO_2 chambers through a gas line connected to a central cylinder system and distributed by fans installed close to the injection hose. The injection of CO_2 was carried out during daylight hours (from 6 am to 6 pm) in the eCO_2 OTCs when the difference between the treatment pairs was less than 200 ppm. The CO_2 injection in the eCO_2 chambers starts on November 1, 2019. The eCO_2 system was adjusted and stabilized during the first two months (i.e., November and December 2019), and after this period, it maintained an average increase in CO_2 concentration of 270 ppm until November 1, 2020 (Fig. S1; aCO_2: 458 ± 1.58; eCO_2: 736.78 ± 4.57).

Soil and plant characteristics description. The OTCs design just enables the monitoring of plants from the understory, so we are considering plants with a maximum height of 3m. Further, we have a variation on average from 100.4 ± 10.0 cm and 123.2 ± 11.5 cm for the height, and 11.72 ± 0.98 and 12.10 ± 0.76 mm for diameter in the chambers with aCO_2 and eCO_2 respectively (Table S1). The total of plants inside the OTCs varied from 8 to 18, with a mean of 15 individuals in the aCO_2 and 12 individuals for eCO_2. Furthermore, we identified a total of 81 different species in the eight OTCs, demonstrating a higher species richness by OTC and between OTCs. The soil chemical and physical properties inside the OTCs follow basically the same pattern previously

described by for the Ferralsols in the Central Amazonian (Quesada et al 2010), with an average of 102.58 mg kg^{-1} of total P where 47% are residual and 52% are in extractable form, 3.7 of pH, 3.06% of carbon and 0.24% of nitrogen (see details by OTC in table S1).

Experiment 1 - Fine root nutrient acquisition mechanisms. In many forests in the central Amazon, a major part of fine root biomass and productivity is happening at the soil surface[19], and in the upper soil layers[48]. We, therefore, monitored fine root productivity, morphological and biochemical traits in the litter layer and in the 15 cm of soil depth in each OTC. **Litter layer:** to monitor fine root colonization in the litter layer (placed horizontally between the mineral soil surface and growing up to the litter layer) we installed two adapted rectangular-shaped ingrowth cores (20 x 15 cm) per OTC in February of 2019. The first collection was realized after 6 months (baseline collection; August 2019; Figure S2), and a week before starting the CO_2 injection we zeroed all the ingrowth cores removing any roots found inside the traps. The next collection was planned for May 2020 (6 months after the start of eCO_2), however, the outbreak of the global pandemic of SARS COVID 19 did not allow us to maintain regular collection intervals, and our sample harvest from the litter layer was realized only after 8 months of start eCO_2 (July 2020; Figure S2). Fine root net productivity (expressed by mg^{-1} cm^2) in the litter layer was determined by carefully collecting all roots from the two ingrowth cores that were in direct contact with the litter layer. Sub-samples of roots were used to determine the morphological parameters and phosphatase activity. **Soil:** to monitor fine root productivity in the soil we installed four 12 cm diameter, 15 cm-deep, root-free ingrowth cores per OTC in February 2019. Similar to the litter layer we collected for the first time in August 2019 (Figure S2) and one week before starting the CO_2 injection (i.e., November 2019) all ingrowth cores were emptied and zeroed (i.e., all roots were removed). After that, the plan was to collect every 3 months, but due to the inability of sampling because of limitations imposed by the global pandemic of COVID 19, we presented the data after one year of eCO_2 starting (i.e., November 2020), with a previous collection in August 2020, therefore with the ideal interval of three months between collections. After the collections, we used two ingrowth cores by OTC to quantify root productivity and morphological parameters of fine roots, and the other two were used to measure fine root phosphatase activity and mycorrhizal colonization. We considered fine roots smaller than 1mm in diameter (< 1mm) to mostly represent absorptive roots (first, second and third orders)[49]. To determine soil fine root productivity, in the field after each collection we manually sampled all roots during a period of 12.5 minutes in five intervals of 2.5 minutes (as an adaptation of the methodology)[50]. The root-free soil was reinserted into the existing hole sampling, and the roots collected were washed and cleaned gently using a brushing to remove soil particles. To extrapolate the amount of roots that would be sampled after the 12.5 minutes we used the cumulative root biomass sampled at each time point (every 2.5 minutes) and tested three different types of simple curves (linear,

polynomial, and logarithmic)[50]. We chose the logarithmic curve that presents the best model fit, the soil fine root productivity was calculated as the dry mass of roots produced per day in the total area of the ingrowth core (mg cm^2 day^1).

Fine root morphology parameters. All fine roots collected from litter cores and fine root subsamples collected from soil cores in the first-time interval (representing more than 50% of the total sample) were scanned in high resolution (600 dpi) and analyzed using WinRHIZO (WinRHIZO Regular, Regent Instruments, Canada) to determine fine root morphological traits. We determined the specific root length (SRL), specific root area (SRA), root tissue density (RTD), and mean root diameter. Then samples were dried for 72 h at 65°C to determine dry root mass [50,51]. SRL (cm mg^{-1}) as the length per unit root dry mass, SRA (cm^2 mg^{-1}) as fine root surface area per unit dry mass, and RTD (mg cm^3) was calculated as root dry mass per unit root volume.

Root phosphatase activity. Fine root subsamples from both litter layer and soil were analyzed for root potential acid phospho-monoesterase activity (phosphatase), which is the phosphatase predominantly produced by plants[52]. The potential root acid phosphatase activity (APase) was measured following an adapted fluorometric microplate assay protocol[51,53]. Approximately 10 mg of clean root subsample from each ingrowth core was incubated for 30 min, gently shaking, with Methylumbelliferyl-phosphate (MUF); in addition, a further subsample was incubated with sodium acetate buffer as a negative control. To stop the reaction 50 µl of 1M NaOH was added to all samples, negative controls, and to methylumbelliferyl standards, then aliquots were pipetted in triplicates into a black 96-well microplate. After 20 minutes the fluorescence was read at 365 nm excitation and 450 nm emission (ref. Tecan Infinite®). The fine root subsamples were scanned and dried at 65° for 72h. Potential root phosphatase activity was expressed in µmol mg^{-1} root dry mass h^{-1}, µmol cm^{-1} root dry mass h^{-1}, and µmol cm^2 root dry mass. We present the APase by mg of root dry mass, in addition we used the APase of root cm^{-1} and root cm^2 of to extrapolate to ecosystem level as total oRL (ELRLP) and (ELRAP) respectively for each OTC.

Mycorrhiza colonization. To determine arbuscular mycorrhiza colonization of roots in in the litter layer we used sub samples of fine roots found inside of the litterbags used to monitor leaf litter decomposition (more details below – litter decomposition design). For roots in the soil we used sub samples collected in the ingrowth cores down to 15 cm of soil depth. After cleaning, the segments of fresh absorptive roots from the first three orders were stored in 50% ethanol. The process of clearing and staining was previously described for tropical roots [51,54,55]. Initially, the roots were cleared using a 2.5% potassium hydroxide (KOH) solution, followed by autoclaving at approximately 120°C for approximately 10 minutes. Subsequently, the roots were subjected for approximately 30 min to an alkaline hydrogen peroxide (H_2O_2) solution for bleaching and acidified using a 2% hydrochloric acid (HCl) solution for further 30 minutes. Then the roots were

immersed in 0.05% Trypan Blue solution a until a consistent blue coloration was achieved. Uniformly stained root fragments were randomly selected from the subsample to quantify the extent of colonization by arbuscular mycorrhizal (AM) fungi by the cross-section method[56]. These fragments were mounted on slides and subjected to a high-resolution optical examination at 10x magnification, enabling the accurate determination of the total length of roots colonized by AM fungi.

Experiment 2 - Leaf litter decomposition. Leaf litter can be a major nutrient source for plants in the studied forest[19], with its importance potentially increasing even further under eCO_2. We therefore conducted a one-year leaf litter decomposition experiment inside the OTCs, starting in September 2020. We used leaves of *Vismia sp.*, to reduce the chemical variability of litter, collected from a single tree recently fallen after a heavy storm in the area close to the experimental site. The leaves were dried at 65° C for 72 h and stored dry. We prepared five litter bags of 2 mm mesh size (20 x 20 cm) and 10 g of dry leaves per OTC. After one year all litterbags were collected and analyzed for mass loss and total nutrient concentration.

Processing of leaf litter decomposition samples. After the collection, the remaining leaves were weighed fresh and then dried at 65 °C for 72 h to determine the water content and dry weight to fresh weight ratio which was used to calculate the total dry weight. Leaf litter mass loss (ML) was calculated as a percentage of total initial mass as

$$ML = (((m_0 - m_1)/m_0) \times 100).$$

with m_0 representing the initial litter dry weight and m_1 the litter dry weight at the collection.

Leaf litter nutrient dynamics. The remaining leaf collected after one year was analyzed for total carbon (C), nitrogen (N), P, and cations. The dried samples were milled to a fine powder. Total C and N were analyzed in an automatic CN analyzer (Vario Max CN, Elemental Analyzer, Germany) by mass spectrometry. Nitro-perchloric acid digestion was used to determine the total concentration of P, potassium (K), calcium (Ca), and magnesium (Mg)[57]. Total P was read on a UV Spectro-photometer (Model 1240, Shimadzu, Kyoto, Japan) and the total cation concentration was measured by atomic absorption spectrophotometry (AAS, 1100 B, Perkin Elmer, Ueberlingen, Germany). Nutrient concentration is presented as g of nutrient by kg of dry leaves ($g\ kg^{-1}$).

Experiment 3 - Soil fine root biomass, microbial activity, and nutrient concentration. We collected two soil samples by OTC in November 2020 to quantify fine root biomass stocks, microbial activity, nutrient concentration, and P fractions in response to eCO_2. Soils were sampled at 0-5 cm and 5-10 cm depth using an auger (ø 10 cm) and then transported to the thematic

laboratory of soils and plants (LTSP) at the National Institute of Amazonian Research (INPA) to sort the roots and sieving the soil to 2 mm for further analyses.

Root biomass stock: fine root biomass was determined following the methodology by Metcalfe et al 2007 as described above. The difference is that the sorting of the roots was carried out in the laboratory and separated by the two different depths (0-5 and 5-10 cm). After sorting, all roots were washed and separated into different diameter classes (<1mm; 1-2mm, and >2mm) and then dried at 65°C for 72 h. We used only the roots considered to be acquisitive (<1mm of diameter) to have a better comparison with the fine root productivity rates. Root biomass was calculated using the area of the auger and the soil depth and expressed in mg cm^2. Fresh soil subsamples were split and weighed to determine **microbial biomass** and **enzymatic activity** analyses within a maximum of fourth days after sampling. Another soil subsample was weighed and dried for 48h at 105 °C to determine soil water content.

Microbial activity: to determine microbial biomass C, N and P we used the chloroform fumigation extraction method of fresh soil within 72 h after soil stock collection[58]. From each sample, 2 g of soil was fumigated with chloroform for 24 h, then the samples were divided into two subsamples (1g each) for extractions with 20 ml 1M KCl to analyze organic extractable C and total extractable N, and another for extractions with 20 ml of 0.5 M $NaHCO_3$ (pH 8.5) to analyze total extractable P. At the same time, another set of samples was used for extraction with the same extractors without chloroform fumigation. Fumigated and non-fumigated extracts of KCl and $NaHCO_3$ were analyzed as previously described by Martins et al. (2021). Microbial C, N, and P were estimated as the difference between concentrations in the fumigated and non-fumigated extracts and expressed by soil dry mass. We measured the potential activity of four different soil extracellular enzymes released by microbes involved in the C, N, and P cycle respectively: cellobiosidase (4-MUF-cellobioside; CB), β-glucosidase (4-MUF-β-D-glucopyranoside; BG), N-acetylglucosominidase (4-MUF-N-acetyl-β-D-glucosaminide; NAG) and acid phosphatase (Methylumbelliferyl-phosphate; APase) using a vortex for 1 min we homogenized 0.5 g of soil and 50 ml of 100 mM sodium acetate buffer, pH 5.5 and then was pipetted into 96 black microplates in triplicates by sample and incubated with the respective substrates for 40 min; in addition, we included substrate and quenching blanks in triplicates per plate on all microplates[53,59,60]. The measurements of the enzyme activities were conducted by fluorescence on a microplate analyzer (TECAN i-control 200Pro, Groedig, Austria) at 365 nm excitation and 450 nm emission and expressed in nmol g^{-1} dry soil h^{-1}. We calculated microbial CNP ratios, the log of C:P enzyme ratio (log (CB + BG) / log APase), the N: P enzyme ratio (log NAG/ logAPase), and the enzyme activity by microbial biomass (i.e., CB: microbial C; NAG: microbial N; APase: microbial P)[61,62].

Nutrient concentration: Total C and N concentrations were analyzed on an elemental analyzer (EA 1100, CE Instruments, Milan, Italy) coupled to a Finnigan MAT Delta Plus IRMS (Thermo Fisher Scientific, MA, USA). Total P was analyzed using a concentrated sulfuric acid (H_2SO_4, 18 *M*) digestion followed by H_2O_2[63]. Furthermore, we used a more comprehensive description of the available P fractions[3,64]. The method followed a sequential extraction, starting with the resin extractable P in water, followed by 0.5M $NaHCO_3$ (pH 8.5, bicarbonate fraction), 0.1M NaOH (hydroxide fraction), and 1M HCl (hydrogen chloride). All extracts have been analyzed for inorganic P_i, and for the $NaHCO_3$ and NaOH extracts the total P was also analyzed by sulfuric digestion (H_2SO_4, 0.9M). Thereby the extraction results in six different fractions: resin P, bicarbonate inorganic P, bicarbonate total P, sodium hydroxide inorganic P, sodium hydroxide total P, and hydrochloric acid P. All seven fractions (including total P) were analyzed for PO_4 concentrations photometrically, and the results are given in $\mu g\, g^{-1}$ dry soil[65]. We calculated the organic fraction (P_o) by the difference between the total fractions (i.e., bicarbonate total, sodium hydroxide total) and their respective inorganic fractions (P_i). With the sum of all labile fractions, we obtain the P extractable, and the residual P was obtained by subtracting the total P and the extractable P[46].

Data analyses. All statistical analyses were performed in R version 4.2.1[66]. To obtain a real effect of elevated CO_2 on our response variables, we calculate a delta elevated CO_2 effect (delta eCO_2) considering the natural spatial variability before starting the increase in CO_2 concentrations by a difference between the collection performed after the start of eCO_2 (8 or 12 months depending on a variable) and the baseline collection (see Figure S2 for details). The delta eCO_2 effect was calculated for all variables considering the differences between the respective OTCs and samples for the different two times. The statistical analysis was realized for each collection separated (baseline, eCO_2, and delta eCO_2 effect) to understand the dynamics of the variables before and after eCO_2 (see Supplementary information). We consider the delta eCO_2 as the real effect of CO_2 on soil and litter fine root dynamic, soil microbial activity, and soil P concentrations. General linear mixed models (GLMM) using the glmmTMB package[67] were used for each variable to test the difference between the treatments (aCO_2 and eCO_2) as fixed factors and OTC identity as random factor to control for environmental and spatial variability. As we are considering the spatial variability with the OTC as a random factor, we use each sample independently as a replication for the different experiments. We fit the models with the *gaussian* family and tested the assumptions for normality and homogeneity of the residuals using the function simulateResiduals by the DHARMa package[68], the variables were log-transformed if needed. In the main text the results are reported graphically as the effect size of eCO_2 calculated with the cohens'd function by effect size package[69].

References

45. Pereira, I. S. *et al.* Performance of laser-based electronic devices for structural analysis of Amazonian terra-firme forests. *Remote Sens.* **11**, (2019).

46. Schaap, K. J. *et al.* Litter inputs and phosphatase activity affect the temporal variability of organic phosphorus in a tropical forest soil in the Central Amazon. *Plant Soil* (2021). doi:10.1007/s11104-021-05146-x

47. Alves, E. G. *et al.* Seasonality of isoprenoid emissions from a primary rainforest in central Amazonia. *Atmos. Chem. Phys.* **16**, 3903–3925 (2016).

48. Cordeiro, A. L. *et al.* Fine-root dynamics vary with soil depth and precipitation in a low-nutrient tropical forest in the Central Amazonia. *Plant-Environment Interact.* 1–14 (2020). doi:10.1002/pei3.10010

49. McCormack, M. L. *et al.* Building a better foundation: improving root-trait measurements to understand and model plant and ecosystem processes. *New Phytol.* **215**, 27–37 (2017).

50. Metcalfe, D. B. *et al.* A method for extracting plant roots from soil which facilitates rapid sample processing without compromising measurement accuracy: Methods. *New Phytol.* **174**, 697–703 (2007).

51. Lugli, L. F. *et al.* Multiple phosphorus acquisition strategies adopted by fine roots in low-fertility soils in Central Amazonia. *Plant Soil* (2019). doi:10.1007/s11104-019-03963-9

52. Turner, B. L. Resource partitioning for soil phosphorus: A hypothesis. *J. Ecol.* **96**, 698–702 (2008).

53. German, D. P. *et al.* Optimization of hydrolytic and oxidative enzyme methods for ecosystem studies. *Soil Biol. Biochem.* **43**, 1387–1397 (2011).

54. Brundrett, M. C., PichéY & Peterson, R. A new method for observing the morphology ofvesicular-arbuscular mycorrhi- zae. *Can J Bot* **62**, (1984).

55. Wurzburger, N. & Wright, S. J. Fine-root responses to fertilization reveal multiple nutrient limitation in a lowland tropical forest. *Ecology* **96**, 2137–2146 (2015).

56. McGonigle, T. P., Miller, M. H., Evans, D. G., Fairchild, G. L. & Swan, J. A. A new method which gives an objective measure of colonization of roots by vesicular—arbuscular mycorrhizal fungi. *New Phytol.* **115**, 495–501 (1990).

57. Malavolta, E., Vitti, G. C. & Oliveira, A. S. *Avaliação doestado nutricional das plantas: princípios e aplicações*. *Associação Brasileira para Pesquisa da Potassa e do Fosfato* (1989).

58. Vance, E. D. & Nadkarni, N. M. Microbial biomass and activity in canopy organic matter and the forest floor of a tropical cloud forest. *Soil Biol. Biochem.* **22**, 677–684 (1990).

59. Marx, M. C., Wood, M. & Jarvis, S. C. A microplate fluorimetric assay for the study of enzyme diversity in soils. *Soil Biol. Biochem.* **33**, 1633–1640 (2001).

60. Saiya-Cork, K. ., Sinsabaugh, R. . & Zak, D. . The effects of long term nitrogen deposition on extracellular enzyme activity in an Acer saccharum forest soil. *Soil Biol. Biochem.* **34**, 1309–1315 (2002).

61. Waring, B. G. Exploring relationships between enzyme activities and leaf litter decomposition in a wet tropical forest. *Soil Biol. Biochem.* **64**, 89–95 (2013).

62. Moorhead, D. L., Sinsabaugh, R. L., Hill, B. H. & Weintraub, M. N. Vector analysis of ecoenzyme activities reveal constraints on coupled C, N and P dynamics. *Soil Biol. Biochem.* **93**, 1–7 (2016).

63. Tiessen, H. & Moir, J. . Total and Organic Carbon, in: Soil Sampling and Methods of Analysis. *Leis Publ., Boca Rat.* 187–199 (1993).

64. Hedley, M. ., Stewart, J. W. . & Chauhan, B. . Changes in inorganic and organic soil phosphorus fractions induced by cultivation practices and by laboratory incubations. *Soil Sci. Soc. Am.* **46**, 970–976 (1982).

65. Murphy, J. & Riley, J. . A modified single solution method for the determination of phosphate in natural waters. *Anal. Chim. Acta* **27**, 31–36 (1962).

66. R Core Team. A language and environment for statistical computing. (2023).

67. Magnusson, A. *et al. Package 'glmmTMB'. Cran* (2020).

68. Florian Harting. DHARMa: ResidualDiagnostics for Hierarchical (Multi-Level/ Mixed) Regression Models. R package version 0.1.5. R package version 0.1.5 (2017).

69. Kelley, K., Stanley, D. & Caldwell, A. *Package ' effectsize '*. (2023). doi:10.21105/joss.02815>.License

Supplementary information

Elevated atmospheric carbon dioxide concentration changes P acquisition strategies in the Amazonian understory

Nathielly P. Martins[1], Lucia Fuchslueger, Laynara F. Lugli, Oscar J. Valverde-Barrantes, Richard J. Norby, Iain P. Hartley, Izabela Aleixo, Fabricio B. Baccaro, Barbara Brum, Raffaello Di Ponzio, Amanda Damasceno, Vanessa R. Ferrer, Katrin Fleischer, Sabrina Garcia, Alacimar Guedes, Florian Hofhansl, David Lapola, Juliane G. Menezes; Anna C. M. Moraes, Ana Caroline Miron, Leonardo Ramos de Oliveira, Cilene Palheta, Iokanam S. Pereira, Maria Pires, Gyovanni Ribeiro, Jessica S. Rosa, Anja Rammig, Flavia D. Santana, Yago R. Santos, Lara Siebert Silva, Bruno Takeshi, Gabriela Ushida and Carlos A. Quesada

***Authors for correspondence:**

Nathielly P. Martins: nathiellymartins9@gmail.com

Lucia Fuchslueger: lucia.fuchslueger@univie.ac.at

Table S1 | Open-top chambers experiment with soil and plant characterization. The baseline description was realized by OTC and showed a mean and standard error (n=4) for your respective treatments of ambient CO_2 (aCO_2) and elevated CO_2 (eCO_2). For the soil data, the values are the mean of two soil cores by OTC, and for height and diameter a mean of the total plant individuals by OTC. The baseline collections were realized on different dates in the year 2019 (see Figure S2 for details).

	aCO_2					eCO_2				
	1	8	9	X	Mean ± SE	2	4	5	Y	Mean ± SE
Total P	82.93	103.05	104.70	127.02	104.43 ± 8.12	79.90	83.49	93.68	129.50	96.64 ± 10.68
Organic P	25.65	24.19	29.10	27.37	26.58 ± 1.71	23.85	22.81	25.03	29.20	25.22 ± 1.40
Inorganic P	21.99	34.94	28.55	24.73	27.55 ± 3.09	21.75	21.20	24.50	26.69	23.58 ± 1.34
Residual P	35.29	43.92	47.04	74.91	50.29 ± 6.90	34.29	39.47	44.15	73.60	47.88 ± 9.28
Carbon (%)	3.69	3.03	3.23	2.70	3.16 ± 0.18	2.50	2.64	3.08	2.95	2.79 ± 0.17
Nitrogen (%)	0.28	0.25	0.26	0.21	0.25 ± 0.01	0.20	0.22	0.23	0.23	0.22 ± 0.01
pH		3.73	3.81	3.66	3.74 ± 0.06		3.71	3.76	3.82	3.76 ± 0.04
Clay (%)		65.31	62.68	61.47	63.15 ± 1.70		56.95	62.75	62.27	61.99 ± 2.31
Sand (%)		12.57	12.03	12.31	12.30 ± 0.34		12.95	11.77	12.74	12.49 ± 0.55
Silt (%)		22.11	25.28	26.21	24.53 ± 1.83		30.10	25.47	20.97	25.51 ± 2.26
Plant individuals	17	13	18	8	15.10 ± 0.57	13	13	13	10	12.38 ± 0.21
Species richness	9	11	14	6		12	7	11	4	
Height (cm)	91.4	77.3	86.1	158.7	100.48 ± 10.0	108.5	112.6	132.3	110	123.41±11.52
Diameter (mm)	12.3	9.96	11.1	14.8	11.72 ± 0.98	13.0	11.1	13.5	10.5	12.10 ± 0.76

The total phosphorus (P) is shown by mg kg^{-1} and the other fractions of P (organic, inorganic, and residual) by µg g^{-1}. The data for plant individuals, height and diameter refers to all individuals within OTCs (including those not identified).

Table S2| Statistical results of elevated CO_2 effect on fine root mechanisms nutrient acquisition in the litter layer and soil. Data were analyzed using generalized linear mixed models with a specific model for each collection data and variable, considering the effect of the treatment as a fixed factor and controlling the spatial variability using the open-top chamber (OTC) as a random factor. The "*baseline*" collections were realized in August 2019 before starting the CO_2 enrichment to characterize the natural spatial variability, the "*elevated CO_2 experiment*" refers to after 8 months under elevated CO_2 for the root in the litter layer and 12 months for the soil (se "figure SX" for details). The delta eCO_2 effect was calculated considering the difference between the collection after the increased CO_2 concentration (i.e., 8 months for the litter and 12 months for the soil) and the baseline.

		Fixed factor treatment; (response variable ~treatment + (1|OTC))											
		Baseline				*Elevated CO_2 experiment*				*Delta time eCO_2 effect*			
		Est.	Std. error	*z*	*P*	Est.	Std. error	*z*	*P*	Est.	Std. error	*z*	*P*
Litter layer	Net root productivity (mg cm^2)	0.05	0.07	0.69	0.48	-0.00	0.28	-0.01	0.98	-0.05	0.26	-0.21	0.83
	SRL (cm mg^{-1})	-0.87	0.55	-1.58	0.11	**5.05**	**2.37**	**2.12**	**0.03**	**7.80**	**1.85**	**4.20**	**<0.001**
	SRA (cm^2 mg^{-1})	-0.06	0.06	-0.95	0.33	0.36	0.28	1.27	0.20	**0.62**	**0.26**	**2.39**	**0.01**
	RTD (mg cm^{-3})	-0.04	0.04	-0.98	0.32	0.08	0.21	0.37	0.70	0.27	0.22	1.24	0.21
	Diameter (mm)	0.07	0.06	1.05	0.29	**-0.07**	**0.03**	**-2.05**	**0.03**	**-0.15**	**0.08**	**-1.96**	**0.04**
	*log APase (nmol mg^{-1} h^{-1})					0.12	0.45	0.28	0.77				
	*log ELRLP					**82.04**	**40.62**	**2.02**	**0.04**				
	*ELRAP					**55.69**	**33.08**	**1.68**	**0.09**				
Soil depth	Biomass (mg cm^2)												
	Productivity (mg cm^2 day^{-1})	-0.00	0.00	-0.40	0.68	**-0.03**	**0.01**	**-2.17**	**0.02**	**-0.03**	**0.01**	**-1.79**	**0.07**
	SRL (cm mg^{-1})	**9.72**	**3.44**	**2.82**	**0.004**	-0.59	4.41	-0.13	0.89	**-9.81**	**4.66**	**-2.10**	**0.03**
	SRA (cm^2 mg^{-1})	**2.41**	**1.04**	**2.30**	**0.02**	-0.22	0.42	-0.52	0.60	**-2.63**	**1.11**	**-2.36**	**0.01**
	log RTD (mg cm^{-3})	-0.00	0.00	-1.42	0.15	**-0.21**	**0.11**	**-1.90**	**0.05**	**-0.21**	**0.11**	**-1.82**	**0.06**
	Diameter (mm)	**-0.17**	**0.09**	**-1.83**	**0.06**	-0.15	0.11	-1.28	0.19	0.02	0.16	0.14	0.88
	Log APase (nmol mg^{-1} h^{-1})	6.97	4.63	1.50	0.13	44.44	39.89	1.11	0.26	37.46	36.77	1.01	0.30
	ELRLP	**65.81**	**26.68**	**2.46**	**0.01**	-6.80	124.82	-0.05	0.95	-68.73	116.83	-0.58	0.55
	ELRAP	**0.97**	**0.41**	**2.35**	**0.01**	0.59	101.14	0.00	0.99	-70.66	90.30	-0.78	0.43
	*Mycorrhiza colonization (%)									**30.25**	**9.65**	**3.13**	**0.001**

The models are fitted using maximum likelihood estimation, statistical significant results are calculated with 95% of probability and shown in boldface type (P <0.1 (higher tendency and significant effects P < 0.05). SRL, specific root length; SRA, specific root area; RTD, root tissue density; APase, acid phosphomonoesterase activity (phosphatase); ELRLP, ecosystem level root length phosphatase; ELRAP, ecosystem level root area phosphatase. *For root phosphatase variables in the litter layer and mycorrhiza colonization in the soil was not possible to realize the baseline characterization, thus we analyze the effect of elevated CO_2 considering the difference with the ambient CO_2 after 8 and 12 months under eCO_2 for the litter and soil respectively.

Table S3- Elevated CO_2 effect on leaf litter decomposition and nutrient dynamic after one year of the field experiment. Statistical parameters are the results of Generalized linear mixed models for each variable. The model considers the effect of the treatment as a fixed factor and controls the spatial variability using the open-top chamber (OTC), run with the Gaussian family.

	Fixed factor coefficients			
	Estimate	Std. error	*z*	*P*
Litter mass loss (%)	-2.077	5.96	-0.34	0.72
Carbon	-2.19	2.48	-0.88	0.37
Nitrogen	-0.16	0.11	-1.47	0.14
Phosphorus	**-0.04**	**0.02**	**-2.09**	**0.03**
Potassium	0.10	0.09	1.06	0.28
Calcium	-0.45	0.78	-0.57	0.56
Magnesium	-0.03	0.28	-0.11	0.91
Mycorrhiza colonization (%)	-1.25	7.096	-0.17	0.86

The models are fitted using maximum likelihood estimation, statistically significant results are calculated with 95% of probability and shown in boldface type ($P < 0.1$ (higher tendency and significant effects $P < 0.05$). The nutrient dynamic is shown in g kg^{1}.

Table S3 – Statistical results of elevated CO_2 effect on soil nutrient concentration. Data were analyzed using generalized linear mixed models with a specific model for each collection data and variable, considering the effect of the treatment as a fixed factor and controlling the spatial variability using the open-top chamber (OTC) as a random factor. The "*baseline*" collections were realized in February 2019 for P variables and August 2019 for other elements, for booths before starting the CO_2 enrichment to characterize the natural spatial variability, the "*elevated CO_2 experiment*" refers to after 12 months under elevated CO_2. The delta eCO_2 effect was calculated considering the difference between the collection after the increased CO_2 concentration (i.e., "elevated CO_2 experiment") and the baseline.

		Fixed factor treatment; (response variable ~treatment + (1|OTC))											
		Baseline				*Elevated CO_2 experiment*				*Delta time eCO_2 effect*			
		Est.	Std. error	*z*	*P*	Est.	Std. error	*z*	*P*	Est.	Std. error	*z*	*P*
Total P		-7.78	12.54	-0.62	0.53	**-7.35**	**3.04**	**-2.42**	**0.01**	0.43	11.19	0.03	0.96
P_t	NaHCO3	-0.76	0.76	-1.00	0.31	-0.84	2.01	-0.41	0.67	-0.07	2.37	-0.03	0.97
	NaOH	**-3.53**	**2.12**	**-1.66**	**0.09**	**-12.24**	**4.29**	**-2.84**	**0.004**	**-8.70**	**3.49**	**-2.49**	**0.01**
P*i*	Resin	-0.09	0.82	-1.13	0.25	**-0.69**	**0.21**	**-3.25**	**0.001**	0.23	0.88	0.26	0.78
	NaHCO3	-0.66	0.45	-1.51	0.13	-0.84	0.52	-1.61	0.10	-0.16	0.79	-0.20	0.83
	NaOH	-2.26	1.63	-1.38	0.16	**-3.25**	**1.22**	**-2.65**	**0.007**	-0.98	1.64	-0.59	0.55
	HCl	-0.13	0.22	-0.59	0.55	0.18	0.15	0.14	0.25	0.31	0.24	1.31	0.18
P_o	NaHCO3	-0.08	0.60	-0.13	0.89	0.71	1.86	0.38	0.69	0.83	2.18	0.38	0.70
	NaOH	-1.27	1.42	-0.89	0.37	-8.98	3.69	**-2.43**	**0.01**	**-7.71**	**2.64**	**-2.91**	**0.003**
Total organic P		-1.35	1.79	-0.75	0.45	-8.89	3.24	**-2.77**	**0.005**	**-7.30**	**3.74**	**-1.95**	**0.05**
Total inorganic P		-4.01	2.73	-1.47	0.14	-4.61	1.49	**-3.07**	**0.002**	-0.59	3.00	-0.19	0.87
Extractable P		-5.37	3.36	-1.59	0.11	-13.90	3.37	**-4.12**	**<0.001**	**-7.83**	**4.62**	**-1.69**	**0.09**
Residual P		-2.41	10.64	-0.22	0.82	5.84	3.59	1.62	0.10	0.16	0.28	0.57	0.56
Carbon (%)		**-0.37**	**0.21**	**-1.72**	**0.08**	-0.24	026	-0.90	0.36	0.20	0.33	0.61	0.53
Nitrogen (%)		**-0.02**	**0.01**	**-1.81**	**0.06**	-0.00	0.01	-0.52	0.60	0.02	0.02	0.93	0.35
Potassium		**-0.02**	**0.01**	**-2.44**	**0.01**	-0.02	0.007	**-2.85**	**0.004**	0.004	0.01	0.41	0.68
Calcium		0.05	0.03	1.49	0.13	-0.04	0.02	-1.46	0.14	**-0.09**	**0.04**	**-1.92**	**0.05**
Magnesium		-0.00	0.01	-0.23	0.81	-0.03	0.01	**-2.04**	**0.04**	-0.03	0.02	-1.18	0.23
Sum of bases		0.01	0.04	0.43	0.66	-0.10	0.05	**-2.08**	**0.03**	-0.12	0.07	-1.58	0.11

The models are fitted using maximum likelihood estimation, statistical significantly results are calculated with 95% of probability and shown in boldface type (P <0.1 (higher tendency and significant effects P < 0.05). The total phosphorus (P) is shown by mg kg^{-1} and the P fractions by µg g^{-1}, the resin, and HCl fractions are obtained first by using a membrane of anion exchange and hydrogen chloride respectively. The $NaHCO_3$ represents the total (Pt), inorganic (Pi), and Organic (Po) P fractions resulting from bicarbonate extraction, and the NaOH represents the total (Pt), inorganic (Pi) and Organic (Po) P fractions resulting by hydroxide extraction. Total organic and inorganic P represents the sum of their respective fractions of $NaHCO_3$ and NaOH. The extractable P represents the total of P which may be available represented by the sum of the organic and inorganic fractions ($NaHCO_3$ and NaOH) plus the resin and HCl, and the residual P is the difference between the total and the extractable P. The sum of bases represents the sum of potassium, calcium, and magnesium concentrations, that are present by extractable fractions in g kg^{-1}.

Table S4| Statistical results of elevated CO_2 effect on soil microbial activity. Data were analyzed using generalized linear mixed models with a specific model for each collection data and variable, considering the effect of the treatment as a fixed factor and controlling the spatial variability using the open-top chamber (OTC) as a random factor. The "*baseline*" collections were realized in August 2019 before starting the CO_2 enrichment to characterize the natural spatial variability, the "*elevated CO_2 experiment*" refers to after 12 months under elevated CO_2 (November 2020). The delta eCO_2 effect was calculated considering the difference between the collection after the increased CO_2 concentration (i.e., "elevated CO_2 experiment") and the baseline.

	Baseline				*Elevated CO_2 effect*				*Delta time eCO_2 effect*			
	Est.	Std. error	Z	*P*	Est.	Std. error	Z	*P*	Est.	Std. error	Z	*P*
Microbial C	53.32	118.82	0.44	0.65	**-77.8**	**39.25**	**-1.98**	**0.04**	-92.2	136.13	-0.67	0.49
Microbial N	-1.10	4.00	-0.27	0.78	-4.74	5.91	-0.80	0.42	0.01	5.49	0.00	0.99
Microbial P	**-1.24**	**0.61**	**-2.01**	**0.04**	**-0.65**	**0.38**	**-1.67**	**0.09**	0.75	0.68	1.10	0.27
Microbial C: N ratio	0.80	2.56	0.31	0.75	0.03	1.96	0.01	0.98	-1.60	2.72	-0.58	0.55
*Microbial C:P ratio	166.4	138.4	1.20	0.22	0.12	0.22	0.56	0.57	-148.4	163.2	-0.91	0.36
*Microbial N: P ratio	0.46	0.32	1.42	0.15	8.12	9.92	0.81	0.41	-28.39	20.55	-1.38	0.16
CB	**5.58**	**3.34**	**1.67**	**0.09**	-0.79	0.93	-0.85	0.39	**-6.41**	**2.63**	**-2.43**	**0.01**
BG	**2.80**	**0.99**	**2.81**	**0.004**	**-0.63**	**0.36**	**-1.71**	**0.08**	**-3.43**	**1.00**	**-3.4**	**<0.001**
NAG	1.85	3.33	0.55	0.57	0.03	0.83	0.04	0.96	-1.82	3.8	-0.48	0.63
AP	-34.82	123.5	-0.28	0.77	**-34.62**	**20.23**	**-1.71**	**0.08**	0.20	118.8	0.00	0.99
C: NAG ratio (log)	0.13	0.21	0.61	0.54	-0.01	0.45	-0.03	0.97	2.80	2.54	1.10	0.26
C: AP ratio (log)	**0.13**	**0.05**	**2.29**	**0.02**	-0.03	0.03	-1.15	0.24	**-0.16**	**0.04**	**-4.03**	**<0.001**
N: P ratio (log)	0.09	0.05	1.50	0.13	0.01	0.03	0.42	0.66	-0.07	0.08	-0.90	0.36
C enzyme: microbial ratio	0.02	0.03	0.65	0.51	-0.00	0.00	-0.14	0.88	-0.02	0.03	-0.77	0.43
N enzyme: microbial ratio	0.01	0.07	0.17	0.86	0.04	0.03	1.30	0.19	0.03	0.08	0.38	0.70
P enzyme: microbial ratio	0.19	0.29	0.65	0.51	12.75	14.17	0.89	0.36	-60.18	42.87	-1.40	0.16

The models are fitted using maximum likelihood estimation, statistical significant results are calculated with 95% of probability and shown in boldface type (P <0.1 (higher tendency and significant effects P < 0.05). Total of carbon (C), nitrogen (N), and phosphorus (P) immobilized on microbial biomass and its stoichiometric ratio. The cellobiosidase (CB) and β-1,4-glucosidase (BG) are enzymes responsible for hydrolyzing the carbon, β-1,4-N-acetylglucosaminidase (NAG) for the nitrogen and acid phosphatase (AP) for the organic phosphorus. Enzyme stoichiometry was calculated using the log ratio of activity rates, the carbon enzymes are represented by the sum of cellobiosidase (CB) and β-1,4-glucosidase (BG) activity. The stoichiometry of enzymes and microbial biomass was obtained by the ratio of CNP enzymes and CNP microbial biomass.

Figure S1 | Open top chamber structure. The figure illustrates (a) the design of an Open Top Chamber (OTC) structure, (b) the canopy open and (c) soil area used for investigating the effect of the increase in the CO_2 concentrations on understory plants. The OTC structure consists of a transparent polypropylene chamber with 3 m of height and 2.4 cm of diameter. Images: Maria Juliana, Flavia Santana.

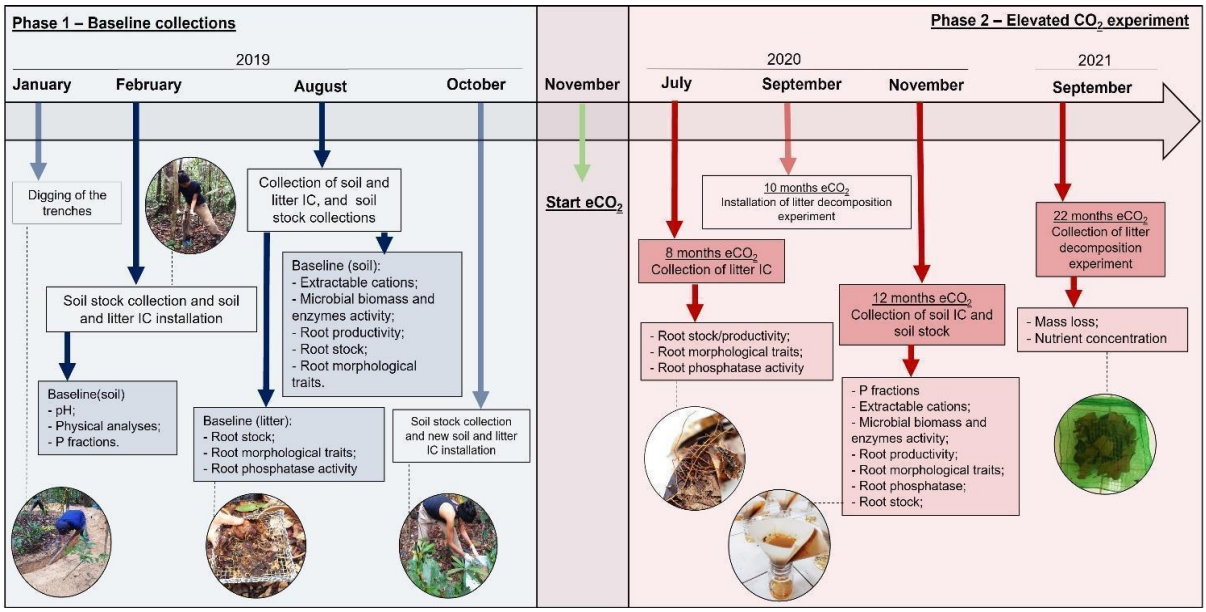

Figure S2 | Timeline of belowground collections of the Open-top chambers experiment. The experiment consists of two phases. The baseline (Phase 1) occurred throughout the year 2019 and this time realized all processes to prepare, install and realize the initial collections to make a complete characterization inside of the OTCs. The soil and surface ingrowth cores were zeroed out before the start of the increase in CO_2 concentrations by November 2019. Phase 2 consists of the currently elevated CO_2 experiment; For the dynamic of fine root up to the litter layer we have a collection after *8 months of elevated CO_2 (July 2020), the litter decomposition experiment was installed in September 2020 and realized a single collection after one year (September 2021). The soil fine root dynamic was collected after *12 months under elevated CO_2 (November 2020), at the same time was collected the root stock and soil samples to analyze nutrient concentrations and microbial activity (microbial CNP biomass and enzymes). *Due to the global pandemic of COVID 19 all the collections were adjusted considering the possibility of going to the field and to the laboratory, this resulted in different times for some variables.

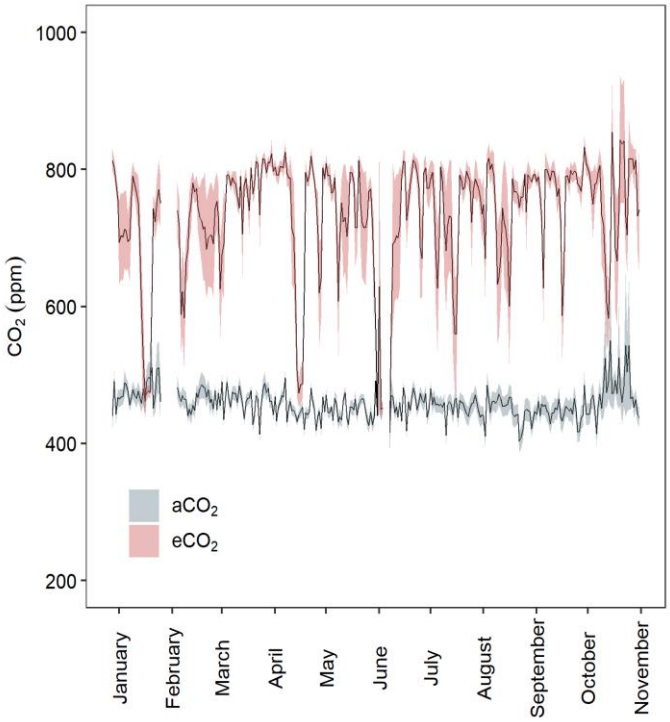

Figure S3 | Concentration of CO_2 inside the Open-top chambers throughout the year 2020. The lines show the daily average and standard error (n=4), the gray lines represent the ambient CO_2 concentration (aCO_2), and the red line is the elevated CO_2 (eCO_2). The data represent the period between November 1, 2019, and November 1, 2020, where 92% of the time has maintained an increase in CO2 concentration on average by 270 ppm.

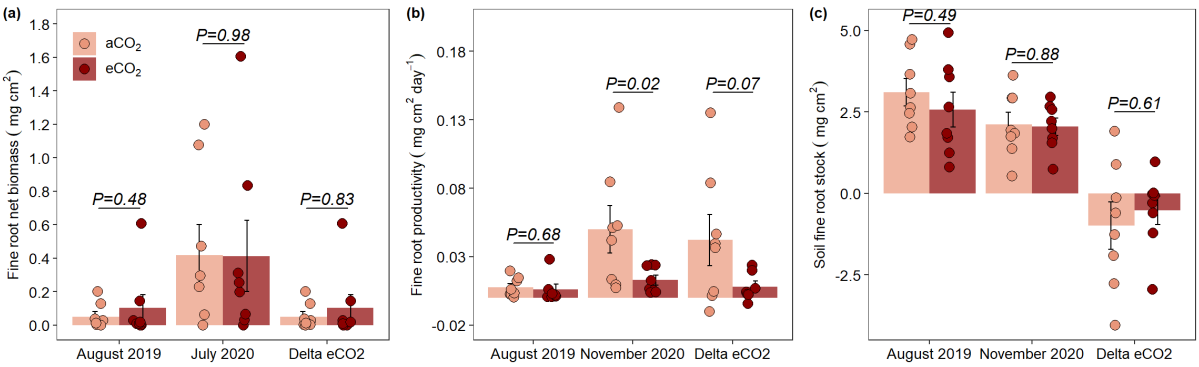

Figure S4 | Elevated CO_2 effect on fine root net biomass in the litter layer (a), fine root productivity (b) fine root stock in the soil (c). For each plot, we show the baseline collections (August 2019) that are realized before to start of elevated CO_2, the collection after 8 months of elevated CO_2 (July 2020) for the litter layer, after 12

months (November 2020) for the soil root, and the delta elevated CO_2 effect for booths (litter and soil). The delta eCO_2 effect was calculated considering the difference between the collection after the increased CO_2 concentration (i.e., 8 months for the litter and 12 months for the soil) and the baseline. Data were analyzed using generalized linear mixed models with a specific model for each collection data and variable, considering the effect of the treatment as a fixed factor and controlling the spatial variability using the open-top chamber (OTC) as a random factor (see "Methods" for details). The numbers at the top of the bars indicate no significant (ns) or significant differences among ambient CO_2 (aCO_2) and elevated CO_2 (eCO_2); *p<0.05, ** p<0.01, and ***p<0.001. The bars showed the mean and standard error of n=8, and the points indicate the samples for each group.

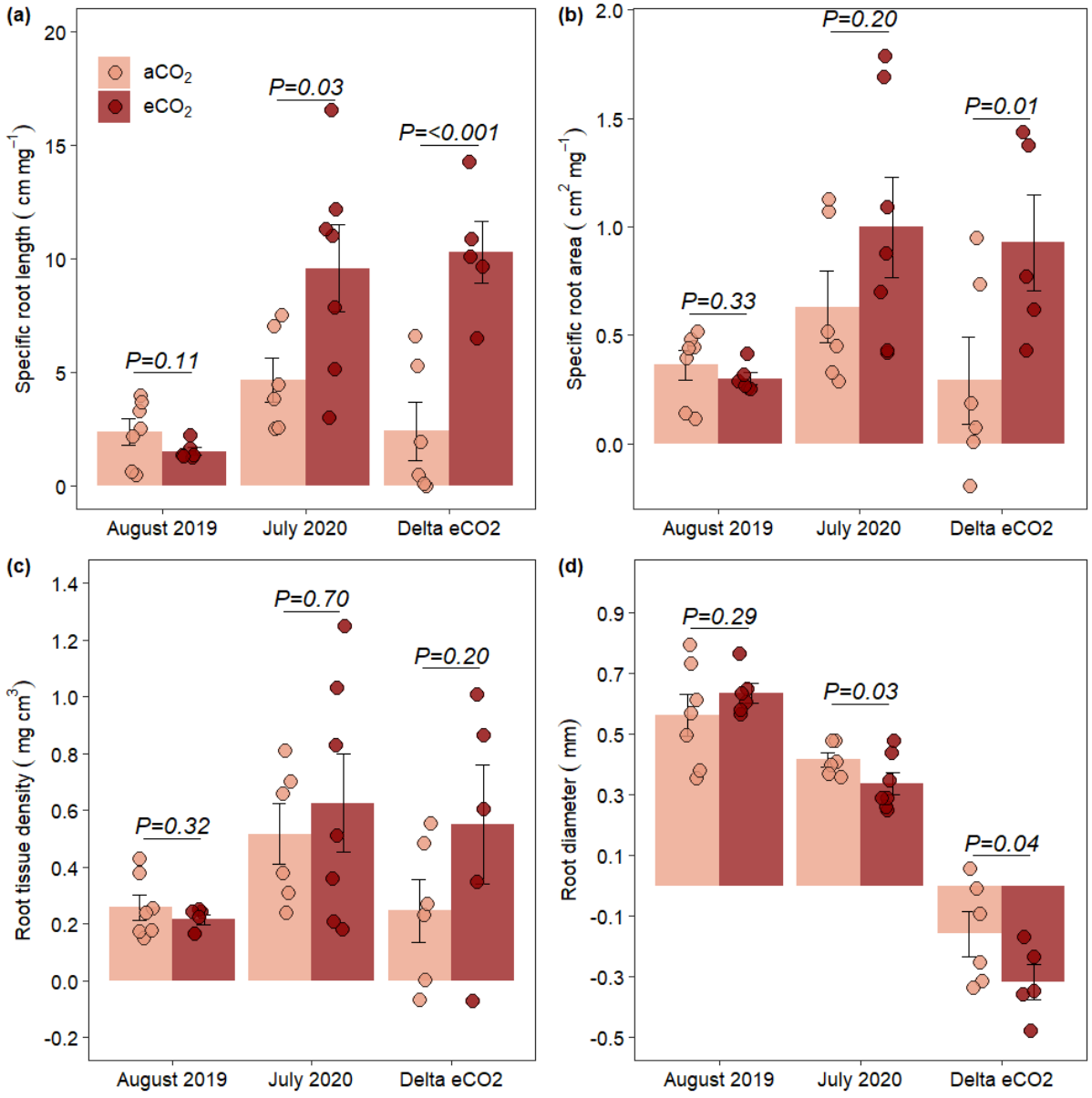

Figure S5 | Elevated CO_2 effect on fine root morphological parameters in the litter layer. (a) specific root length (SRL), (b) specific root area (SRA), (c) root tissue density (RTD), and (d) root diameter. For each plot, we show the baseline collections (August 2019) that are realized before the start of elevated CO_2, the collection after 8 months of elevated CO_2 (July 2020), and the delta elevated CO_2 effect. The delta eCO_2 effect was calculated considering the difference between the collection after the increased CO_2 concentration (i.e., 8 months for the litter) and the baseline. Data were analyzed using generalized linear mixed models with a specific model for each collection data and variable, considering the effect of the treatment as a fixed factor and controlling the spatial variability using the open-top chamber (OTC) as a random factor (see "Methods" for details). The numbers at the top of the bars indicate no significant (ns) or significant differences among ambient CO_2 (aCO_2) and elevated CO_2

(eCO_2); *p<0.05, ** p<0.01, and ***p<0.001. The bars showed the mean and standard error of n=8, and the points indicate the samples for each group.

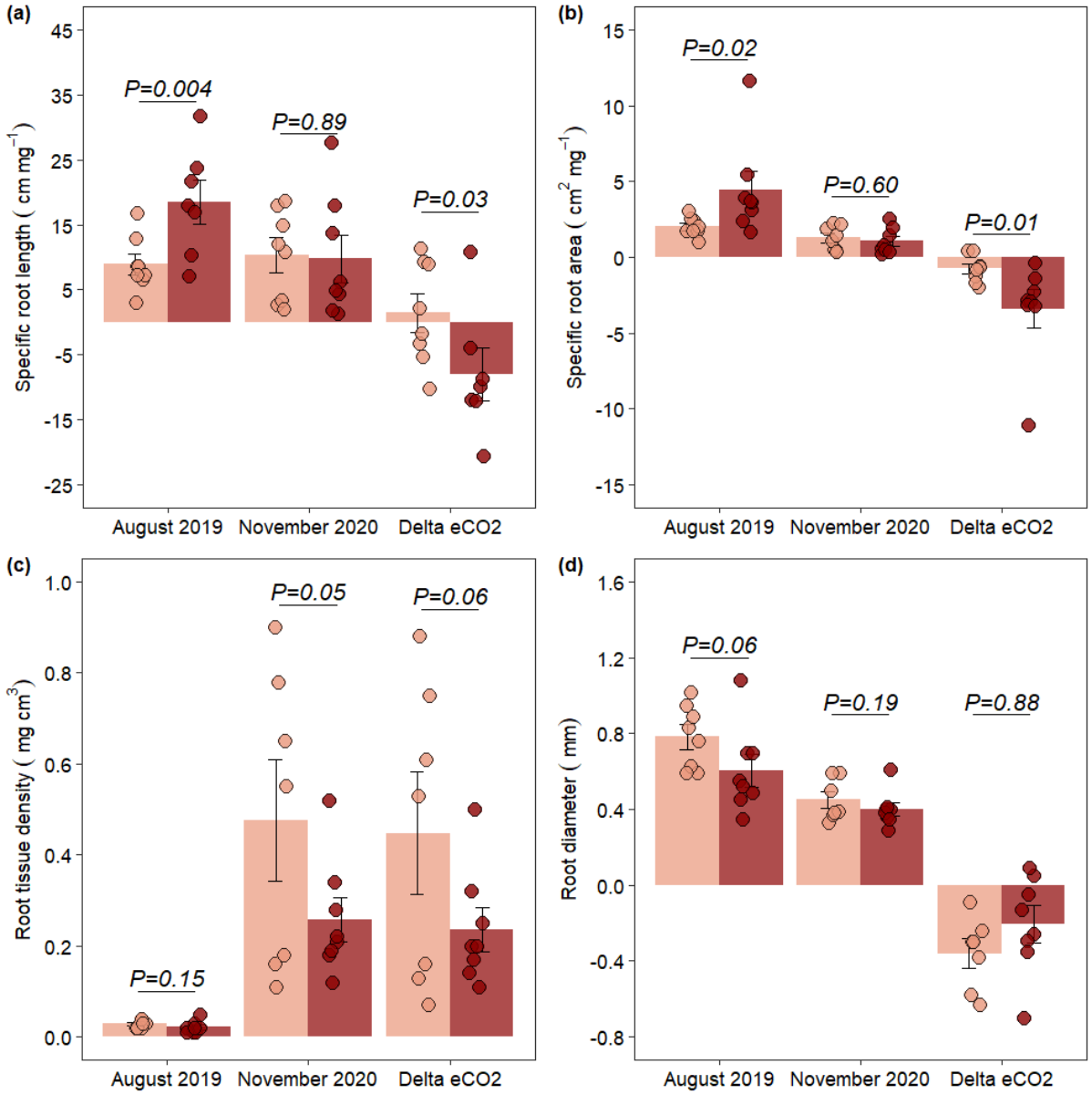

Figure S6 | Elevated CO_2 effect on fine root morphological parameters in the soil. (a) specific root length (SRL), (b) specific root area (SRA), (c) root tissue density (RTD), and (d) root diameter. For each plot, we show the baseline collections (August 2019) that are realized before the start of elevated CO_2, the collection after 12 months of elevated CO_2 (November 2020), and the delta elevated CO_2 effect. The delta eCO_2 effect was calculated considering the difference between the collection after the increased CO_2 concentration (i.e., 12 months) and the baseline. Data were analyzed using generalized linear mixed models with a specific model for each collection data and variable, considering the effect of the treatment as a fixed factor and controlling the spatial variability using the open-top chamber (OTC) as a random factor (see "Methods" for details). The numbers at the top of the bars indicate no significant (ns) or significant differences among ambient CO_2 (aCO_2) and elevated CO_2 (eCO_2); *p<0.05, ** p<0.01, and ***p<0.001. The bars showed the mean and standard error of n=8, and the points indicate the samples for each group.

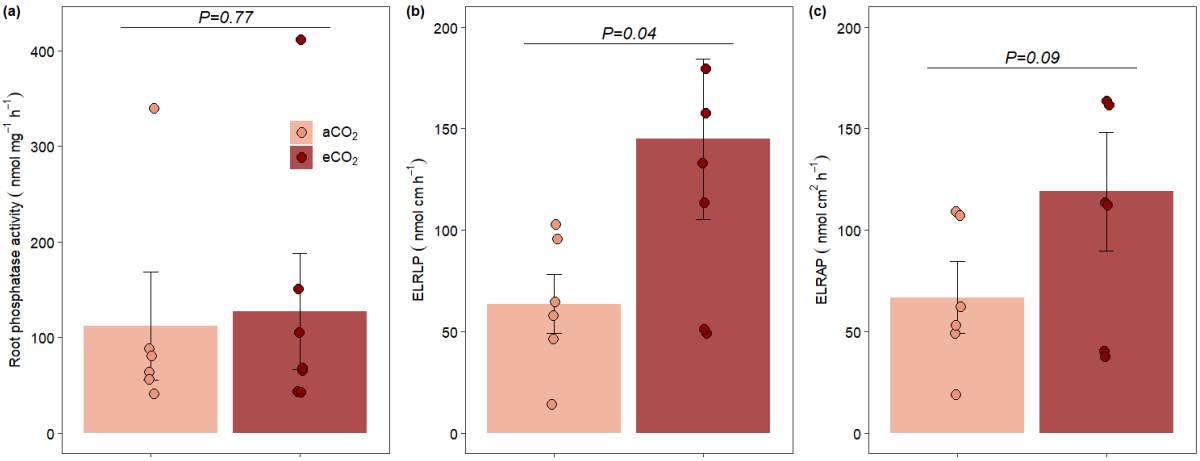

Figure S7 | Elevated CO_2 effect on fine root acid phosphatase activity in the litter layer. Effects of eCO_2 on (a) root phosphatase activity by mg of the dry root, (b) ecosystem upscale of root phosphatase activity by cm to total SRL (ELRLP), (c) ecosystem upscale of root phosphatase activity by cm to total SRA (ELRAP). For each plot, we are shown only the collection after 8 months of elevated CO_2 (July 2020). Data were analyzed using generalized linear mixed models considering the effect of the treatment as a fixed factor and controlling the spatial variability using the open-top chamber (OTC) as a random factor (see "Methods" for details). The numbers at the top of the bars indicate no significant (ns) or significant differences among ambient CO_2 (aCO_2) and elevated CO_2 (eCO_2); *p<0.05, ** p<0.01, and ***p<0.001. The bars showed the mean and standard error of n=8, and the points indicate the samples for each group.

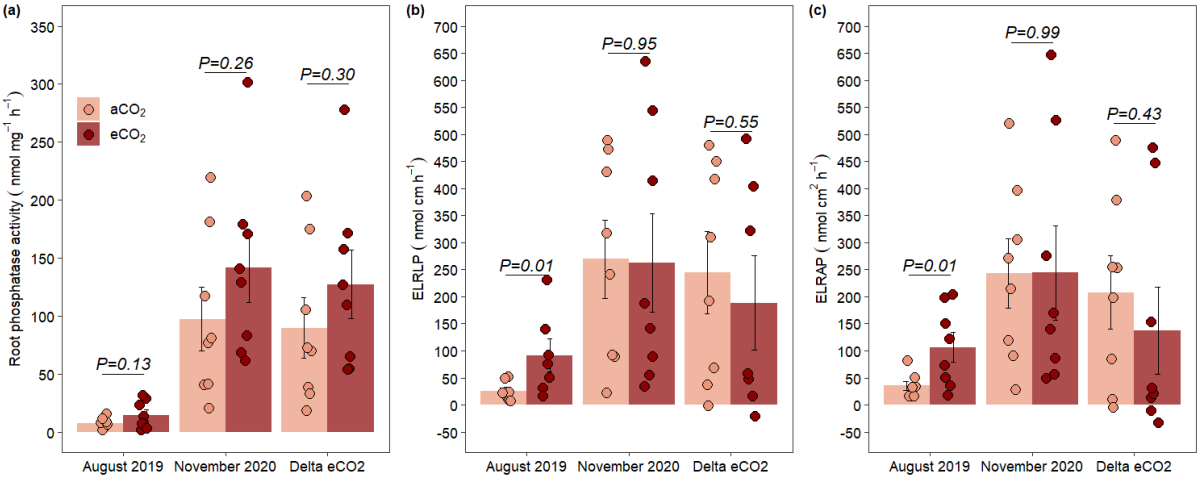

Figure S8 | Elevated CO_2 effect on fine root acid phosphatase activity in the soil. Effects of eCO_2 on (a) root phosphatase activity per mg of dry root, (b) ecosystem upscale of root phosphatase activity by cm to total root length (ELRLP), (c) ecosystem upscale of root phosphatase activity by cm to total root area (ELRAP). For each plot, we show the baseline collections (August 2019) that are realized before the start of elevated CO_2, the collection after 12 months of elevated CO_2 (November 2020), and the delta elevated CO_2 effect. The delta eCO_2 effect was calculated considering the difference between the collection after the increased CO_2 concentration (i.e., 12 months) and the baseline. Data were analyzed using generalized linear mixed models with a specific model for each collection data and variable, considering the effect of the treatment as a fixed factor and controlling the spatial variability using the open-top chamber (OTC) as a random factor (see "Methods" for details). The numbers at the top of the bars indicate no significant (ns) or significant differences among ambient CO_2 (aCO_2) and elevated CO_2 (eCO_2); *p<0.05, ** p<0.01, and ***p<0.001. The bars showed the mean and standard error of n=8, and the points indicate the samples for each group.

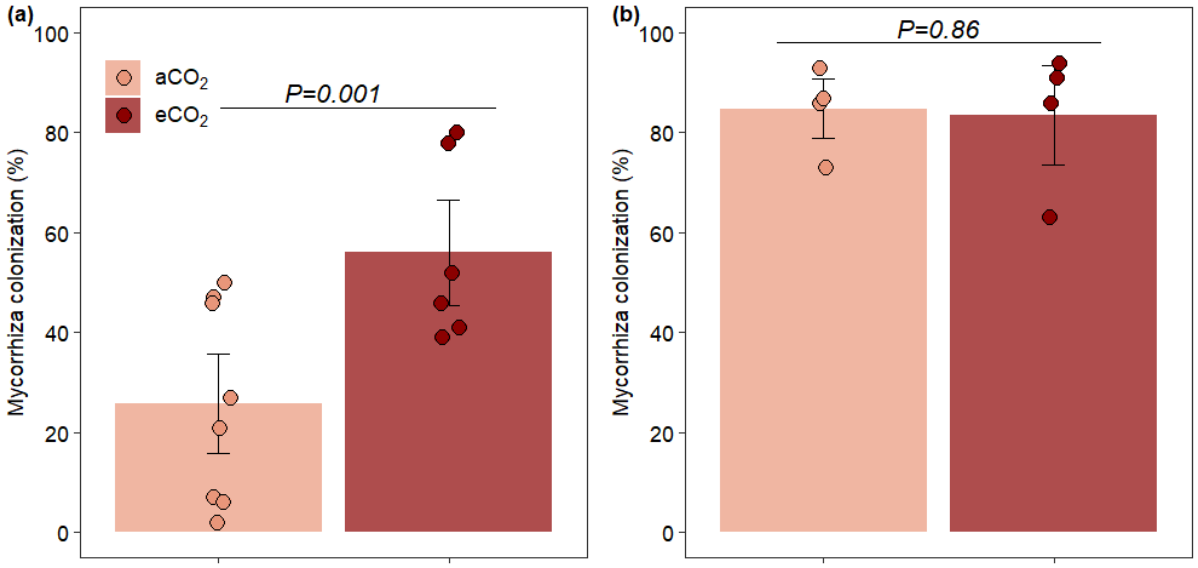

Figure S9 | Elevated CO_2 effect on total root arbuscular mycorrhiza colonization (% of root length) in the soil and litter. The graphic represents a collection after 12 months under elevated CO_2 (November 2020) for the soil and for the litter (September 2021). For the litter we used the data of fine root growing inside of the litter bags in the litter decomposition experiment. Data were analyzed using generalized linear mixed models considering the effect of the treatment as a fixed factor and controlling the spatial variability using the open-top chamber (OTC) as a random factor (see "Methods" for details). The numbers at the top of the bars indicate no significant (ns) or significant differences among ambient CO_2 (aCO_2) and elevated CO_2 (eCO_2); *p<0.05, ** p<0.01, and ***p<0.001. The bars showed the mean and standard error of n=8 for the soil plot with the points indicate the samples for each group, and n=4 for the litter with the points indicate a single sample by OTC.

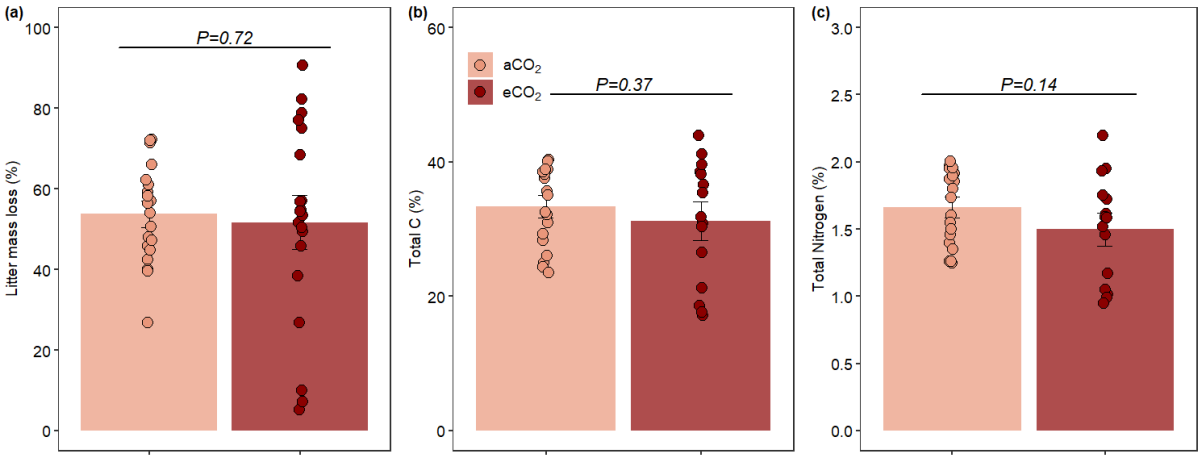

Figure S10 | Elevated CO_2 effect on litter decomposition parameters. (a) litter mass loss, (b) a total of carbon (C) and (c) nitrogen (N) in the litter mass after one year in the field exposed under elevated CO_2. Data were analyzed using generalized linear mixed models considering the effect of the treatment as a fixed factor and controlling the spatial variability using the open-top chamber (OTC) as a random factor (see "Methods" for details). The numbers at the top of the bars indicate no significant (ns) or significant differences among ambient CO_2 (aCO_2) and elevated CO_2 (eCO_2); *p<0.05, ** p<0.01, and ***p<0.001. The bars showed the mean and standard error of n=20, and the points indicate the samples for each group.

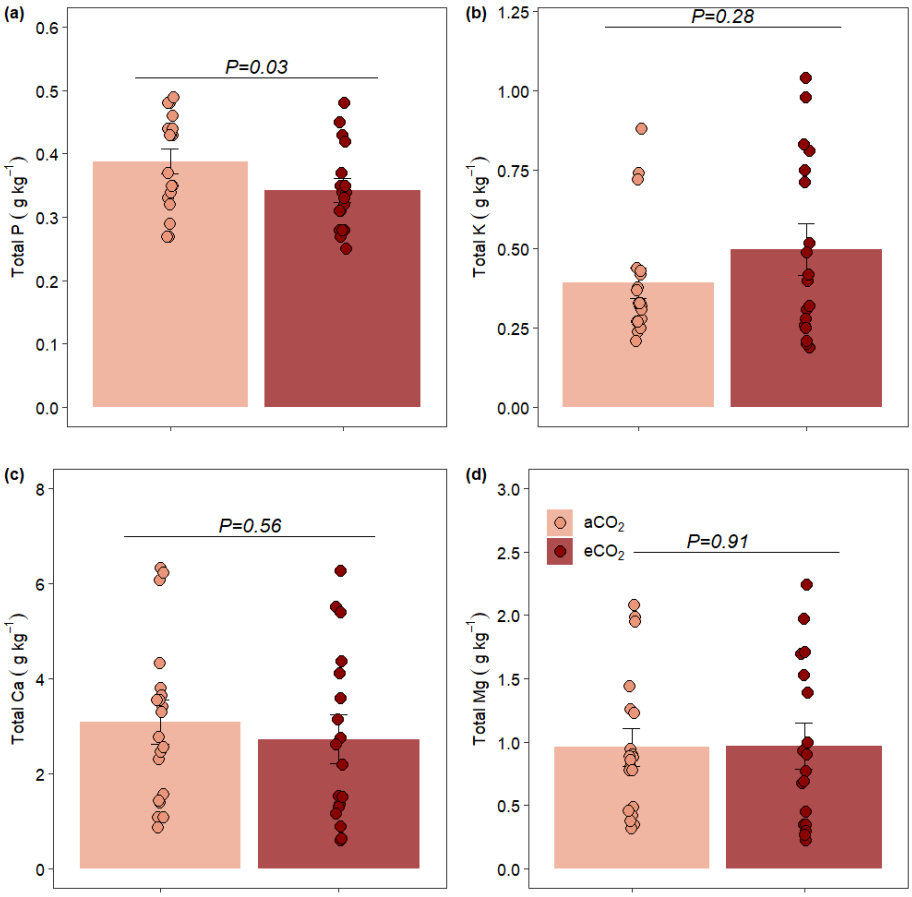

Figure S11 | Elevated CO_2 effect on leaf litter nutrient concentration. (a) total phosphorus (P), (b) total potassium (K), (c) total calcium (Ca), and (d) total magnesium (Mg) in the leaf litter mass after one year in the field exposed under elevated CO_2. Data were analyzed using generalized linear mixed models considering the effect of the treatment as a fixed factor and controlling the spatial variability using the open-top chamber (OTC) as a random factor (see "Methods" for details). The numbers at the top of the bars indicate no significant (ns) or significant differences among ambient CO_2 (aCO_2) and elevated CO_2 (eCO_2); *p<0.05, ** p<0.01, and ***p<0.001. The bars showed the mean and standard error of n=20, and the points indicate the samples for each group.

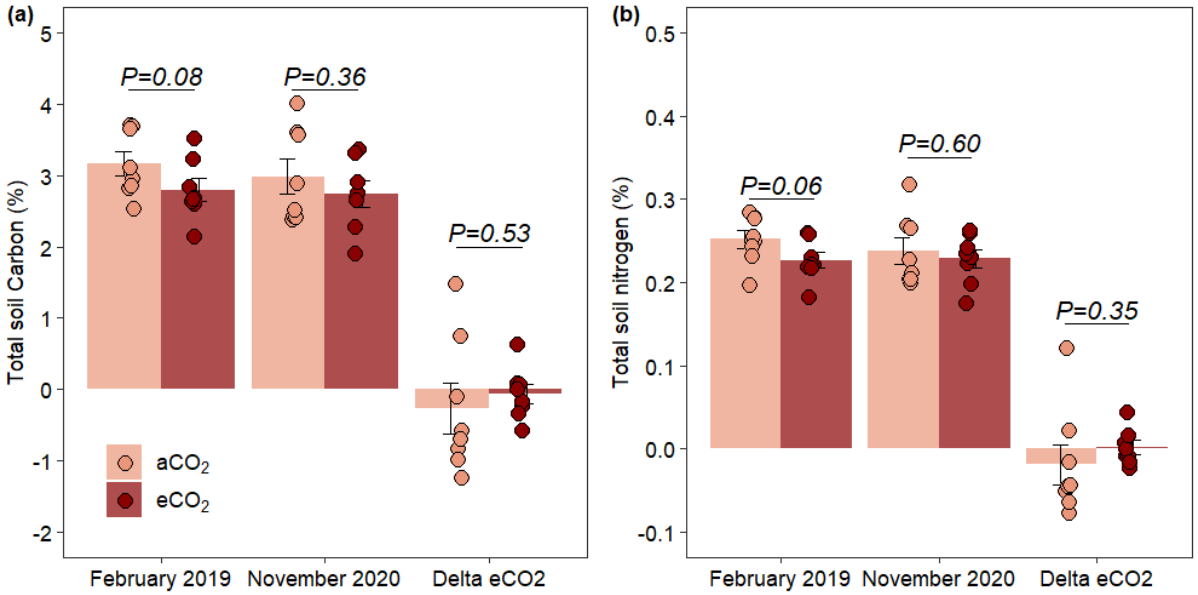

Figure S12 | Elevated CO_2 effect on soil carbon and nitrogen dynamic. The (a) percent of total soil carbon and (b) the percent of total soil N for baseline collections (August 2019) that are realized before to start of elevated CO_2, the collection after 12 months of elevated CO_2 (November 2020), and the delta elevated CO_2 effect. The delta eCO_2 effect was calculated considering the difference between the collection after the increased CO_2 concentration (i.e., 12 months) and the baseline. Data were analyzed using generalized linear mixed models with a specific model for each collection data and variable, considering the effect of the treatment as a fixed factor and controlling the spatial variability using the open-top chamber (OTC) as a random factor (see "Methods" for details). The numbers at the top of the bars indicate no significant (ns) or significant differences among ambient CO_2 (aCO_2) and elevated CO_2 (eCO_2); *p<0.05, ** p<0.01, and ***p<0.001. The bars showed the mean and standard error of n=8, and the points indicate the samples for each group.

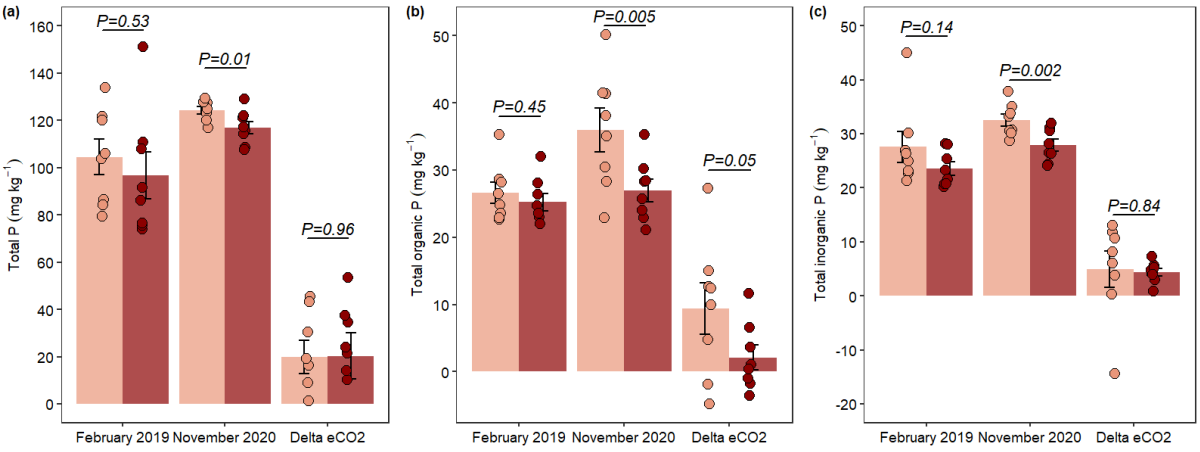

Figure S13 | Elevated CO_2 effect on soil phosphorus dynamic. The (a) total phosphorus (P) was obtained by sulfuric digestion, (b) total organic, and (c) inorganic P was obtained by the Hedley soil P fractionate methodology. Total organic (P_O) and inorganic (P_i) P fractions represent the sum of their respective fractions of $NaHCO_3$ and NaOH. For each plot, we show the baseline collections (August 2019) that are realized before the start of elevated CO_2, the collection after 12 months of elevated CO_2 (November 2020), and the delta elevated CO_2 effect. The delta eCO_2 effect was calculated considering the difference between the collection after the increased CO_2 concentration (i.e., 12 months) and the baseline. Data were analyzed using generalized linear mixed models with a specific model for each collection data and variable, considering the effect of the treatment as a fixed factor and controlling the spatial variability using the open-top chamber (OTC) as a random factor (see "Methods" for details). The numbers at the top of the bars indicate no significant (ns) or significant differences among ambient CO_2 (aCO_2) and elevated CO_2 (eCO_2); *p<0.05, ** p<0.01, and ***p<0.001. The bars showed the mean and standard error of n=8, and the points indicate the samples for each group.

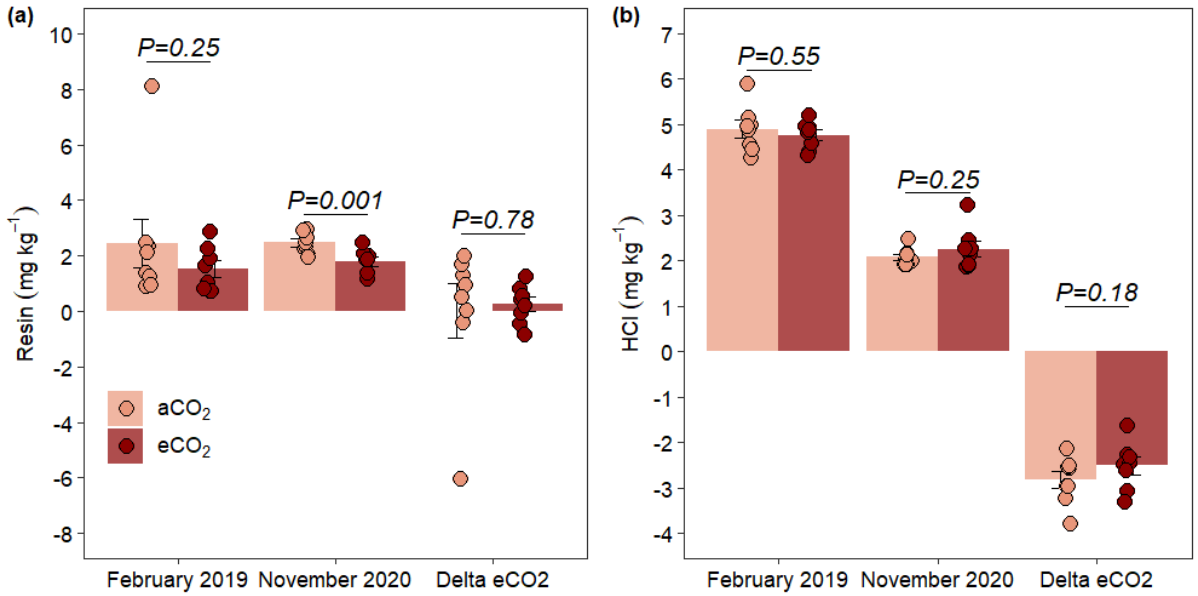

Figure S14 | Elevated CO_2 effect on soil phosphorus fractions. The soil P fractions were obtained by the Hedley soil P fractionate methodology (see "Methods" for details), the resin P fraction (a) was the first fraction obtained by a membrane of anion exchange, followed by the extraction of (b) hydrogen chloride fraction (HCl). For each plot, we show the baseline collections (February 2019) that are realized before the start of elevated CO_2, the collection after 12 months of elevated CO_2 (November 2020), and the delta elevated CO_2 effect. The delta eCO_2 effect was calculated considering the difference between the collection after the increased CO_2 concentration (i.e., 12 months) and the baseline. Data were analyzed using generalized linear mixed models with a specific model for each collection data and variable, considering the effect of the treatment as a fixed factor and controlling the spatial variability using the open-top chamber (OTC) as a random factor (see "Methods" for details). The numbers at the top of the bars indicate no significant (ns) or significant differences among ambient CO_2 (aCO_2) and elevated CO_2 (eCO_2); *p<0.05, ** p<0.01, and ***p<0.001. The bars showed the mean and standard error of n=8, and the points indicate the samples for each group.

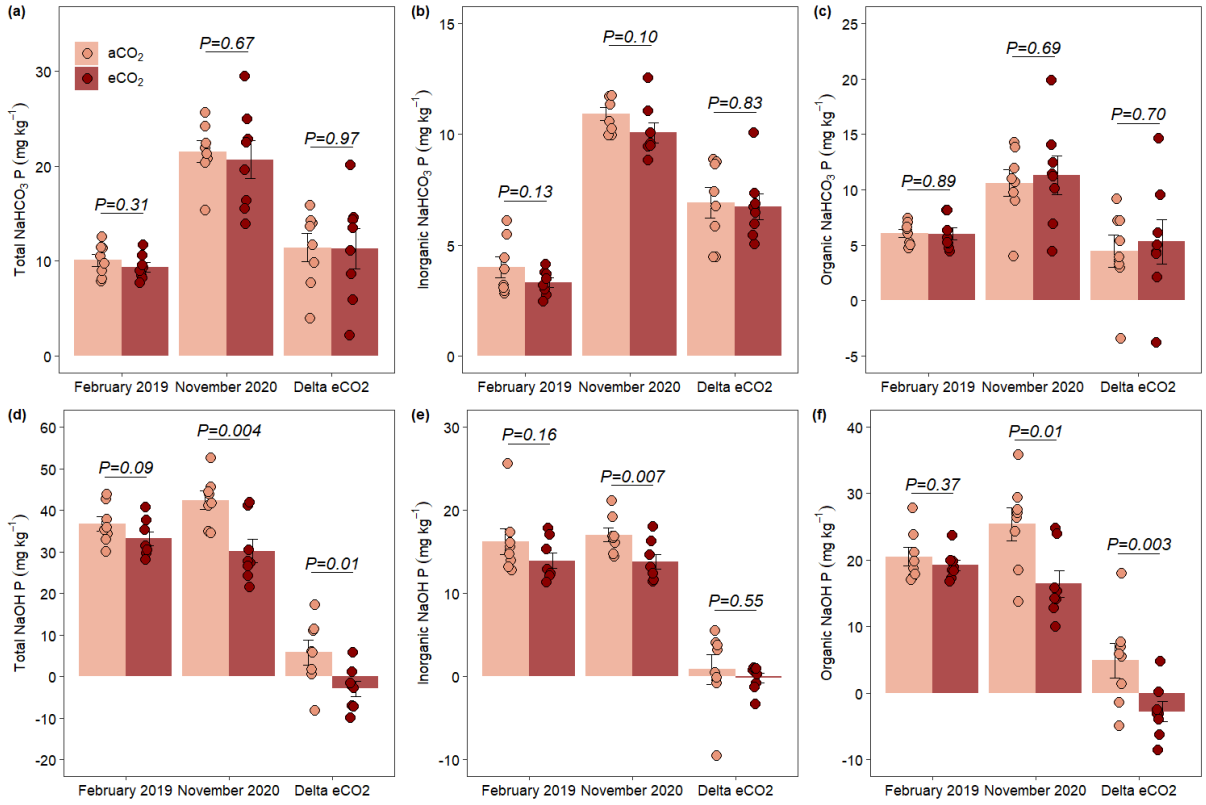

Figure S15 | Elevated CO_2 effect on soil phosphorus fractions. The soil P fractions were obtained by the Hedley soil P fractionate methodology (see "Methods" for details), the $NaHCO_3$ represents the fractions of P resulting from bicarbonate extraction: (a) total bicarbonate P, (b) inorganic bicarbonate P and (c) organic bicarbonate P (difference between total and inorganic). The NaOH P fractions resulted from the hydroxide extraction: (d) total hydroxide P, (e) inorganic hydroxide P, and (f) organic hydroxide P (difference between total and inorganic). For each plot, we show the baseline collections (February 2019) that are realized before the start of elevated CO_2, the collection after 12 months of elevated CO_2 (November 2020), and the delta elevated CO_2 effect. The delta eCO_2 effect was calculated considering the difference between the collection after the increased CO_2 concentration (i.e., 12 months) and the baseline. Data were analyzed using generalized linear mixed models with a specific model for each collection data and variable, considering the effect of the treatment as a fixed factor and controlling the spatial variability using the open-top chamber (OTC) as a random factor (see "Methods" for details). The numbers at the top of the bars indicate no significant (ns) or significant differences among ambient CO_2 (aCO_2) and elevated CO_2 (eCO_2); *p<0.05, ** p<0.01, and ***p<0.001. The bars showed the mean and standard error of n=8, and the points indicate the samples for each group.

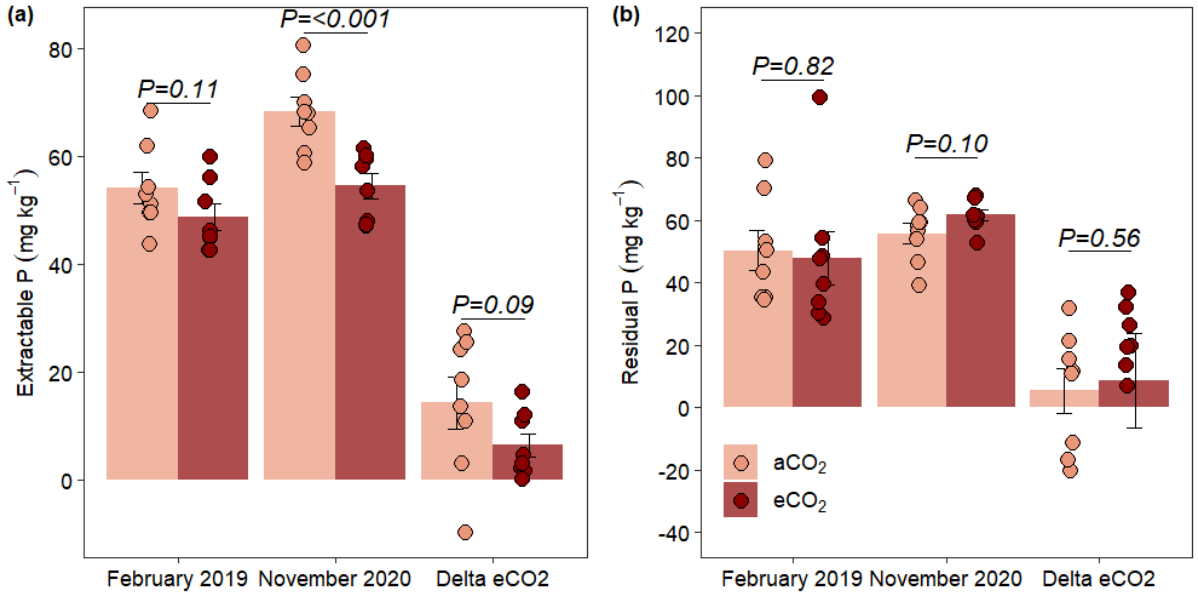

Figure S16 | Elevated CO_2 effect on soil phosphorus fractions. The soil P fractions were obtained by the Hedley soil P fractionate methodology (see "Methods" for details), the (a) extractable P represents the total of P which may be available represented by the sum of the organic and inorganic fractions ($NaHCO_3$ and NaOH) plus the resin and HCl. The (b) residual P was obtained by the difference between total and extractable P and represents the unavailable P. For each plot, we show the baseline collections (February 2019) that are realized before the start of elevated CO_2, the collection after 12 months of elevated CO_2 (November 2020), and the delta elevated CO_2 effect. The delta eCO_2 effect was calculated considering the difference between the collection after the increased CO_2 concentration (i.e., 12 months) and the baseline. Data were analyzed using generalized linear mixed models with a specific model for each collection data and variable, considering the effect of the treatment as a fixed factor and controlling the spatial variability using the open-top chamber (OTC) as a random factor (see "Methods" for details). The numbers at the top of the bars indicate no significant (ns) or significant differences among ambient CO_2 (aCO_2) and elevated CO_2 (eCO_2); *p<0.05, ** p<0.01, and ***p<0.001. The bars showed the mean and standard error of n=8, and the points indicate the samples for each group.

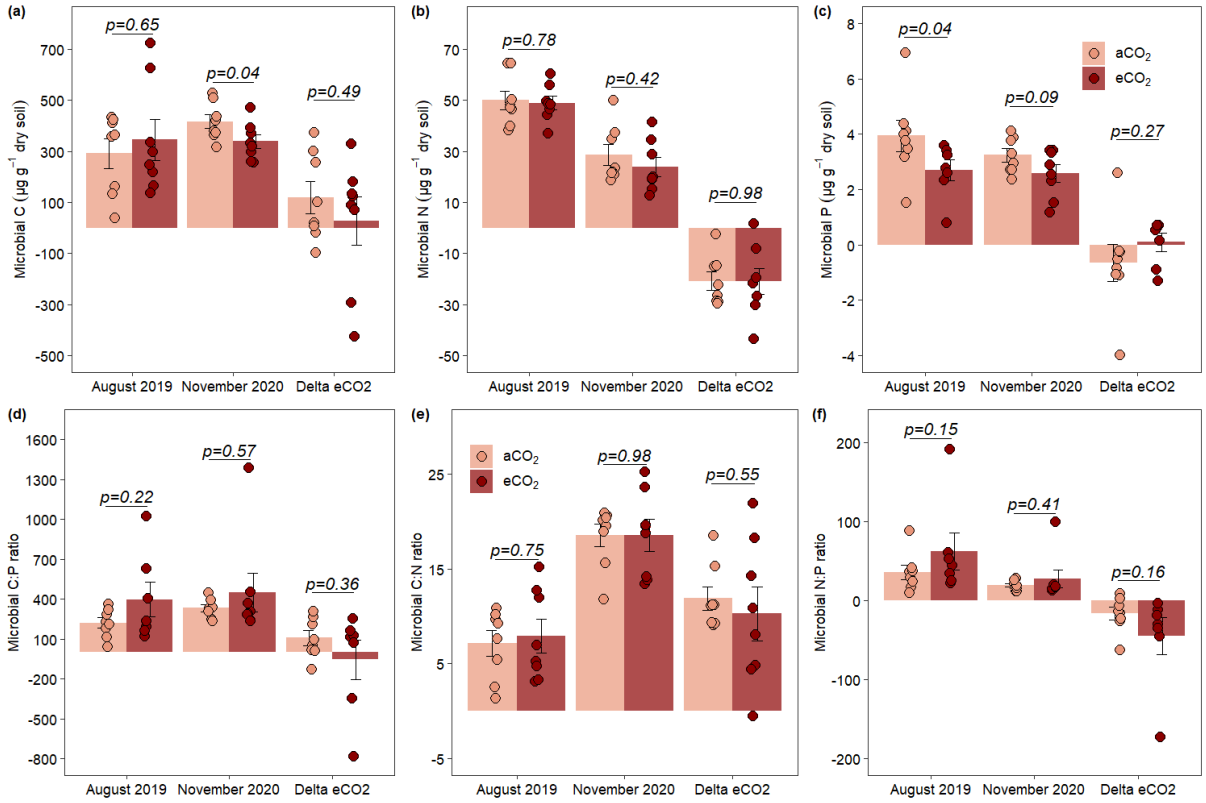

Figure S17 | Elevated CO_2 effect on soil microbial biomass and stoichiometry. Total of (a) carbon (b) nitrogen and (c) phosphorus immobilized on microbial biomass and the microbial ratio of (d) carbon and phosphorus, (e) carbon and nitrogen, and (d) nitrogen and phosphorus. For each plot, we show the baseline collections (August 2019) that are realized before the start of elevated CO_2, the collection after 12 months of elevated CO_2 (November 2020), and the delta elevated CO_2 effect. The delta eCO_2 effect was calculated considering the difference between the collection after the increased CO_2 concentration (i.e., 12 months) and the baseline. Data were analyzed using generalized linear mixed models with a specific model for each collection data and variable, considering the effect of the treatment as a fixed factor and controlling the spatial variability using the open-top chamber (OTC) as a random factor (see "Methods" for details). The numbers at the top of the bars indicate no significant (ns) or significant differences among ambient CO_2 (aCO_2) and elevated CO_2 (eCO_2); *p<0.05, ** p<0.01, and ***p<0.001. The bars showed the mean and standard error of n=8, and the points indicate the samples for each group.

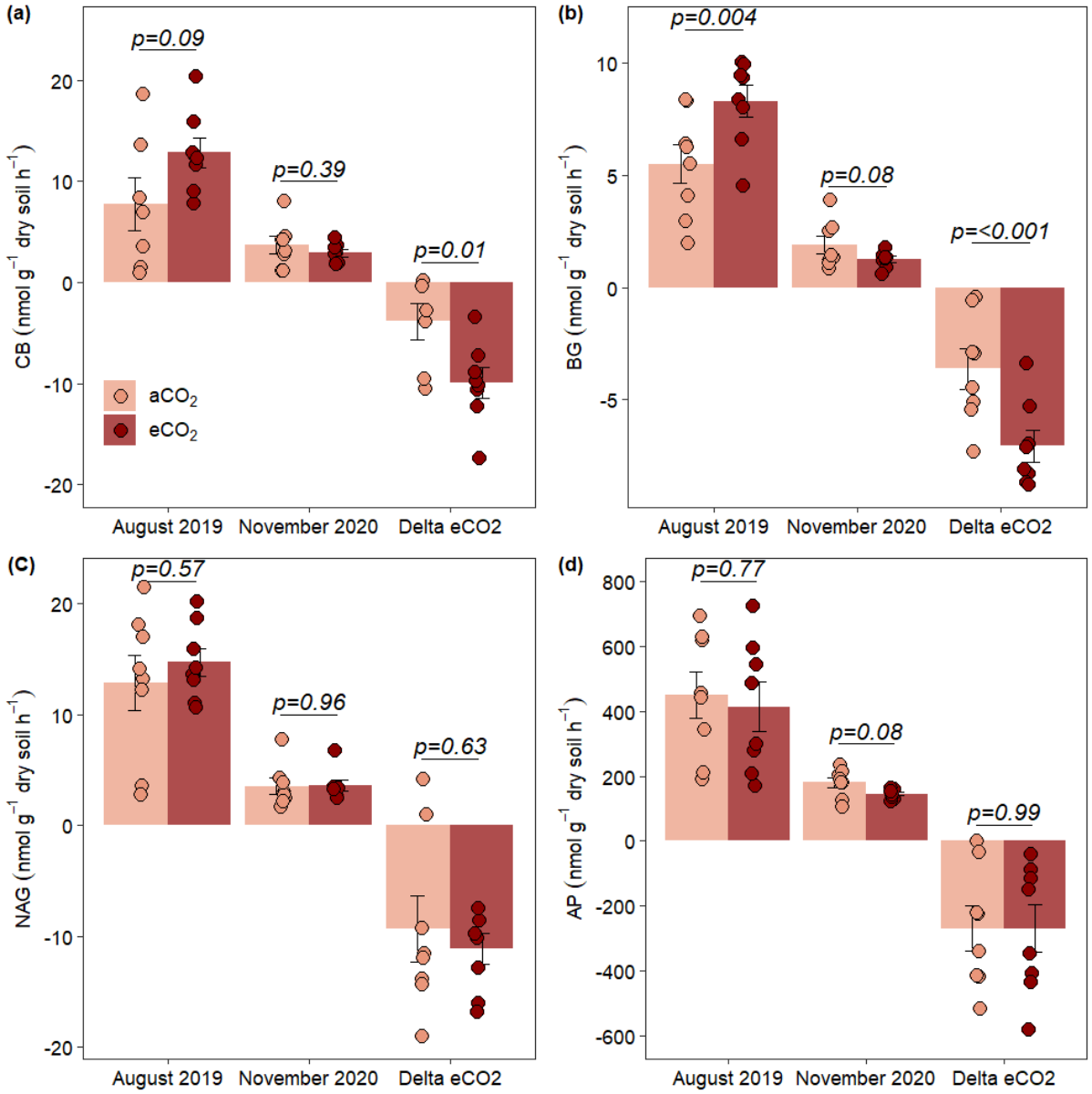

Figure S18 | Elevated CO_2 effect on soil enzymes activity. The (a) cellobiosidase (CB) and (b) β-1,4-glucosidase (BG) are responsible for hydrolyzing the carbon, (c) β-1,4-N-acetylglucosaminidase (NAG) for the nitrogen and (d) acid phosphatase (AP) for the organic phosphorus. For each plot, we show the baseline collections (August 2019) that are realized before the start of elevated CO_2, the collection after 12 months of elevated CO_2 (November 2020), and the delta elevated CO_2 effect. The delta eCO_2 effect was calculated considering the difference between the collection after the increased CO_2 concentration (i.e., 12 months) and the baseline. Data were analyzed using generalized linear mixed models with a specific model for each collection data and variable, considering the effect of the treatment as a fixed factor and controlling the spatial variability using the open-top chamber (OTC) as a random factor (see "Methods" for details). The numbers at the top of the bars indicate no significant (ns) or significant differences among ambient CO_2 (aCO_2) and elevated CO_2 (eCO_2); *p<0.05, ** p<0.01, and ***p<0.001. The bars showed the mean and standard error of n=8, and the points indicate the samples for each group.

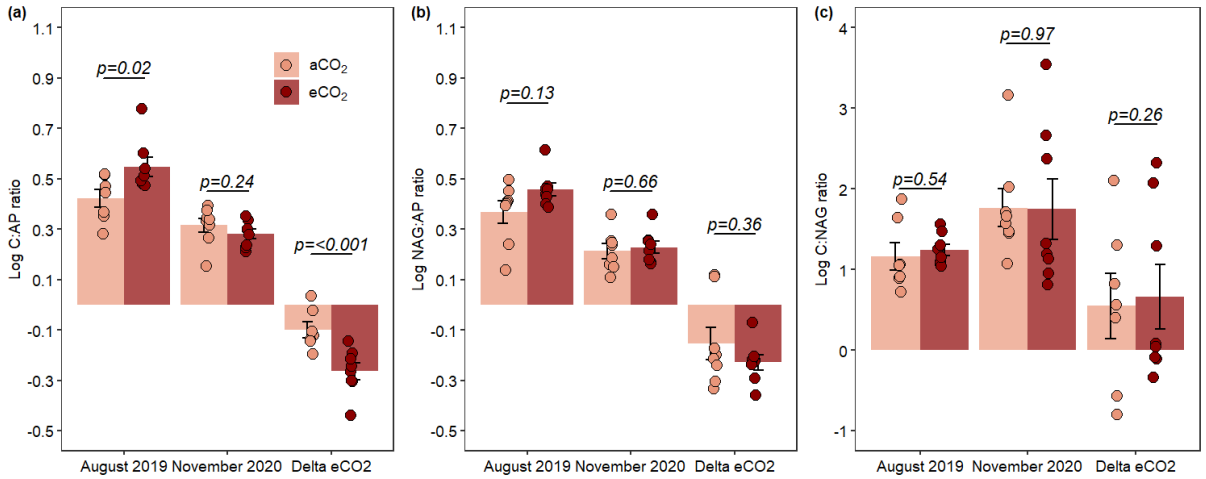

Figure S19 | Elevated CO_2 effect on soil enzymes stoichiometry. The stoichiometry was obtained by the log ratio, and the carbon enzymes are represented by the sum of cellobiosidase (CB) and β-1,4-glucosidase (BG) activity. The ratio of investment for (a) carbon and phosphorus acquisition is shown by the ratio of the total of C enzymes by acid phosphatase; (b) nitrogen and phosphorus acquisition investments are represented by the ratio of β-1,4-N-acetylglucosaminidase (NAG) and acid phosphatase (AP); and (c) the carbon and nitrogen acquisition investments are represented by the ratio of the total of C enzymes and β-1,4-N-acetylglucosaminidase (NAG). For each plot, we show the baseline collections (August 2019) that are realized before the start of elevated CO_2, the collection after 12 months of elevated CO_2 (November 2020), and the delta elevated CO_2 effect. The delta eCO_2 effect was calculated considering the difference between the collection after the increased CO_2 concentration (i.e., 12 months) and the baseline. Data were analyzed using generalized linear mixed models with a specific model for each collection data and variable, considering the effect of the treatment as a fixed factor and controlling the spatial variability using the open-top chamber (OTC) as a random factor (see "Methods" for details). The numbers at the top of the bars indicate no significant (ns) or significant differences among ambient CO_2 (aCO_2) and elevated CO_2 (eCO_2); *p<0.05, ** p<0.01, and ***p<0.001. The bars showed the mean and standard error of n=8, and the points indicate the samples for each group.

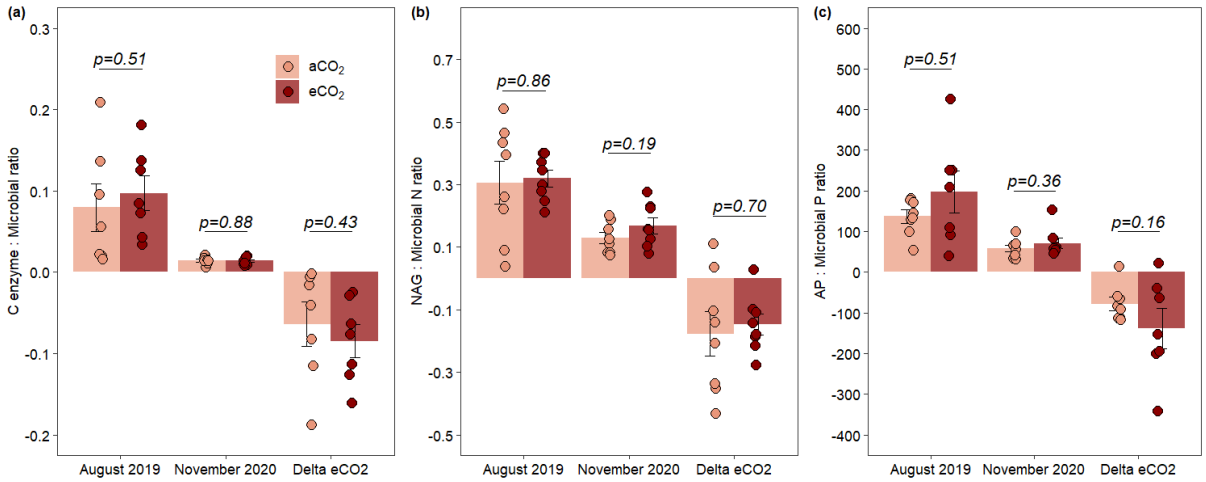

Figure S20| Elevated CO_2 effect on stoichiometry of soil enzymes and microbial biomass. The carbon enzymes are represented by the sum of cellobiosidase (CB) and β-1,4-glucosidase (BG) activity. (a) the ratio of carbon enzymes and C microbial biomass; (b) the ratio of nitrogen enzyme activity (β-1,4-N-acetylglucosaminidase) and nitrogen microbial biomass; (c) the ratio of phosphorus enzyme activity (acid phosphatase) and phosphorus microbial biomass. For each plot, we show the baseline collections (August 2019) that are realized before the start of elevated CO_2, the collection after 12 months of elevated CO_2 (November 2020), and the delta elevated CO_2 effect. The delta eCO_2 effect was calculated considering the difference between the collection after the increased CO_2 concentration (i.e., 12 months) and the baseline. Data were analyzed using generalized linear mixed models with a specific model for each collection data and variable, considering the effect of the treatment as a fixed factor and controlling the spatial variability using the open-top chamber (OTC) as a random factor (see "Methods" for

details). The numbers at the top of the bars indicate no significant (ns) or significant differences among ambient CO_2 (aCO_2) and elevated CO_2 (eCO_2); *$p<0.05$, ** $p<0.01$, and ***$p<0.001$. The bars showed the mean and standard error of n=8, and the points indicate the samples for each group.

Síntese

Uma das grandes questões científicas atuais é compreender como as florestas – e em especial as tropicais, que armazenam aproximadamente metade do carbono (C) estocado na biomassa vegetal no planeta responderão às mudanças climáticas (Pan et al. 2011; Koch, Hubau, and Lewis 2021). Nas últimas duas décadas, foi observada uma redução na capacidade da floresta Amazônica em atuar como sumidouro, o que pode estar relacionado ao aumento recente da mortalidade de árvores ou a uma desaceleração no aumento de alocação de C decorrente do crescimento de árvores devido a uma possível saturação no efeito de fertilização por CO_2 (Brienen et al. 2015; Hubau et al. 2020). A discrepância entre as projeções climáticas que indicam o potencial de a floresta atuar como este importante sumidouro de C nas próximas décadas e o que está sendo observado através dos dados *in situ* pode estar relacionado com a pouca representatividade dos ciclos de nutrientes – e em especial o do fósforo (P) nos modelos climáticos atuais (Hofhansl et al. 2016; Fleischer et al. 2019). Considerando que aproximadamente 60% dos solos da Amazônia são limitados por P e que a disponibilidade deste recurso limita a produtividade líquida da floresta Amazônica (Quesada et al. 2012; Cunha et al. 2022), compreender as múltiplas estratégias de aquisição de nutrientes das plantas e microrganismos é essencial para obter projeções mais acuradas sobre a resposta da floresta Amazônica às alterações climáticas.

Nesse sentido, nós avaliamos a influência da presença das raízes finas e aliviação na limitação de P na decomposição de detritos de madeira, que são considerados uma importante fonte de nutrientes, mas também um importante estoque de C na Amazônia, já que a decomposição desse material resulta em uma liberação de CO_2 para a atmosfera. Os nossos resultados indicaram que a presença das raízes finas acelera a decomposição dos detritos de madeira, mas o efeito direto na liberação de nutrientes só foi observado nas últimas coletas do experimento e nos detritos de menor densidade. Indicando que a qualidade do material orgânico, é um importante fator para a mobilização direta dos nutrientes através das raízes finas. Ainda, ao aliviar a limitação de P, observamos um aumento na decomposição dos detritos e na liberação de alguns nutrientes como o P, cálcio (Ca) e magnésio (Mg), o que sugere que a comunidade microbiana responsável por decompor os detritos de madeira é limitada pela disponibilidade de P. Assim, com a maior disponibilidade deste recurso, os microrganismos tendem a decompor o substrato à procura principalmente de C para atingir o seu equilíbrio estequiométrico (razão C:P). Os nossos resultados indicam os detritos de madeira como uma importante fonte de nutrientes, porém em condições naturais com baixa disponibilidade de P, a decomposição dos detritos de madeira

ocorre ao longo de décadas. Ou seja, uma fonte de nutrientes a longo prazo, podendo ser acelerada pela capacidade das plantas em investir na aquisição direta através da proliferação das raízes nesses substratos.

Estudos anteriores simulando o aumento nas concentrações de CO_2, realizados principalmente em florestas temperadas limitadas por nitrogênio (N), sugerem que a capacidade da floresta em alocar C para a sua biomassa depende diretamente da capacidade das plantas em superar a limitação de nutrientes (Finzi et al. 2007). Os nossos resultados indicam uma surpreendente plasticidade das plantas de sub-bosque da floresta Amazônica em investir o C extra assimilado via fotossíntese em múltiplas estratégias para aumentar a eficiência na aquisição de nutrientes nos diferentes compartimentos (serapilheira e primeiras camadas de solo).

Na camada da serapilheira, local com maior acúmulo das frações orgânicas e onde ocorre continuamente a ciclagem de nutrientes, em condições de aumento nas concentrações de CO_2, as plantas aumentaram o comprimento e área específica das raízes e reduziram o diâmetro possibilitando um maior volume de serapilheira explorado. Além disso, observamos uma maior atividade da fosfatase por comprimento total das raízes, que pode ser responsável pela redução na concentração do P total na serapilheira em processo de decomposição. Diferente da mineralização do N que ocorre através da oxidação do C via enzimas extracelulares produzidas pelos microrganismos (com produção de CO_2), a mineralização do P ocorre via hidrólise com o auxílio da enzima fosfatase sem a necessidade de realizar a decomposição do C presente no material orgânico (sem a produção de CO_2) (McGill and Cole 1981; Nannipieri et al. 2011; Dijkstra et al. 2013). Assim, o fato de as florestas tropicais aumentarem a eficiência na aquisição do seu nutriente limitante (P) sem aumento o fluxo de CO_2 liberado através da decomposição do material orgânico pode resultar em um saldo positivo na alocação de C em relação à fertilização por CO_2, sendo um importante processo que pode diferenciar a magnitude da resposta das florestas temperadas e as florestas tropicais ao aumento de CO_2.

Nas primeiras camadas do solo, nós observamos uma redução na produtividade das raízes finas, acompanhado de uma redução no comprimento e área específica das raízes em condições de aumento de CO_2. Por outro lado, foi observado um aumento no percentual de colonização por micorrizas arbusculares, indicando que o mecanismo para aumentar a área explorada foi "terceirizado" através da simbiose com os fungos micorrízicos, ao contrário do observado na camada da serapilheira onde as plantas alteraram suas estruturas morfológicas das raízes. De certa forma o custo-benefício em investir na associação com as micorrizas se mostrou mais

eficiente até o período estudado. No entanto, os nossos resultados indicam uma redução nas enzimas extracelulares responsáveis pela quebra das moléculas de C, sugerindo mudanças na dinâmica de C abaixo do solo que podem estar relacionadas à uma menor demanda dos microrganismos por C. Além disso, observamos uma redução na concentração do P orgânico do solo decorrente de um aumento na mineralização deste nutriente, sem alterações na fração do P inorgânico ou na concentração de P na biomassa dos microrganismos, o que pode sugerir uma maior absorção pelas plantas. Apesar desta redução na fração orgânica do P, não foram observadas alterações na atividade da fosfatase no solo ou raízes em condições de aumento de CO_2, sugerindo que além de aumentar a eficiência na aquisição de nutrientes as micorrizas arbusculares podem estar possivelmente influenciando bioquimicamente na disponibilidade do P.

Em síntese, os nossos resultados indicam que os detritos de madeira e as folhas presentes na camada da serapilheira são uma importante fonte de nutrientes, e as plantas podem intensificar a ciclagem ou mobilização direta de nutrientes através da proliferação das raízes finas. Além disso, apesar das possíveis diferenças em relação à intensidade e ao tempo de resposta das plantas de sub-bosque em comparação às de dossel ou emergentes, os nossos resultados representam um importante avanço na compreensão da resposta da floresta Amazônica frente às alterações climáticas. A surpreendente resposta das plantas investindo em múltiplas estratégias para aquisição de nutrientes, juntamente com alterações na dinâmica de P em resposta ao aumento nas concentrações de CO_2, sugerem que a disponibilidade desse nutriente realmente é um fator que restringe a resposta das florestas tropicais ao efeito de fertilização por CO_2. Nossa hipótese é que, embora a resposta das árvores adultas do dossel possa seguir estratégias semelhantes de mudanças nas estratégias de aquisição de P, a magnitude da mudança pode ser maior, pois elas podem acessar muito mais recursos. Nesse sentido, nossos resultados contribuem para uma maior representatividade dos processos relacionados a ciclagem de nutrientes, principalmente relacionados ao ciclo do P e as múltiplas estratégias para aquisição de nutrientes nos modelos terrestres globais, obtendo com isso a possibilidade de projeções mais acuradas em relação a resposta das florestas tropicais às mudanças climáticas.

Referencias

Brienen, R. J.W., O. L. Phillips, T. R. Feldpausch, E. Gloor, T. R. Baker, J. Lloyd, G. Lopez-Gonzalez, et al. 2015. “Long-Term Decline of the Amazon Carbon Sink.” *Nature* 519 (7543): 344–48. https://doi.org/10.1038/nature14283.

Cunha, Hellen F.V., Flavia Delgado Santana, Izabela Fonseca Aleixo, Anna Martins Moraes, Sabrina Garcia, Raffaello Di Ponzio, Erick Oblitas Mendoza, et al. 2022. “Direct Evidence for Phosphorus Limitation on Amazon Forest Productivity,” no. September 2021. https://doi.org/10.1038/s41586-022-05085-2.

Dijkstra, Feike A, Yolima Carrillo, Elise Pendall, and Jack A Morgan. 2013. “Rhizosphere Priming: A Nutrient Perspective.” *Frontiers in Microbiology* 4 (July): 216. https://doi.org/10.3389/fmicb.2013.00216.

Finzi, Adrien C, Richard J Norby, Carlo Calfapietra, Anne Gallet-Budynek, Birgit Gielen, William E Holmes, Marcel R Hoosbeek, et al. 2007. “Increases in Nitrogen Uptake Rather than Nitrogen-Use Efficiency Support Higher Rates of Temperate Forest Productivity under Elevated CO 2.” www.pnas.org/cgi/content/full/.

Fleischer, Katrin, Anja Rammig, Martin G. De Kauwe, Anthony P. Walker, Tomas F. Domingues, Lucia Fuchslueger, Sabrina Garcia, et al. 2019. “Amazon Forest Response to CO2 Fertilization Dependent on Plant Phosphorus Acquisition.” *Nature Geoscience* 12 (September): 736–741. https://doi.org/10.1038/s41561-019-0404-9.

Hofhansl, Florian, Kelly M. Andersen, Katrin Fleischer, Lucia Fuchslueger, Anja Rammig, Karst J. Schaap, Oscar J. Valverde-Barrantes, and David M. Lapola. 2016. “Amazon Forest Ecosystem Responses to Elevated Atmospheric CO2 and Alterations in Nutrient Availability: Filling the Gaps with Model-Experiment Integration.” *Frontiers in Earth Science* 4 (February): 1–9. https://doi.org/10.3389/feart.2016.00019.

Hubau, Wannes, Simon L. Lewis, Oliver L. Phillips, Kofi Affum-Baffoe, Hans Beeckman, Aida Cuní-Sanchez, Armandu K. Daniels, et al. 2020. “Asynchronous Carbon Sink Saturation in African and Amazonian Tropical Forests.” *Nature* 579 (7797): 80–87. https://doi.org/10.1038/s41586-020-2035-0.

Koch, Alexander, Wannes Hubau, and Simon L. Lewis. 2021. “Earth System Models Are Not Capturing Present-Day Tropical Forest Carbon Dynamics.” *Earth’s Future* 9 (5): 1–19. https://doi.org/10.1029/2020EF001874.

Kuzyakov, Yakov., J K. Friedel, and K. Stahr. 2000. “Review of Mechanisms and Quantification of Priming Effects.” *Soil Biology and Biochemistry* 32 (11–12): 1485–98. https://doi.org/10.1016/S0038-0717(00)00084-5.

McGill, W B, and C V Cole. 1981. “Comparative Aspects of Cycling of Organic C, N, S and P through Soil Organic Matter.” *Geoderma* 26: 267–86. https://doi.org/doi.org/10.1016/0016-7061(81)90024-0.

Nannipieri, P, L Giagnoni, L Landi, and G Renella. 2011. “Role of Phosphatase Enzymes in Soil.” In *Phosphorus in Action. Biological Processes in Soil Phosphorus Cycling*, 26:215–43. https://doi.org/10.1007/978-3-642-15271-9.

Pan, Yude, Richard a Birdsey, Jingyun Fang, Richard Houghton, Pekka E Kauppi, Werner a Kurz, Oliver L Phillips, et al. 2011. “A Large and Persistent Carbon Sink in the World’s Forests.” *Science* 333: 988–93. https://doi.org/10.1126/science.1201609.

Quesada, C. A., O. L. Phillips, M. Schwarz, C. I. Czimczik, T. R. Baker, S. Patiño, N. M. Fyllas, et al. 2012. “Basin-Wide Variations in Amazon Forest Structure and Function Are Mediated by Both Soils and Climate.” *Biogeosciences* 9 (6): 2203–46. https://doi.org/10.5194/bg-9-2203-2012.